Organophosphorus polymers, blends and composites: Applications in Li-ion batteries, optics and gas sorption

A Thesis Submitted for the degree of

DOCTOR OF PHILOSOPHY

By

Anjana K. O.

Reg. No. 14CHPH06



School of Chemistry
University of Hyderabad
Hyderabad, India-500 046

July 2020

Organophosphorus polymers, blends and composites: Applications in Li-ion batteries, optics and gas sorption

A Thesis Submitted for the degree of

DOCTOR OF PHILOSOPHY

By

Anjana K. O.

Reg. No. 14CHPH06



School of Chemistry
University of Hyderabad
Hyderabad, India-500 046

July 2020

CONTENTS

DEC	LARATION	(i)	
CERTIFICATE			
ACK	ACKNOWLEDGEMENTS		
LIST	LIST OF SCHEMES		
LIST OF TABLES		(vi)	
		(ix)	
COMMON ABBREVIATIONS SYNOPSIS (
	Chapter 1		
	Introduction		
1.1.	Introduction to polymers	1	
1.2.	Polymer blends and composites	2	
1.3.	Phosphorus based small molecules and polymers	3	
1.4.	Li ion batteries and Phosphorus based polymers	5	
	1.4.1. Lithium ion batteries and their significance	5	
	1.4.2. History of electrolytes used in Li-ion battery	7	
	1.4.3. Theories explaining mechanism of ionic conductivity	9	
1.5.	Phosphorus based polymers as tunable refractive index materials	11	
	1.5.1. Basics of refractive index and why tunability of refractive index is		
	important	11	
	1.5.2. Principles of ellipsometry and why is it unique	13	

1.5.	Polymer films as membranes for gas separation	16
1.7.	Scope of the thesis	19
1.8.	References	21
	Chapter 2	
C	catechol based polyphosphates with tunable micros	tructure-
	assisted Li-ion conductivity as solid polymer elect	rolytes
2.1.]	Introduction	31
2.2.]	Results and discussion	33
	2.2.1. Synthesis and characterization of polymers	33
	2.2.2. Microstructure of polymers P1-P4	35
	2.2.3. Thermal properties of P1-P4	37
	2.2.4. Conductivity studies	39
	2.2.5. Fabrication of coin cell	45
2.3.	Conclusions	46
2.4.]	Experimental section	47
	2.4.1. Materials and instrumentation	47
	2.4.2. General synthetic procedure of polyphosphates (P1-P4)	48
	2.4.3. Preparation of solid polymer electrolytes SPE1-SPE4	48
	2.4.4. Measurements of impedance of solid polymer electrolytes	49
2.5.]	References	49

Chapter 3

Poly(methyl methacrylate)/polyphosphate blends with tunable refractive indices for optical applications

3.1. Introduction	59
3.2. Results and discussion	61
3.2.1. FT-IR spectra and interaction between polymers in blend	65
3.2.2. AFM topography and uniformity of the blends	66
3.2.3. Absorption behavior of polyphosphates	68
3.2.4. Thermal analysis of the polyphosphates and their blends	69
3.2.5. Study of refractive indices of polymer blends	71
3.2.5.1. PB5 series	73
3.2.5.2. PB6 series	75
3.2.6. Tunability in optical properties of PB5 and PB6 blends	77
3.3. Conclusions	78
3.4. Experimental section	79
3.4.1. Materials and instrumentation	79
3.4.2. General synthetic procedure for the polymers P5 and P6	79
3.4.3. Sample preparation for ellipsometry and data analysis	80
3.5. References	80
Chapter 4	
Polyvinyl Alcohol-Phytic Acid Polymer Films as Pro	mising
Gas/Vapor Sorption Materials	
4.1. Introduction	87
4.2. Result and discussion	88

4.2.	1. Production	of PVA/PA films and their characterization	88	
4.2.	2. Morphology	of PVA/PA films	91	
4.2.3. Thermal and mechanical properties of composite PVA/PA films				
4.2.1. Production of PVA/PA films and their characterization 4.2.2. Morphology of PVA/PA films 4.2.3. Thermal and mechanical properties of composite PVA/PA films 4.2.4. Gas sorption properties of PVA/PA films 4.2.4.1. Dynamic Vapor Sorption Analysis (DVS) 4.2.4.2. Brunauer-Emmet-Teller (BET) studies 4.3. Conclusions 4.4. Experimental section 4.4.1 Materials and instrumentation 4.4.2 General Synthetic Protocol 4.4.3 Testing of mechanical strength 4.4.4 Gas sorption experiments 4.5. References				
	4.2.4.1.	Dynamic Vapor Sorption Analysis (DVS)	96	
	4.2.4.2.	Brunauer-Emmet-Teller (BET) studies	97	
4.3. C	onclusions		101	
4.4. E	xperimental se	ction	101	
4.4.	1 Materials and	linstrumentation	101	
4.4.2 General Synthetic Protocol				
4.4.3 Testing of mechanical strength				
4.4.	4 Gas sorption	experiments	102	
4.5. R	eferences		102	
		Chapter 5		
Sum	mary and F	uture perspective	113	
P	ublications		116	
P	osters and oral	presentations	116	

DECLARATION

I hereby declare that the matter embodied in the thesis entitled "Organophosphorus polymers, blends and composites: Applications in Li-ion batteries, optics and gas sorption" is the result of investigations carried out by me in the School of Chemistry, University of Hyderabad, India under the supervision of Prof. K. Muralidharan.

In keeping with the general practice of reporting scientific investigations, due acknowledgements have been made wherever the work described is based on the findings of other investigators. Any omission, which might have occurred by oversight or error, is regretted.

Certifical

K. M. 27/7/2000

K. MURALIDHARAN

Professor School of Chemistry University of Hyderabad Hyderabad - 500 046.



CERTIFICATE

This is to certify that the thesis entitled "Organophosphorus polymers, blends and composites: Applications in Li-ion batteries, optics and gas sorption" submitted by Anjana K.O. bearing registration number 14CHPH06 in partial fulfillment of the requirements for the award of Doctor of Philosophy (Ph.D.) in the School of Chemistry is a bonafide work carried out by her under my supervision and guidance. This thesis is free from plagiarism and has not been submitted previously in part or full to this or any other University/Institution for any degree or diploma. This thesis is free from plagiarism and has not been submitted previously in part or in full to this or any other University or Institution for award of any degree or diploma. Further the student has one publication before submission of the thesis for adjudication and has produced evidences for the same in the form of reprints.

Parts of this thesis have been:

- A. Published as the following article:
 - 1. A. K. Othayoth, B. Srinivas, K. Murugan and K. Muralidharan, Opt. Mat. 2020, 104, 109841-109851.
- B. Presented in the following conferences:
 - 1. International Conference on Materials Science and Technology (ICMST), 2019. held at VSSC Trivandrum from 10-13 October, 2018.
 - 2. SPSI Macro 2018, 15th International Conference on Polymer Science and Technology, held at IISER Pune, India from 19-22 December, 2018.

Further, the student has passed the following courses towards the fulfillment of coursework requirement for Ph.D.:

Sl. No.	Cou	rse Code	Title	Credits	Pass/Fail
1	CY-	801	Research Proposal	3	Pass
2	CY-	805	Instrumental Methods-A	3	Pass
- 3	CY-	806	Instrumental Methods-B	3	Pass
4	CY-	504	Chemistry of Materials	3	Pass

Prof. K. Muralidharan 7/7/2

(Thesis supervisor)

K. MURALIDHARAN

Professor
School of Chemistry
University of Hyderabad
Hyderabad - 500 046.

Dean

School of Chemistry

School of Chemistry
University of Hyderabad
P.O. Central University

Authors Hyderabad 500 046

ACKNOWLEDGEMENT

My heartfelt thanks are due to my Ph.D. supervisor **Prof. K. Muralidharan** who gave me the opportunity to explore my research interests. His support, guidance and suggestions at every stage of my research are immensely valued. I have enjoyed whatever bit of research I have done here because of the freedom in research given by him. I heartfully acknowledge **Prof. M. Durgaprasad** without whom, I would not be able to complete my Ph.D. My respect and gratitude to him is beyond what words can express.

I thank all the teaching and non-teaching staff of School of Chemistry, University of Hyderabad for helping me at different stages directly and indirectly. I specially thank my DC members **Prof. Tushar Jana and Prof. R. Nagarajan** for their support. And special thanks to **Prof. T. P. Radhakrishnan** for his questions, discussions and valuable suggestions at the right time, for it motivated me to investigate further about the basics and rectify some flaws.

I sincerely thank **Dr K. Murugan** from ARCI, Hyderabad for helping me with ellipsometric studies and the numerous useful discussions associated. I also thank **Dr. Shanmugharaj** from VELS University, Chennai for helping us with the fabrication of coin cells and Dr. H. Vignesh Babu for setting up the platform for conductivity studies in our lab. Special note of thanks to Mr. Sunil (FESEM), Mr. Durgesh (NMR), and Mr. Durgaprasad (FESEM and AFM).

I was also fortunate enough to have wonderful teachers during my M.Sc. at NIT Calicut and all of them have inspired me through their own ways of teaching. I am grateful to all my M. Sc. teachers including Prof. G. Unnikrishnan, Dr. C Arunkumar, Dr. Suni Vasudevan, Dr. Lisa Sreejith, Dr. C. Lakshmi, Dr. Soney Varghese, Dr. N. Sandhyarani, Dr. P. Parameswaran and Dr. A. Sujith and B.Sc. teachers Mrs. B. Lakshmidevi, Dr. Gigy Abraham, Dr. Sr. Neetha, Sr. Asha, Mrs. Dhanusha and Mrs. Tina. I must also acknowledge my intermediate teachers Mrs. Suma and Mr. Vineesh who were a great source of inspiration for me to pursue Chemistry.

Friends are an integral part of life and of course they made my days here more enjoyable. I whole heartedly thank Divya, Arun, Nagamaiah, Anju, Soumya, Archana, Radhika, Priya, Bhavana, Rahulettan, Jeladhara, Jeena, Jhansi, Shyam, Ramar, Sugandhi and Reshma for all those wonderful time. A special note of gratitude to Divya, Arun and Ranjani akka for standing

by me at crucial situations. I also express my gratitude towards my lab seniors Narayana anna and Srinu anna for teaching, supporting and motivating me at different points of my Ph.D. I am grateful to labmates Venky, Manzoor, Anju, Hemanth, Srinu anna, Mani anna, Aneesh anna, Ramu anna, Mohan anna, Prachuritha and Ramakrishna for creating a friendly and supportive environment in the laboratory. The times we have spent together as a group will always be fondly remembered. Also, the project students who were a part of my lab work- Ashwini, Jaseel. Soumick, Vikas and Chittemma were a great help and support and I acknowledge them with lots of love.

My parents, my sister, and my husband-these people have strongly supported me throughout the journey and still continue to do so. To them of course, no thanksgiving words can encompass the feeling and I dedicate my thesis work to these wonderful people in my life.

Acknowledgements are due to all those who have helped me through this journey; both positive and negative I must say, because positive people gave me confidence and support and negative people made me believe in my strengths, which otherwise I would have never realized. And now I strongly believe everything that happens in life is an experience and experience is the greatest teacher ever. As our former President and missile man of India, Dr. APJ Abdul Kalam said "Difficulties in your life do not come to destroy you, but to help you realize your hidden potential and power. Let difficulties know that you too are difficult."

Anjana

List of Schemes

1.1.	Mechanism of lithium ion conductivity by polyether host	11
1.2.	A schematic representation of the method of ellipsometric analysis by suitable	
	theoretical model selection	16
2.1.	Schematic representation of the syntheses of polymers P1-P4	33
3. 1.	Schematic representation for the syntheses of polymers P5 and P6	61
4.1	Synthesis of PVA/PA polymeric films	89

List of figures

1.1	Different possible chemical environments of phosphorus	4
1.2	Illustration of working of a typical lithium ion battery	6
1.3	Instrumentation set up for ellipsometer and the original instrument	15
1.4	Relationship between hydrogen permeability and H ₂ /N ₂ selectivity	17
1.5	Applications of focus of the thesis	20
2.1 2.2	Infrared spectra of polymers P1-P4 (a) The energy minimized structure of P3 obtained using MM2 force field by	35
	Chem3D software	36
	(b) A schematic illustration of structural framework of polymer matrices that can	
	support the movement of Li-ions through solid polymer electrolytes	36
2.3.	FESEM images of polymers P1-P4	37
2.4.	TGA and DSC plots of polyethers P1-P4 (a and b), SPE3 (c and d)	39
2.5.	Temperature dependent Nyquist plots of SPE1	41
2.6 .	Temperature dependent Nyquist plots of SPE2	42
2.7.	Temperature dependent Nyquist plots of SPE3	43
2.8.	Temperature dependent Nyquist plots of SPE4	44
2.9.	Arrhenius plots of temperature dependent conductivities of a) SPE1 b) SPE2	
	c) SPE3 d) SPE4	45
2.10	(a) The assembly of various components making up a coin cell (b) Voltage-time	
	graph obtained by the charge discharge cycling studies.	46
3.1.	Polymers P5 and P6 casted into films by solvent casting	62
3.2.	A schematic representation of the sample coated on SLG	63
3.3.	Images of samples illustrated for their transparency (a) PB510 (b) PB520 (c)	
	PB550 (d) PB560 (e) PB580 (f) P5 (g) PB610 (h) PB620 (i) PB650 (j) PB660 (k)	
	PB680 (l) P6 (m) PMMA	64

3.4.	(a) IR spectra of the polymers and blends of PB5 series (b) IR spectra of the	
	polymers and blends in PB6 series (c) IR spectra of the blends of PB6 series showing	ıg
	the region 3200-3550 cm ⁻¹ illustrating intermolecular hydrogen bonding.	65
3.5.	AFM topography (right) and phase (left) images of P5 (a and b), PB510 (c	
	and d),PB580(e and f), PB660 (g and vi 'B620 (i and j), P6 (k and l).	68
3.6.	(a) Absorption spectra of P5 and P6 (b) Absorption spectra of P5 and P6 (c)	
	Extinction coefficients of blends of P6.	69
3.7.	The thermogravimetric analyses of all the samples in PB5 and PB6 series in figure	
	(a and b).	70
3.8.	Ellipsometric spectra for the samples spin-coated on a glass substrate (experimental	
	data and model fit are shown) (a) PB510 (b) PB520 (c) PB550 (d) PB560 (e) PB580)
	(f) P5 (g) PB610 (h) PB620 (i) PB650 (j) PB660 (k) PB680 (l) P6 (m) PMMA.	7 1
3.9.	(a) Ellipsometric spectra of a sample (PB580) spin-coated on a glass	
	substrate (experimental data and model fit are shown) (b) variation of refractive	
	index with wavelength and (c) uniqueness fit for the sample PB580.	7 4
3.10 .	(a) Variation of refractive indices with wavelengths for PB5 series (b) Variation	
	of refractive indices with different weight percentages for PB5 series.	75
3.11 .	(a) Variation of refractive indices with wavelengths for PMMA, PB610, PB620	
	and P6 (b) Variation of refractive indices with wavelengths for PB650, PB660 and	
	PB680 (c) Variation of refractive indices with different weight percentages for PB6	
	series (d) a representative plot (PB660) of variation in n and k with wavelength.	76
3.12 .	Abbe values of blends of PB5 series plotted at increasing weight percentages of P5.	7 8
4.1.	Images of various polymeric films showing its transparency and film forming	
	nature (a)PVA (b) 9:1 PVA/PA (c) 4:1 PVA/PA (d) 3:1 PVA/PA (e) 3:2 PVA/PA	
	(f) 1:1 PVA/PA (g) 2:3 PVA/PA.	9(
4.2.	FT-IR spectra of the polymeric films.	91
4.3.	The cross-sectional FESEM images of the polymeric films showing their	
	morphology (a) PVA (b) 9:1 PVA/PA (c) 4:1 PVA/PA (d) 3:1 PVA/PA (e) 3:2	
	PVA/PA (f) 1:1 PVA/PA (g) 2:3 PVA/PA.	92
4.4.	The cross-sectional FESEM images of the polymeric films showing their	
	porosity(a) PVA (b) 9:1 PVA/PA (c) 4:1 PVA/PA (d) 3:1 PVA/PA(e) 3:2	

	PVA/PA (f) 1:1 PVA/PA (g) 2:3 PVA/PATGA spectra of the polymeric films.	93
4.5.	TGA spectra of the polymeric films.	94
4.6.	Stress-strain graph of the polymeric films.	96
4.7.	Gravimetric vapor sorption spectra of the polymeric films.	97
4.8.	BET adsorption desorption isotherms of the polymeric films.	100
4.9.	Graphs showing variation in specific surface area (a) and average pore size (b)	
	with increasing PA content.	100

List of tables

2.1 .	Molecular weights of polymers P1-P4	34
2.2.	Thermal stability analysis of polymers P1-P4 and SPEs	38
2.3.	Li-ion conductivities of SPE1- SPE4 (10%- 40%) at various temperature	40
3.1.	NMR data and molecular weight distribution of P5 and P6	61
3.2.	Phosphates (P5 or P6) and PMMA blends and their weight ratio	62
3.3.	Refractive indices of polyphosphate blends with PMMA.	76
3.4.	Abbe values of PB5 blends	77
4.1.	Various polymer composites synthesized and the distribution of PVA and PA in	
	them	89
4.2.	Mechanical properties of the samples	95
4.3.	Vapor sorption properties of the samples	96
4.4.	Specific surface area and average pore size of the samples	98

Common abbreviations

NMR Nuclear Magnetic Resonance

FTIR Fourier Transform Infrared

UV Ultraviolet

PEO Polyethylene oxide

PMMA Polymethyl methacrylate

PVA Polyvinyl Alcohol

PA Phytic Acid

SPE Solid Polymer Electrolyte

T_g Glass transition Temperature

M_n Number average molecular weight

M_w Weight average molecular weight

PDI Polydispersity Index

DMSO Dimethylsulfoxide

DCM Dichlorormethane

DMAc Dimethyl acetamide

THF Tetrahydrofuran

TGA Thermogravimetric Analysis

DSC Differential Scanning Calorimetry

GPC Gel Permeation Chromatography

FESEM Field Emission Scanning Electron Microscopy

AFM Atomic Force Microscopy

DVS Dynamic Vapour Sorption Analysis

RI Refractive Index

HRIP High Refractive Index Polymer

MSE Mean Squared Error

LED Light Emitting Diode

MSCM Molecular Sieve Carbon Membrane

DNA Deoxyribonucleic acid

RNA Ribonucleic acid

ATP Adenosine Triphosphate

PVA Polyvinyl Alcohol

PA Phytic Acid

BET Brunauer-Emmett-Teller

UTM Universal Testing Machine

LIB Lithium Ion Battery

EMC Ethyl Methyl Carbonate

LiTFSI Lithium bis(trifluoromethanesulfonyl) imide

SLG Soda Lime Glass

VASE Variable Angle Spectroscopic Ellipsometer

SYNOPSIS

The thesis entitled "Organophosphorus polymers, blends and composites: Applications in Li-ion batteries, optics and gas sorption" consists of four chapters.

Chapter 1: Introduction

Chapter 1 begins with the general introduction of polymers, blends, and composites and then discusses phosphorus, phosphorus-containing polymers, and small molecules. Further, the general applications of these moieties, and then specifically, the three different applications explored in this thesis, are discussed. These applications include polymers as electrolytes in lithium-ion batteries, tunable refractive index materials, and polymeric membranes for gas sorption applications (figure 1). The chapter ends with a brief description of the future scopes of the thesis.

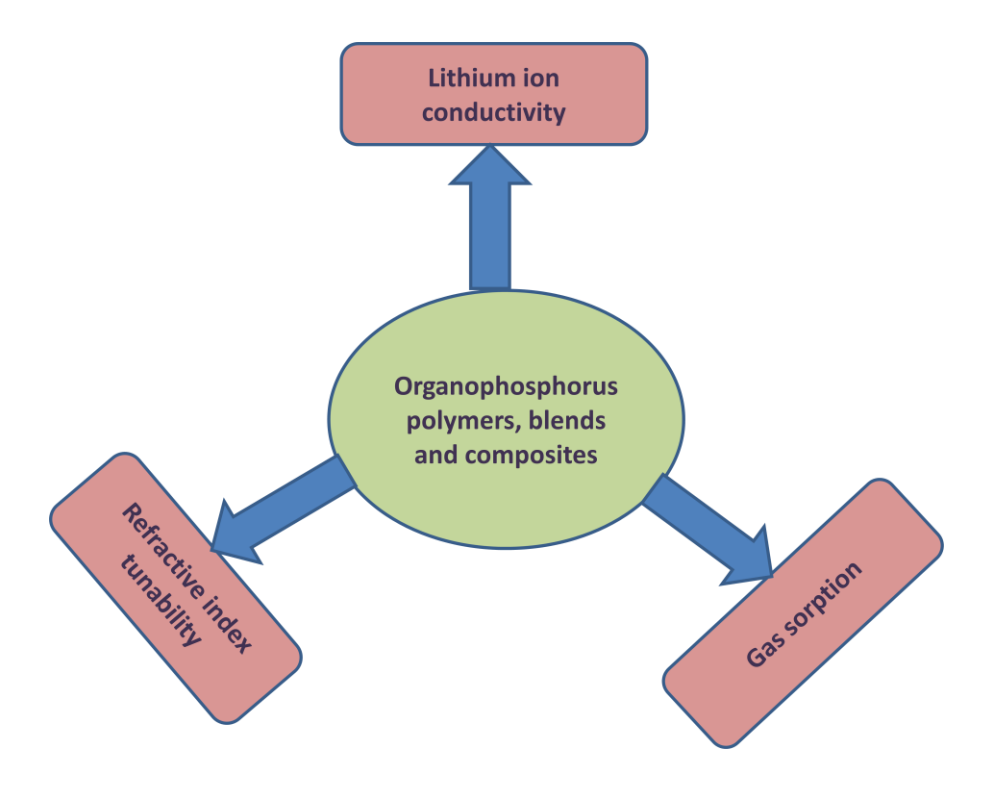


Figure 1: Applications of focus of the thesis.

Chapter 2: Tunable microstructure-assisted Li-ion conductivity in catechol based polyphosphates for solid electrolytes in Li-ion battery

This chapter describes the syntheses, characterization, and Li-ion conductivity of phosphorus-containing polyethers (**P1-P4**) for solid polymer electrolyte applications in Li-ion batteries. The polymers described in this chapter are thermally stable with high molecular weight, porous nature, and tubular morphology. The conductivity of one of the solid polymer electrolytes prepared from P3 with 20 wt% of LiTFSI was 1.4×10^{-3} S cm⁻¹ at 80 °C (figure 2), and P1 with 40 wt% of LiTFSI was 1.2×10^{-3} S cm⁻¹ at 80 °C. Remaining all polymers (P1- P4) showed good conductivity at RT (~10⁻⁴ S cm⁻¹). The high conductivity achieved is explained by the porous nature of the polymers.

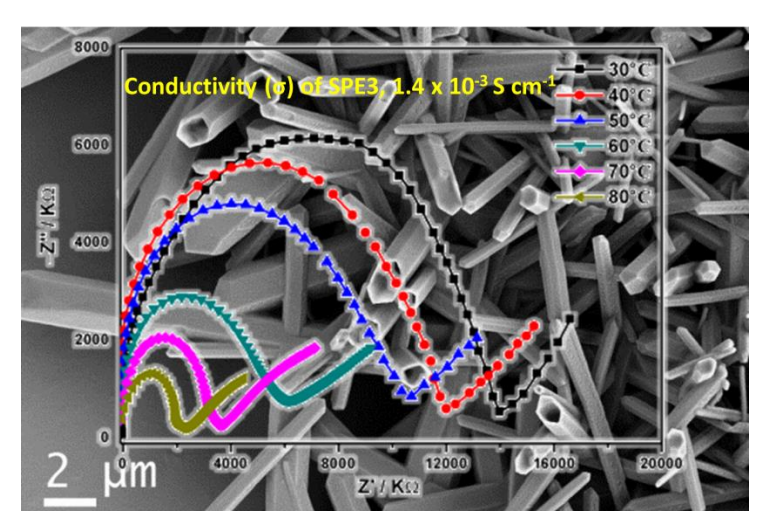


Figure 2: Nyquist plot for SPE3 which showed the highest conductivity with 20 weight % of LiTFSI at various temperatures. The hollow tubular morphology of the polymer, P3 is shown in the background.

Chapter 3: Poly(methyl methacrylate)/polyphosphate blends with tunable refractive indices for optical applications

In chapter 3, we have studied two different phosphorus polyethers (**P5** and **P6**) blended with poly(methyl methacrylate) (PMMA) to find their applicability in optics. We have investigated the refractive indices of these polymer blends using ellipsometry. Tuning the refractive indices is a needed strategy for optical applications. Tunability is achieved in our materials by altering the ratio of PMMA to **P5** or **P6**. The RI tunability of 0.05 was observed in the PB5 series and 0.1 in

the PB6 series. The approach is found to be ideal and straightforward for obtaining homogeneous blends with varying degree of RI. The PB5 series showed reasonable values of abbe numbers compared to the conventional lens materials, with a maximum value of 56 achieved in the case of PB520 blend. These results show that the synthesized polymer blends are promising as optical materials with refractive index tunability from 0.97- 1.57 at 589.3nm. While PB5 series could be useful for lens kind of applications, the PB6 series with higher weight percentages of P6 could be useful as optical filters (figure 3).

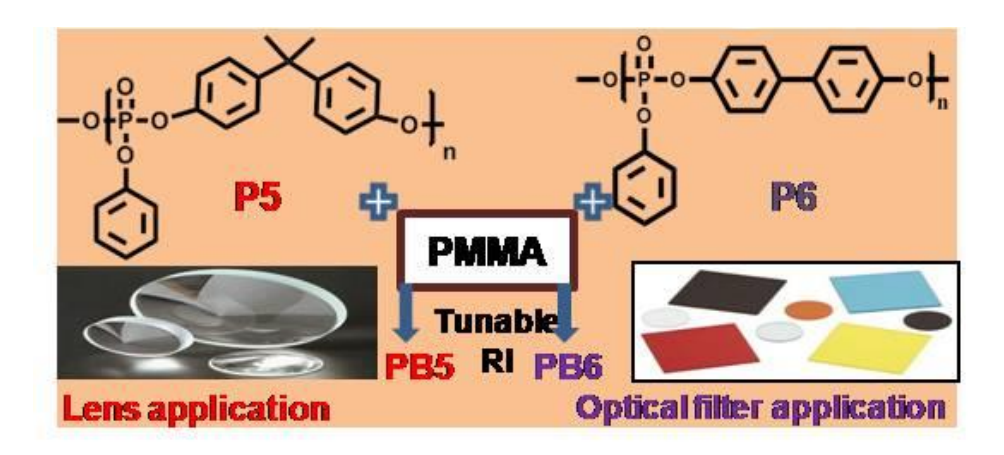


Figure 3: A graphical representation illustrating the applications of polymer blends synthesized by blending the polyphosphates P5 and P6 with PMMA.

Chapter 4: Polyvinyl Alcohol-Phytic Acid Polymer Films as Promising Gas/Vapor Sorption Materials

The whole idea of this work was to synthesize and characterize PVA/PA films for studying its gas sorption properties. Phytic acid is being a bulky molecule, unable to pack efficiently in the solid-state, could trap sufficient free volume. From FESEM analysis, the morphology of these films is found to be layered leaf-like, which may help in trapping gas molecules and thereby help in gas sorption. The mechanical properties of these films are also quite interesting as one of the films, 2:3 PVA/PA showed the highest elongation at break of 372%. Vapor sorption analysis is a piece of clear evidence that these films can adsorb and desorb gaseous molecules and shows a general trend of increasing vapor sorption with an increase in weight percent of phytic acid. In particular, 2:3 PVA/PA polymer film shows the highest vapor sorption with 0.15g moisture

content per gram of the sample. By BET analysis, the films were found to be mesoporous. Specific surface area (Figure 4) and average pore size of the films, as compared to the pure PVA, were found to increase with the gradual increase in PA. Further, the selectivity and permeability of these polymeric films have to be investigated to understand the applicability of the films for practical purposes.

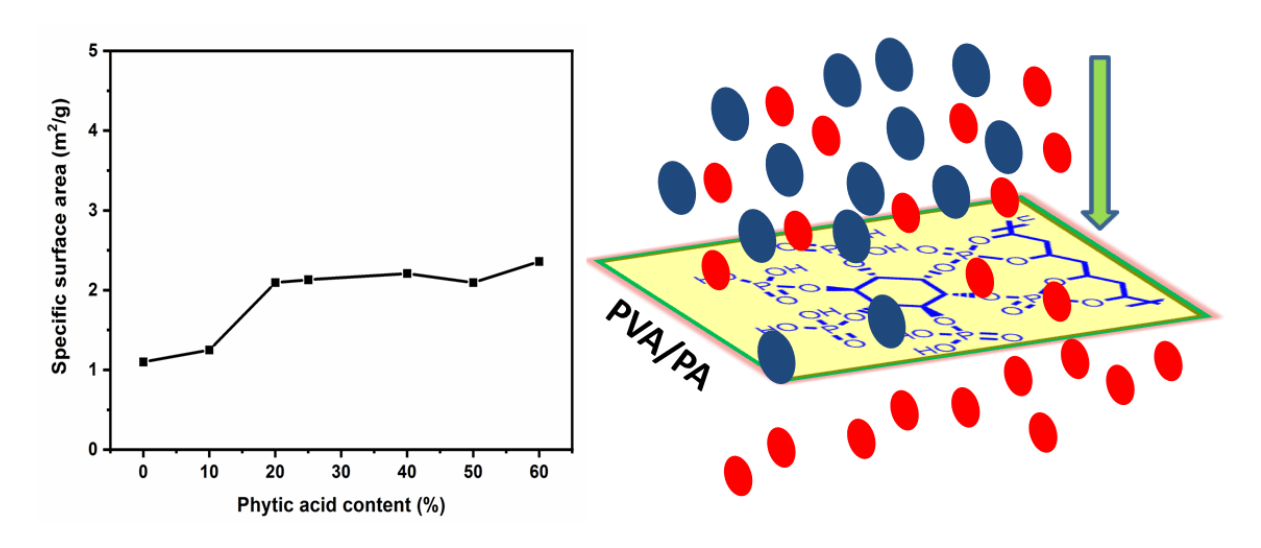


Figure 4: Variation of specific surface area with increase in phytic acid content and graphical representation showing PVA/PA membrane for gas separation application.

Chapter 5: Summary and future perspective

The thesis is summarized, and the possible extension of the work is also discussed in this chapter.

Chapter 1

Introduction

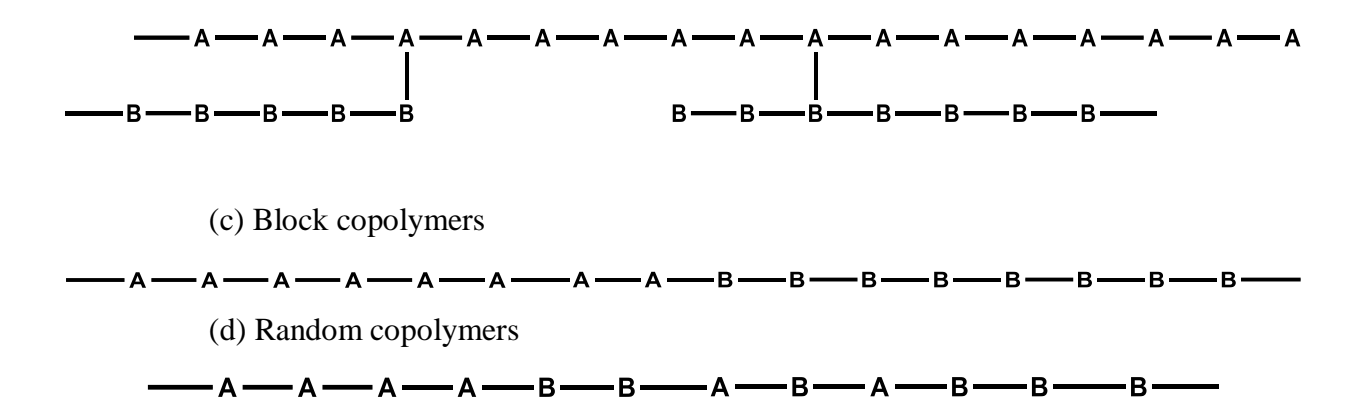
1.1. Introduction to polymers

Life on earth originated when the simple chemical compounds like methane, ammonia, and carbon-dioxide combined under certain conditions to form the basis of life-proteins, which is basically a polymeric compound. A polymer is a chain molecule consisting of repeated subunits. The word "poly" means many, and "mer" means parts. Polymers have so intimately been bound to our daily lives that we cannot imagine a day without them. Not only the synthetic ones, but we also have quite more number of biopolymers like proteins, DNA, RNA, and lipids, which make up a crucial part of the human body. The plant-based polymers like rubber, silk, cellulose are also equally beneficial to humankind. The existence of macromolecules was accepted by researchers worldwide mainly due to the efforts of Staudinger¹ and Carothers² in the 1920s.

Depending on the repetition of monomers, they are classified as:

- (i) Homopolymers these polymers contain a single monomer repeating throughout the chain.
- (ii) Copolymers these polymers contain at least two different monomers along the chain. They are further divided into:
 - (a) Alternating copolymers

(b)Graft copolymers



Based on the processes of polymerization, there are two major categories:

- (i) Addition polymers: Consecutive addition of monomer molecules results in the addition polymer. This reaction is also known as chain polymerization (e.g., PVC, Teflon etc.).
- (ii) Condensation polymers: In this process, a step-by-step growth polymerization reaction occurs through condensation reactions leaving small molecules like water or methanol as byproducts (e.g., Proteins, Nylon etc.).

1.2. Polymer blends and composites

A polymer blend is a single-phase material obtained by mixing at least two polymers and has different physical properties than the parent polymers. On the other hand, a polymer composite is a multiphase material with a polymer matrix and reinforcing filler. The filler and matrix maintain their identity even after forming a composite and have their own physical and chemical properties intact. Based on miscibility, polymer blends could be classified into three types:

- 1] <u>Completely miscible blends</u>: In these blends have homogeneity in the range of at least a nanometer scale. These blends have a single glass transition temperature (Tg). Characteristically, their Tg value lies in between those of the parent polymers. E.g., PS/PPO.
- 2] <u>Partially miscible blends</u>: As the name suggests, these are partially miscible polymers, i.e., a small part of one of the polymer dissolves in the other to form compatible blends. The polymers retain individual Tg values but slightly shifted towards the Tg of the blend. E.g., PC/ABS.

3] <u>Fully immiscible blends</u>: These blends have highly inhomogeneous morphology and hence do not find use unless it is made compatible with the help of a compatibilizer. The individual polymers retain their Tg values. E.g., PA/ABS.

Polymer composites can be classified based on the polymer matrix present in them as:

- 1] <u>Thermoplastic matrix composite</u>: Matrix can be melted, molded, and remolded without changing its physical properties. These composites are quite tough, have excellent impact resistance and damage tolerance. They are less dense than thermoset matrix composites and hence a good alternative for weight critical applications.
- 2] <u>Thermoset matrix composite</u>: Matrix once cured into solid form cannot be melted or remolded. These composites are durable and have good fatigue strength but brittle and have low impact resistance. They are useful for high heat applications.

1.3. Phosphorus based small molecules and polymers

The name phosphorus meaning light-bearer is derived from the faint glow produced when white phosphorus undergoes oxidation. Phosphorus is classified as a pnictogen along with nitrogen, arsenic, antimony, and bismuth. Phosphorus is the eleventh most abundant element on earth and contribute upto 1.1% of the human body by weight. Phosphates are found in DNA, RNA, ATP, and phospholipids, which are crucial for human survival. Organophosphorus compounds are an integral part of fertilizers, pesticides, detergents, nerve agents, and many more.

Phosphorus-containing polymers are quite fascinating from a research point of view due to their numerous applications in various fields. For example, they are used as corrosion inhibiting agents,³ dispersants, flame retardants, complexing agents, proton-conducting membranes in fuel-cell,^{4,5}and as flame retardants.^{6,7}Also, they have good complexing properties^{8,9} and affinity to bind metals.^{10,11}Phosphorus atoms can exist in different possible chemical environments, as shown in figure 1.1 leading to differences in properties also.¹².

Figure 1.1: Different possible chemical environments of phosphorus.

phosphorus-based polymers are known Varieties such as polyphosphates, polyphosphonates, polyphosphoesters, phosphonated poly(meth)acrylates, and polyphosphazenes. 13 Many phosphorus-based like polymers polyphosphoesters, polyphosphonates, phosphonated poly(meth)acrylates, and polyphosphates are blood compatible and biodegradable. They also showed strong interactions with bones, dentin, or enamel, enhancing their biomedical applications. Addition of a phosphonic functional groups to the polymers increased its adhesion ablity on teeth because of the formation of a complex with calcium in hydroxyapatite (HAP).^{21,22}Hence, these functionalized polymers could be employed in bone tissue engineering. Polymers withphosphorus also act as carriers for bioactive molecules. Polymers derived from 2-methacryloyloxyethyl phosphorylcholine are mainly attractive owing to their biomimetic nature.

Polyphosphazenes have phosphorus and nitrogen atoms alternating in the skeleton. They are advantageous due to the availability of easy synthetic strategies to introduce different side chains. It is well known for polymer electrolyte kind of applications. The first reported polyphosphazene electrolyte, poly[bis(2-(20-methoxyethoxy)phosphazene) (referred as

MEEP), ¹⁴showed an Li-ion conductivity values at room temperature as 10⁻⁵ S cm⁻¹. This value is two times higher compared to that of pure PEO based SPEs. However, they have unsatisfactory dimensional stability and flow slowely under pressure. To increase the dimensional and mechanical stability many process have been attempted. Some of them are UV irradiation¹⁵, chemical cross-linking by bifunctional reagents¹⁶ and unsaturated groups¹⁷, interpenetrating network created thorough oxyethylene side groups¹⁸ and blend composites¹⁹ were tried. Though the solid polymer electrolytes (SPEs) produced using polyphosphazene polymer with ether side chain showed Li-ion conductivity higher than PEO-salt based polymer electrolytes, the values are considerably less than the minimum value required for practical utility.

Polyphosphate derivatives are also equally attractive due to their biodegradability and biocompatibility. Under physiological conditions, they undergo enzymatic digestion of phosphate linkages. ²⁴Certain phosphonates like poly(oxyethylene H-phosphonates) were utilized for biomedical applications owing to their water-solubility, low toxicity, biocompatibility, controlled biodegradability, and easy functionalizability. ²⁵⁻³⁰ When clinically tested, a well-known chemical radioprotector cysteamine was incorporated into poly-(oxyethylene phosphate), its drug dose required for efficient radioprotection and toxicity was reduced. ³¹Modified, water-soluble polyphosphates holding the BCEA group were used in chemotherapy.

Biodegradable copolymers having lactide ester linkages and phosphonates in the main chain of polymer were explored. Paclitaxel delivery from polyphosphoesters was evaluated³² for their antitumor activity. It was found to be active continuously over 60 days in vitro and in vivo. It was useful for the controlled and targeted delivery of neurotrophic proteins to the treatment of various diseases attacking the nervous system.³³ Poly(phosphoesters), due to their adjustable biodegradability and biocompatibility, are used to make nerve guide conduits. Under physiological conditions, they can couple fragile biomolecules and result in various physicochemical properties.^{34,35} Polymer micelles formed bypoly(ε-caprolactone) and polyphosphoester block copolymers were investigated for their in vivo biomedical applications. Molecular weights of these polyphosphoester copolymer were controlled to adjust the lower critical solution temperature.³⁶

1.4. Li-ion batteries and phosphorus based polymers

1.4.1. Li-ion batteries and their significance

Li-ion batteries are lightweight and provide the highest energy density per weight. The lightest element Li posses the highest oxidation potential compared to other elements, and can be handled safely in electrochemical processes. ^{39,40} Hence Li metal is suitable for Rechargeable high energy density batteries. The Li-ion cells are an integral part of the portable, entertainment, computing, and telecommunication types of equipment used in our daily lives. A typical Li-ion battery is constructed using a graphite anode and lithium metal oxide (e.g., LiCoO₂, LiMnO₂) as the cathode. The electrolyte consist of a salt of lithium (e.g., LiPF₆, LiBF₄) dissolved in an organic solvent (e.g., dimethyl carbonate, ethylene carbonate). ³⁸ Figure 1.2 shows a typical configuration of Li-ion battery. The overall reaction happening can be depicted below.

 $6C + LiMO_2 \rightleftharpoons Li_xC_6 + Li_{(1-x)}MO_2, x \sim 0.5, voltage \sim 3.7V$

e'

A

e'

Li'

O

Li'

O

Li'

O

Li conducting organic Li 1.xCO2

Aluminum

electrolyte

Aluminum

Li-ion batteries are of different kinds based on the cathode used and the chemistry involved. Some of the interesting batteries are discussed below.

Figure 1.2: Illustration of working of a typical lithium ion battery.³⁷

current collector

(i) Lithium Titanate battery (LTO)

collector

These batteries are highly advantageous since they can operate at shallow temperatures like -40 °C. They have rapid charge and discharge rates but have their energy density quite low (30-110 Wh/kg) and a low voltage of about 2.4 V.

(ii) <u>Lithium Cobalt-Oxide battery (LCO)</u>

These are found in portable electronic equipment like cell phones, cameras, and laptops. The major disadvantages of these batteries are the low discharge rates, cost of cobalt and the risk involved when these are damaged. However, they have a high energy density in the range 110-190 Wh/kg.

(iii) <u>Lithium Iron Phosphate battery (LFP)</u>

These batteries are used in medical equipments and power tools because of their advantages like low overheating and fire risks. They also have a longer life. Their energy density is in the range of 95-140 Wh/kg, but possess lower volumetric capacity.

(iv) Lithium Nickel Manganese Cobalt Oxide battery (NMC)

These batteries have a longer life and do not cause overheating, and hence used in e-bikes, power tools and electric power trains. However, cobalt is quite expensive, and these batteries have lower energy densities (95-130Wh/kg).

(v) <u>Lithium Manganese Oxide battery (LMO)</u>

These are used mostly in cell-phones, and laptops and hybrid vehicles. These batteries are safe, have a longer life, low cost, with high discharge rates but low energy density in the range 110-120 Wh/kg.

1.4.2. History of electrolytes used in Li-ion battery

A battery is fabricated with three inevitable components. These important components are; a cathode, an anode, and an electrolyte. The commercial Li-ion battery use mostly graphite as an anode and lithium cobalt oxide, lithium iron phosphate, and lithium manganese oxide as the cathode. The material used as electrolyte could be organic or inorganic solvent-based electrolytes or molten salts. ⁴⁷The problem is lithium metal in contact with liquid electrolytes, lithium-metal electrodes may generate fire and explosion. Consequently, use of a thin polymer membrane as a replacement for of the liquid electrolyte with would be appropriate. After the invention of ionic conductivity in poly(ethylene oxide)⁴¹ (PEO) added with salt of alkali metals by Wright and

coworkers in 1973, the polymer based electrolytes were promoted for batteries in 1978. Polymer electrolytes combine the advantages of ease of processing and solid-state electrochemistry.^{42,43}

The research on solid polymer electrolytes (SPE) has grown up recently for electrochemical device applications giving importance to safety issues. 48 With P. V. Wright and M.B. Armand's studies on the complexes formation of PEO polymer with alkali metal salts, 50,51 the topic received more attention. Several polymers were investigated as SPE such as poly(siloxanes), poly(acrylates), poly(vinylpyrrolidine), poly(ethylenesuccinate), poly(vinylalcohol), and poly(phosphazenes). 52 Among the many polymers studied, PEO was identified as facile 53 for several reasons; some of them are listed below.

- (i) It has low cost.
- (ii) It is soluble in many solvents and hence easily processable.
- (iii) It has a high donor number.
- (iv) It has a relatively high dielectric constant.
- (v) It has a T_g value, which causes to high plasticity. This helps in having intimate contact with electrodes.
- (vi) PEO with high molecular weight has the high viscosity. This high viscosity helps the material to resist creeping at high temperatures.
- (vii) It has no toxicity.

Thermal runaway and consequent rise in temperature creates chances of explosion or fire in lithium batteries. ⁷⁰Hence flame retardancy is a great challenge for battery manufacturers. Usually phosphorus-based organic compounds are mixed with electrolytes used for Li-ion batteries as the flame-retardant constituent. The possible advantages of using solid polymer electrolytes compared to liquid electrolytes are the following: ⁷¹

- (i) Improved safety with no leakage problems.
- (ii) They are non-volatile.
- (iii) Probability of avoiding the destructive decomposition at the electrodes.
- (iv) The problem of dendrite formation could be solved by introducing the non-porous and solid electrolyte metallic lithium.
- (v) Easy to fabricate and hence cheaper manufacture of cell.

- (vi) Since they are all-solid-state batteries they do not require casing made by heavy steel.

 The cell weight could be considerably reduced.
- (vii) Cell will have good shape flexibility.
- (viii) They will have improved shock resistance.

1.4.3. Theories explaining mechanism of ionic conductivity

Ionic conductivity can be expressed by $\sigma = nem$ where n denotes the "effective number of mobile ions", e denotes the "elementary electric charge", and m represents the "ion mobility", respectively. Thus, the equation implies that if more salt dissociates in polymer higher will be the value of n and higher will be the ionic conductivity. Also, the Li+ transference number should be high (the charge transported by lithium cations equated to the total number of charge transported gives the Li+ ion transference number). ^{43,45}In polymer electrolytes, ionic conductivity has a contribution from both cations and anions. However, in polyelectrolytes, the ionic conductivity is governed solely by the movement of cations. This restriction is since the anions are fixed as a part of the polymer chains. Hence, they are known as "single-ion conductors." There area few examples where it was proposed that for Li+ alone conducting polymers. ⁴⁶However, practically the conductivities of these polymers were found to be only about 1% that of ordinary SPEs. This low conductivity is primarily due to the inadequate dissociation of Li+ in those materials.

For practical purposes, the SPEs should have broad electrochemical stability, typically between 0 - 4.5 V and an ionic conductivity as high as 10^{-3} S cm⁻¹at room temperature. Also, it should be compatible with high voltage cathodes and low voltage anodes. However, the current SPEs have a low lithium transference number (in the range 0.2 - 0.3) and a low conductivity (in the range 10^{-5} S cm⁻¹) at room temperature.⁴⁹ initially, it was considered that the crystalline domains are majorly contributing towards ionic conductivity. Contradictorily, later studies in this direction established that amorphous phase as the sole cause for ionic conductivity.⁴⁴

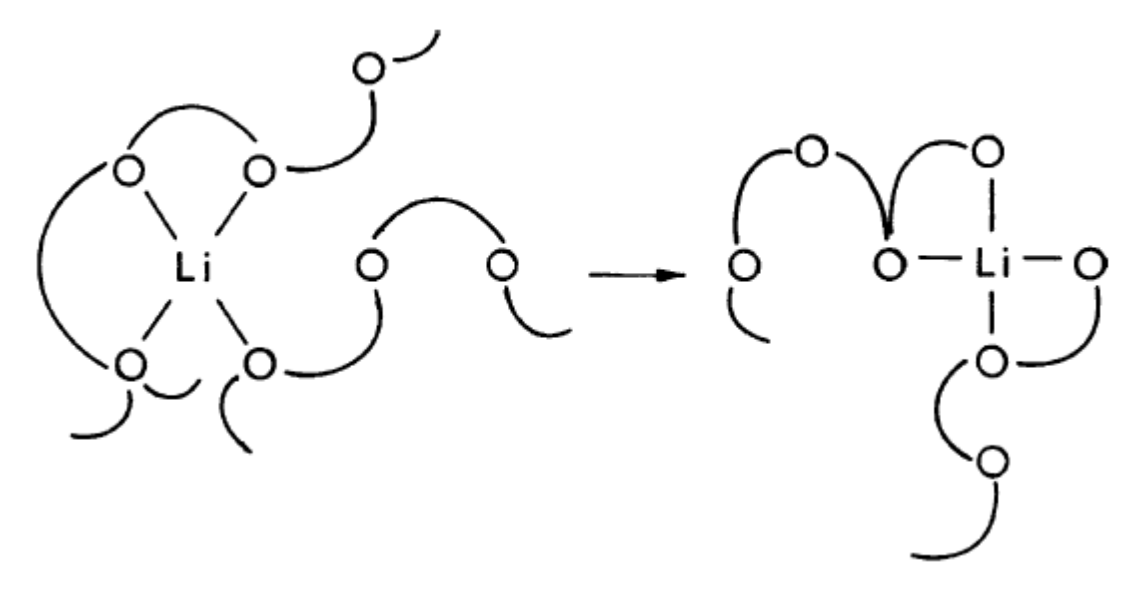
In 1973, Wright et al. explained the possible crystallization of polymers and that this property influence and reduce its ionic conductivity.⁴¹ This finding concludes that for the satisfactory performance of a battery, the operating temperatures should be around 70 °C, i.e., it should be well above the m.p. of the polymeric crystals. This requirement is impractical for portable electronics, though not an issue for many other applications like in electric vehicles. Also, there are problems associated with the complete dissociation of the polymer electrolyte,

since this does not happen most of the times.⁵⁴ The ions exist in aggregated form with reduced movement and hence resulting in low conductivity.

Numerous studies on PEO-based electrolytes concentrated on how to increase their ionic conductivity by controlling their crystallinity. Production of polymer composites using ceramic fillers was found to be an alternative. Though the fillers show good conductivity, their interface with polymer showed huge impedance (e.g., NASICON, LiAlO₂, β -alumina), which challenges this idea. When the polymer melt is cooled down, the crystallization centers turn into poorly developed spherulites. This change improves the amorphous nature of the material and physically increasing the conductivity. Nevertheless, this process also has its flaws. For example, when there is high filler loading, grains may agglomerate and segregate, blocking the smooth movement of ions. 66-69

Different theories are available explaining ionic conductivity in SPEs. One such theory proposed by Bruce et al.⁷² takes into account of atoms possesing lone pairs of electrons (e.g., oxygen, nitrogen) as electron donors of the polymer chains. These atoms coordinate loosely to Li-ion. Therefore, lithium salt no more exists as aggregates but exists in a solvated state. In an amorphous polymer, the ionic conductivity is supported by the local segmental motion of polymeric chains above its Tg.⁷³⁻⁷⁵As a result of the polymeric chains' local dynamics, the free volume is created and destroyed continuously. Thus, lithium-ion moves forward in the polymeric system facilitated by the local chain dynamics (Scheme 1.1).

In crystalline polymer electrolytes, there is yet another mechanism of ionic conductivity provided the vacant sites for ion migration were already present in the structure. In such cases, ion hopping could occur when sufficient energy is available for the hopping. There is no dependence on local chain dynamics in that case. Similar is the case with amorphous electrolytes when there are sufficient voids created within by steric hindrance of bulky groups. These bulky groups prevent efficient packing and create disorders, which will, in turn, enhance ionic conductivity by the hopping mechanism.



Scheme 1.1: Mechanism of lithium ion conductivity by polyether host. ⁷⁶

1.5. Phosphorus based polymers as tunable refractive index materials

1.5.1. Basics of refractive index and why tunability of refractive index is important

The Refractive index (RI) of any material is dimensionless quantity. This parameter describes the extent to which the path of light is bent or refracted upon passing through the material. It is a fundamental physical property used to check the purity of a sample. The equation below explains the basic definition of RI.

$$n = c/v$$

Here, c represents the "speed of light" in vacuum (~3×10⁸ m/s) and v represents the "phase velocity of light" in that particular medium. The RI value of water is 1.333, and it denotes that light travels 1.333 times slower in water than in vacuum. RI is a complex number given by the equation below.

$$n = n + i\kappa$$

Where n is the real part corresponding to the RI and the imaginary part κ is known as "extinction coefficient". While n indicates the "phase velocity", κ corresponds to the "strength of absorption loss" at a particular wavelength. The n and κ components of the complex RI are connected to each other via the Kramers – Kronig relations. In general, if the medium is fully transparent, RI is real and if the medium is absorbing light, the index of refraction is complex. The standard measurements of RI are performed on exposure to the yellow doublet Sodium-D line (wavelength 589.29 nm) and reference medium is air at standardized pressure and temperature.

Many factors which include polarizability, molecular geometry, polymer backbone orientation, and the chain flexibility are crucial in determining the RI of a polymer. Similarly, there are other factors like molar refractivity and molar volume which may influence the RI of the polymer. The "Abbe number" is a measure of the dispersion (variation of RI vs wavelength) of the material, with high values of V_D indicating low dispersion.

$$V_D = \frac{n_D - 1}{n_F - n_C}$$

Where n_D is the wavelength corresponding to sodium D (589.3 nm) line, n_F the wavelength corresponding to hydrogen F (486.1 nm), and n_C is the RI of the material corresponding to wavelength of hydrogen C (656.3 nm) line. Abbe number and RI are inversely related. In general polymers show RI in between 1.30 and 1.70.

A polymer that has an RI greater than 1.50 is referred to as a high-refractive-index polymer (HRIP). Lenses, reflectors, optical waveguides, photonic crystals, antireflection films, light-emitting diode (LED) materials, and holographic recording materials are all made of such high RI optical materials. Fr-84 Several inorganic optical materials are also known with impressive strength, hardness, and rigidity along with a high RI above 2.0. However, they possess several other undesirable features like high densities and low flexibility of processing. On the other hand, organic polymer materials are lightweight and flexible. The major problems associated with these organic polymers is that they possess high optical dispersion, low solubility, large birefringence, and strong absorption in the visible region. The incorporation of groups with high

molar refractions (phosphorus and sulfur atoms, aromatic groups, and halogen atoms) increases the RI of the organic polymers as is clear from the classical Lorentz-Lorenz equation. ⁸⁶ Lorentz-Lorenz equation relates RI to mean polarizability and molar volume. It also helps to estimate RI of the material by adding up the individual molar refraction values contributed by the functional groups and repeating units. ^{86,87}

$$\frac{n^2 - 1}{n^2 + 1} = \frac{4\pi}{3} N\alpha = \sum_{i} (R_{LL})_{i}$$

In the equation, N denotes "number of molecules per unit volume", α denotes "mean polarizability" and R_{LL} denotes "individual molar refraction values". Many compounds were designed following this basic principle such as polythiourethane, ^{88,89} polyphosphazenes, ^{90,91} poly[S-alkylcarbamate], ⁹² epoxypolymers, episulfide-type polymers, ⁹³ poly(thioether sulfone), ⁹⁴ showed RI from 1.60 to 1.76. The elements having high molar refractions are able to increase the RI value of polymers, retaining a high Abbe number. However, using this strategy, it is challenging to improve RI of polymer beyond 1.8. ⁹⁵

The optical properties of hybrid materials may be modified by changing their chemical composition. This tunability helps to produce step-index or graded-index optical waveguide materials having desired reproducible RI. A graded-index optical fibre is characterized by a gradually decreasing RI value with increasing distance from the core. In fact, human eye is the most miraculous example of graded-index optics in nature. On the other hand, step-index optical fibres have separate refractive indices for the core and cladding (usually core with a uniform and higher refractive index and cladding with a low refractive index).

Polymer blends, on the other hand, are a physical mixture of different polymers. ⁹⁶ Blending is very useful for improving the properties of polymeric materials. The properties are determined by the miscibility of polymers in the blend. ⁹⁷These blends are prepared by various techniques; among them, solution blending technique is used frequently in the laboratory-scale synthesis of polymer blends. ⁹⁸

1.5.2. Principles of ellipsometry and why is it unique

Since RI and κ of a thin film sample are difficult to measure directly, the parameters are obtained indirectly from various other measurable quantities like transmittance (T), reflectance (R), or ellipsometric parameters (Ψ and δ), which are dependent on them. Further, a theoretical model is fitted with the experimentally measured parameters R or T, or ψ and δ , and thereby n and κ are construed. Spectroscopic ellipsometry is an optical method used to measure dielectric properties such as a dielectric function or complex refractive index of thin films. It basically analyses the variation in polarization concerning R or T and equates these values to a theoretical model that fits with the experimental data. It provides information about roughness, thickness, electrical conductivity, composition, doping concentration, crystalline nature, and many other properties.

Ellipsometry derives its name from the elliptical polarization of light that is used. Light being a transverse wave can undergo circular, elliptical, or linear polarization. Confinement of the electric or magnetic field vectors to a particular plane along the direction of propagation is known as "linear polarization" or "plane polarization" of electromagnetic radiation. On the other hand, "circularly polarized" light comprises two plane waves equal in amplitude but differ in phase by 90°. The waves with unequal amplitudes constitute the "elliptically polarized" light.

Figure 1.3 illustrated the rudimentary instrumentation set up of an ellipsometer. In this instrument, electromagnetic radiation is emitted from the source is linearly polarized using a polarizer. This polarized light further passes over an optional compensator (consisting of a quarter-wave plate and a retarder) and then made to fall on a sample. The sample reflects the radiation and passes it onto a compensator (optional) and second polarizer. The second polarizer is also known as an analyzer. Finally, electromagnetic radiation reaches the detector.

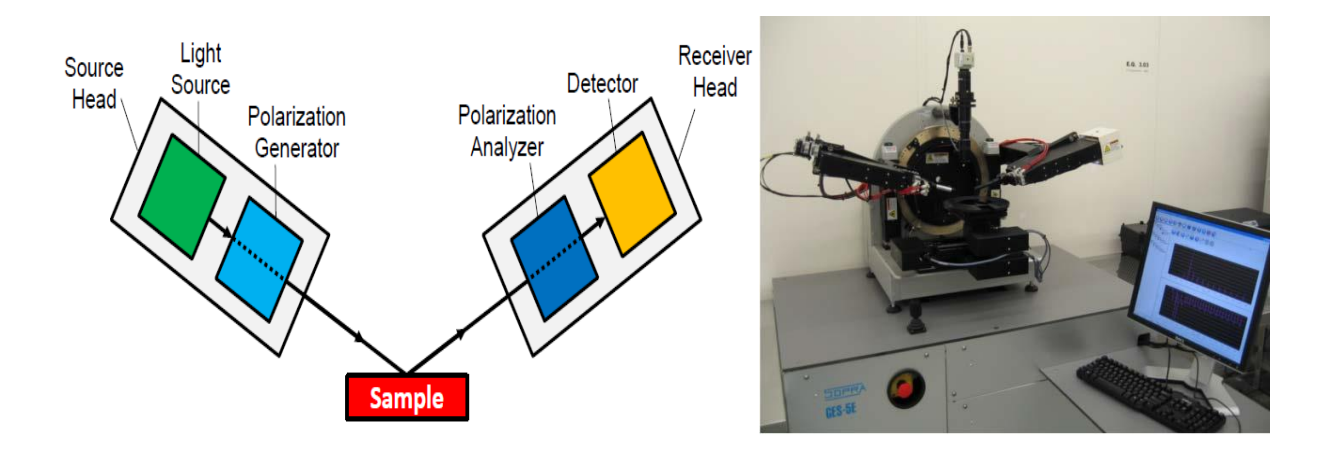
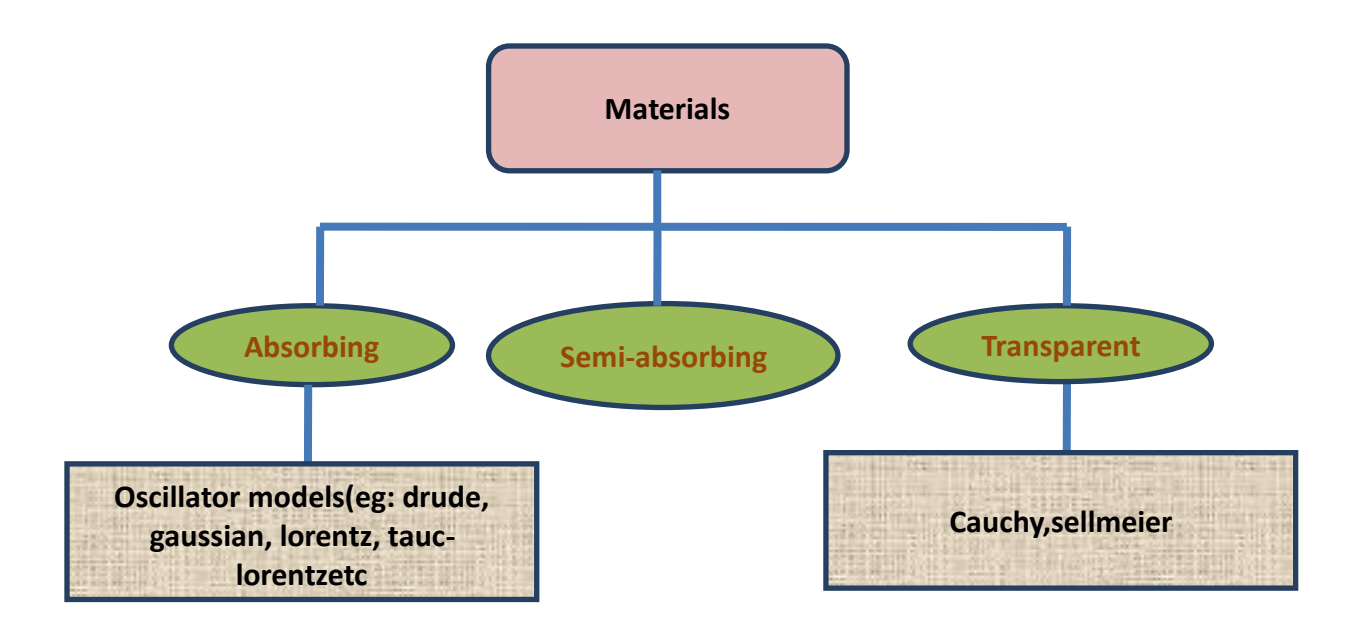


Figure 1.3: Schematic diagram of a spectroscopic ellipsometry measurement (left)⁹⁹ and the original ellipsometer instrument(right)

Ellipsometry experiment is performed mostly, keeping the instrument in the reflection setup. In most models, the sample is considered a combination of different discrete layers that are optically homogeneous. The changes happening in the polarization of the incident light upon interaction with the material is measured by phase difference (Δ) and amplitude ratio (Ψ). The change in polarization depends on the material properties and helps in the contact-free determination of optical constants and thickness of films with high accuracy.

The foremost disadvantage of this technique is that it is an indirect method, and hence a model-based analysis is required to construe the optical constants using the ellipsometric parameters obtained from the instrument. Also, a significant challenge is the direct inversion of Ψ and Δ and is not possible to avoid it unless the samples are homogeneous, isotropic, and infinitely thick films. The fit between experimental and calculated model data is identified in terms of a parameter called Mean Squared Error (MSE). The smaller is the value of MSE, and the better is the fit. This fit is ensured with the help of the Levenberg-Marquardt algorithm..

Thus to start with the material has to be analyzed if it is absorbing, semi-absorbing or transparent (Scheme 1.2). If it is absorbing oscillator models like Drude, Gaussian, Lorentz, Tauc-Lorentz etc. could be used, and for transparent samples, Cauchy or Sellmeier models are generally used. For semi-absorbing materials, combinations of models from either category are used.



Scheme 1.2: A schematic representation of the method of ellipsometric analysis by suitable theoretical model selection.

1.6. Polymer films as membranes for gas separation

Jean Antoine (Abbé) Nollet (in 1748) studied naturally obtained pig bladder as a membrane. The pig bladder was observed to be more permeable to water compared to ethanol. This report was the first semi-permeable membrane. Nowadays, polymer membranes are commonly used for commercial gas separation applications like to separate CO₂ from natural gas, N₂ from the air, and H₂ from the mixtures of hydrocarbons in the petrochemical process. There are two basic parameters, i.e., permeability coefficient (P_A) and selectivity (α A/B), that define the performance of a membrane. 104

Permeability coefficient,
$$P_A = \frac{Gas \ flux \times membrane \ thickness}{pressure \ difference \ across \ membrane}$$

Gas selectivity
$$(\alpha_{A/B}) = \frac{P_A}{P_B}$$

 P_A in the above equation denotes the permeability of the gas which is comparatively more permeable and P_B denotes the permeability of the less permeable gas in the pair of two gases. When a film is more permeable, less area of membrane is sufficient to purify a given amount of any gas, and this reduces the cost required for production considerably. Similarly, when the film is more selective, the products can be obtained with higher purity. Unfortunately, these two properties are mostly in inverse relation for many polymers. With the help of H_2/N_2 separation factors and hydrogen permeability coefficients in the case of many polymers, Robeson quantified the theory shown in figure 1.4. The line indicates an "upper bound" for the permeability and selectivity combinations of known membranes for the mixture of H_2/N_2 gases. The best performance materials are found in the upper right corner of figure 1.4.

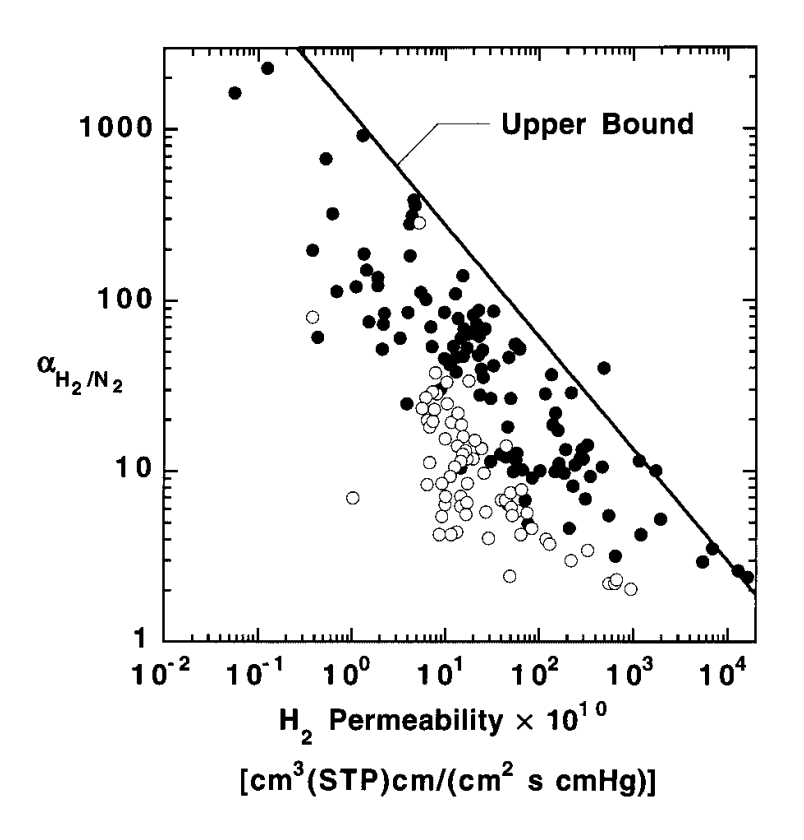


Figure 1.4: Relationship between hydrogen permeability and

 H_2/N_2 selectivity and the empirical upper bound relation (figure taken from ref 109).

A semi-permeable membrane is a thin polymeric film that behaves as a barrier between two phases through which transport of those substances happens differentially. This differential transport can occur as a result of differences in concentration, electrical potential, and pressure across the medium.¹¹¹ Stearic nature and polarity of organic moiety of the polymer chains determine the permeability of a polymeric membrane. Also, the shape and size of bulky groups in the main and side chains of polymers dictate the packing, density, and rigidity.¹¹²

The common gas separation applications¹¹³ involve separation of oxygen and nitrogen for oxygen enrichment and inert gas generation, separation of water from hydrocarbons for natural gas dehydration, separation of water from air for air dehumidification, separation of hydrocarbons from the air for pollution control, separation of helium from hydrocarbons and for helium recovery.

A membrane could be categorized as porous or non-porous membranes (or dense membranes) depending on selectivity and flux density. A porous membrane contains voids constructed by random inter-connected pores. It is very similar to a conventional filter by structure and function. The separation process by porous membrane depends mainly on the permeate character, pore-size, and the molecular size of the polymer membrane. They exhibit high flux but low selectivity values. These membranes are prepared from a polymer solution by solution casting, stretching, track etching, sintering, and phase separation.

Non-porous membranes posses high selectivity, but the flux is usually low. One advantage with non porous membranes is that, if their solubility in the membrane varies considerably, even permeants of similar sizes can be separated. Melt extrusion or solution-casting method is used to produce dense membrane. Polymer membranes are widely used to isolate carbon dioxide from other gases like hydrogen, oxygen, nitrogen and methane, decarbonation of gases, food packaging, and treatment of natural or industrial gases. 113, 114

The structural regularity of polymers favors close packing, enhancing density and rigidity, thereby selective permeability. For instance, polyether sulfones (PES) chains form an ordered structure and hence have better bulk density than polysulfones (PSF) that contain an aliphatic isopropylidene moiety leading to irregular packing arrangement. Owing to the same reason, isotropic PES showed increased selectivity for the gas pairs like H₂/N₂, He/CH₄, O₂/N₂and CO₂/CH₄, compared to cellulose acetate or bisphenol-A polysulphone. In 2001, Fuertes reported that membranes with micropore size 3–5 Å could effectively separate gas molecules whose effective diameters are smaller than 4Å from their mixtures by molecular

sieving.¹¹⁷ These are called Molecular Sieve Carbon Membranes (MSCM) because here, the gas transport depends only on the size of molecules of gas rather than the effects of adsorption.

There are various processes that are widely used in industrial membrane separation of gases. Six important processes are listed below.

- (i) Gas separation.
- (ii) Reverse osmosis
- (iii) Electrodialysis
- (iv) Pervaporation
- (v) Microfiltration
- (vi) Ultrafiltration

Gas separation process is still in its developing stages. Most of the membranes available currently for gas separation are functioning based on the solution-diffusion mechanism.

1.7. Scope of the thesis

Phosphorus-containing polymers and small molecules find diverse applications in our day to day life, and still many left unexplored. The thesis focuses on three diverse applications of organophosphorus polymers, their blends, and composites. The applications include Li-ion conductivity, refractive index tunability, and gas sorption (figure 1.5). All these applications are quite distinct from each other, and the requirements for the same vary drastically.

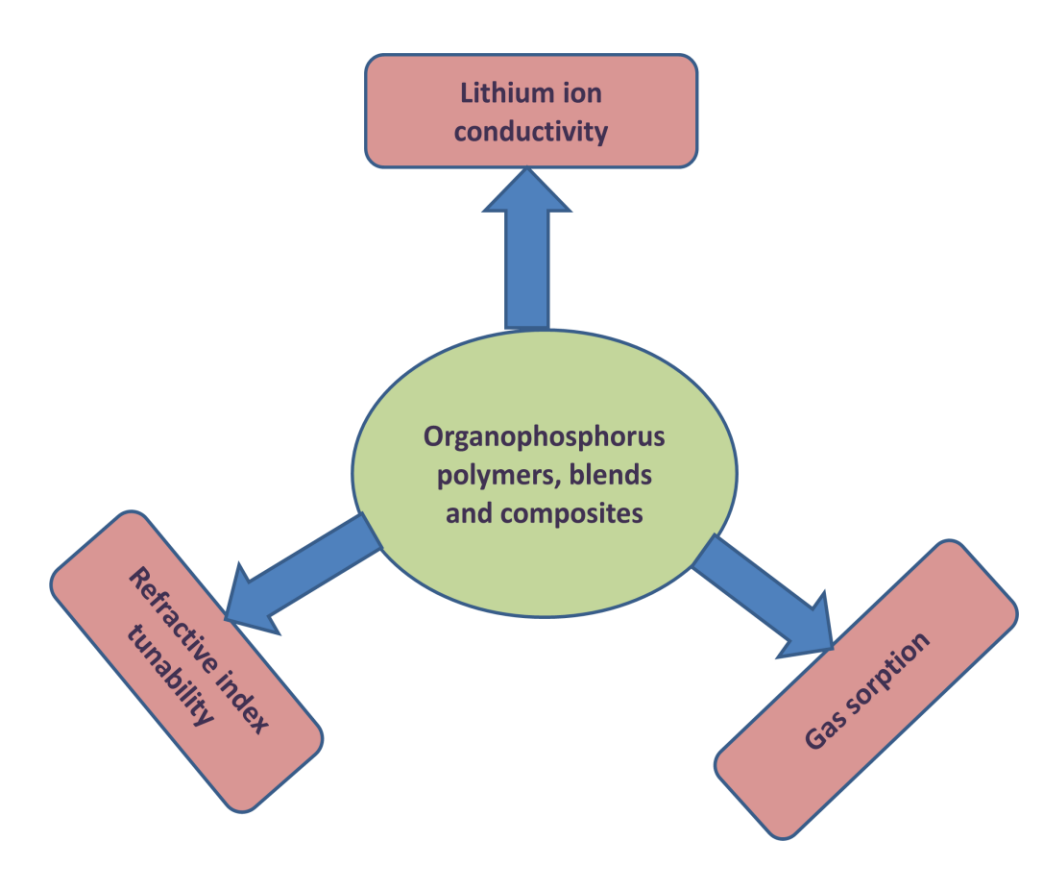


Figure 1.5: Schematic representation of applications of focus in the thesis

Commercial electrolytes used in the Li-ion batteries contains salts of lithium dissolved in some organic solvents, but they inherently possess the risk of leakage and fire hazard. On the other hand, the polymer electrolytes compared to liquid electrolytes, have no leakage of electrolytes, and no combustible products evolve from the reactions at electrode. It also avoids the internal shortage at the electrode surface. 118–123 But the major challenge with these SPEs are their low Li-ion conductivity at room temperature and small values of lithium transference number. Hence, to improve these drawbacks and achieve SPEs that can fulfill practical requirements is still a challenging area of extensive research. In this regard, we have synthesized phosphorus polyethers and met the conductivity of about 10-4 S cm-1 and 10-3 S cm-1 at room temperature and 80 °C, respectively, for most SPEs..

The tunability of the refractive index is as important as the property itself. Often we require graded-index polymer fiber for various applications, for instance, high-speed data communication.¹²⁴ Hence it is crucial to know how we can tune the refractive index of a material for a specific use. There are several ways how we can achieve this. At the molecular level, the

introduction of sulfur, halogen, and phosphorus may increase the refractive index because of polarizability change. At the bulk level, the addition of some inorganic fillers or blending with another polymer may help in altering the refractive index. We have focused on the blending technique and studied how the refractive index changes with an increase in the amount of organophosphorus polymer in the blend. Besides, these blends showed a refractive index tunability from 0.97- 1.57 at 589.3 nm. Still, there are many variants of organophosphorus polymers, and it is required to study systematically how the variations in the percentage ratios of these polymers help in tuning the RI.

The study of gas separation using various kinds of natural and synthetic membranes is a field of intense research interests. 125,126 Differential permeation principle separates the components from their mixtures. So the membrane is crucial, and it is required to tune with several factors like permeability, selectivity, and diffusivity to determine the membrane's efficiency. In this regard, we need to explore more and more membrane materials that can fulfill current requirements. 127 Phytic acid is a bulky molecule with the potential to create sufficient free volume when mixed with a polymer and made a composite, with the polymer being the matrix and phytic acid acting as filler. As a first step towards this, pore size and volume of these composites prepared with different weight ratios were estimated with the help of BET. All the films were mesoporous, and the introduction of PA has increased the pore size and specific surface area of the film compared to pure PVA, though not drastically. Further, the selectivity and permeability of these polymer films have to be studied using different pairs of gases to understand the kind of applications for these polymer films.

1.8. References

- [1] H. Staudinger, Ber. Dtsch. Chem. Ges., 1920, **B53**, 1073-1085.
- [2] W. H. Carothers, J. Am. Chem. Soc., 1929, **51**, 2548-2559.
- [3] L. H. Taboada, M. Guzmann, K. Neubecker, A. Goethlich, PCT Int. Appl., 2008.
- [4] T. Bock, R. Muelhaupt, H. Moehwald, Macromol. Rapid Comm. 2006, 27, 2065.
- [5] J. Parvole, P. Jannasch, *Macromol.*, 2008, **41**, 3893.

- [6] J. Canadell, B. J. Hunt, A. G. Cook, A. Mantecon, V. Cadiz, *Polym. Degrad. Stab.*, 2007, 92, 1482.
- [7] H. Singh, A. K. Jain, J. Appl. Polym. Sci., 2009, 111, 1115.
- [8] T. P. Knepper, *Trends Anal. Chem.*, 2003, **22**, 708.
- [9] E. M. Jon, V. V. Adrabinska, Coord. Chem. Rev., 2005, 249, 2458.
- [10] A. Clearfield, Curr. Opin. Solid State Mater. Sci., 1996, 1, 268.
- [11] M. Essahli, G. Colomines, S. Monge, J. J. Robin, A. Collet, B. Boutevin, *Polymer*, 2008, 49, 4510.
- [12] M. V. Chaubal, A. S. Gupta, S. T. Lopina, D. F. Bruley, *Crit. Rev. Ther. Drug Carrier Syst.* 2003, **20**, 295.
- [13] S. Monge, B. Canniccioni, A. Graillot, and J. J. Robin, *Biomacromolecules*, 2011, **12**, 1973–1982.
- [14] M. Essahli, G. Colomines, S. Monge, J. J. Robin, A. Collet, B. Boutevin, *Polymer*, 2008, **49**, 4510–4518.
- [15] L. H. Taboada, M. Guzmann, K. Neubecker, A. Goethlich, PCT Int. Appl., 2008, 28.
- [16] T. P. Knepper, *Trends Anal. Chem.*, 2003, **22**, 708–724.
- [17] E. M. Jon, V. V. Adrabinska, Coord. Chem. Rev., 2005, 249, 2458–2488.
- [18] J. Canadell, B. J. Hunt, A. G. Cook, A. Mantecon, V. Cadiz, *Polym. Degrad. Stab.*, 2007, **92**, 1482–1490.
- [19] S. Chang, N. D. Sachinvala, P. Sawhney, D. V. Parikh, W. Jarrett, C. Grimm, *Polym. Adv. Technol.*, 2007, **18**, 611–619.
- [20] S. Monge, B. Canniccioni, A. Graillot, and J. J. Robin, *Biomacromolecules*, 2011, **12**, 1973–1982.
- [21] L. Y. Mou, G. Singh, J. W. Nicholson, Chem. Commun., 2000, 345–346.

- [22] B. P. Fu, X. M. Sun, W. X. Qian, Y. Q. Shen, R. R. Chen, M. Hannig, *Biomaterials*, 2005, **26**, 5104–5110.
- [23] B. I. Dahiyat, M. Richards, K. W. Leong, J. Control. Release, 1995, 33, 13.
- [24] M. L. Renier, D. H. Kohn, J. Biomed. Mater. Res., 1997, 34, 95 –104.
- [25] E. Bezdushna, H. Ritter, K. Troev, *Macromol. Rapid Commun.*, 2005, **26**, 471–476.
- [26] I. Gitsov, F. E. Johnson, J. Polym. Sci., Part A: Polym. Chem., 2008, 46, 4130–4139.
- [27] N. Koseva, P. Kurcok, G. Adamus, K. Troev, M. Kowalczuk, *Macromol. Symp.*, 2007, **253**, 24 –32.
- [28] K. Kossev, A. Vassilev, Y. Popova, I. Ivanov, K. Troev, *Polymer*, 2003, 44, 1987–1993.
- [29] L. Bai, R. Y. Chen, Y. Y. Zhu, *Chin. Chem. Lett.*, 2002, **13**, 29 –32.
- [30] R. Tzevi, P. Novakov, K. Troev, D. M. Roundhill, J. Polym. Sci., Part A: Polym. Chem., 1997, 35, 625–630.
- [31] R. Georgieva, R. Tsevi, K. Kossev, R. Kusheva, M. Balgjiska, R. Petrova, V. Tenchova, I. Gitsov, K. Troev, *J. Med. Chem.*, 2002, **45**, 5797–5801.
- [32] S. K. Dordunoo, W. C. Vineek, M. Chaubal, Z. Zhao, R. Lapidus, R. Hoover, W. B. Dang, S. Svenson, Ed. ACS Symposium Series 924, American Chemical Society, Washington DC, 2006.
- [33] X. Y. Xu, H Yu, S. J. Gao, H. Q. Mao, K.W. Leong, S. Wang, *Biomaterials*, 2002, **23**, 3765–3772.
- [34] S. Wang, A. C. A. Wan, X. Y. Xu, S. J. Gao, H. Q. Mao, K. W. Leong, H. Yu, *Biomaterials*, 2001, **22**, 1157–1169.
- [35] A. C. A. Wan, H. Q. Mao, S. Wang, K. W. Leong, L. Ong, H. Yu, *Biomaterials*, 2001, 22, 1147–1156.
- [36] Y. C. Wang, Y. Li, X. Z. Yang, Y. Y. Yuan, L. F. Yan, J. Wang, *Macromolecules*, 2009, **42**, 3026–3032.

- [37] B. Scrosati, J. Garche, J. Power Sources, 2010, **195**, 2419–2430.
- [38] W. V. Schalkwijk, B. Scrosati, Advances in Lithium-ion Batteries, Kluwer Academic/Plenum, Boston, 2004.
- [39] W. H. Meyer, Adv. Mater., 1998, **10**, 439.
- [40] K. Brandt, Solid State Ion., 1994, 69, 173.
- [41] D. E. Fenton, J. M. Parker, P. V. Wright, *Polymer*, 1973, 14, 589.
- [42] M. Armand, M. Duclot, French Patent 7832976, 1978.
- [43] M. Armand, Solid State Ion., 1994, 69, 309-319.
- [44] C. Berthier, W. Gorecki, M. Minier, M. B. Armand, J. M. Chabagno, P. Rigaud, *Solid State Ion.*, 1983, **11**, 91.
- [45] P. G. Bruce, C.A. Vincent, Faraday Discuss. Chem. Soc., 1989, 88, 43.
- [46] S. Takeoka, H. Ohno, E. Tsuchida, *Polym. Adv. Technol.*, 1993, **4**, 53.
- [47] A. M. Stephan, Eur. Polym. J., 2006, 42 (1), 21.
- [48] F. M. Gray, Solid polymer electrolytes-fundamentals and technological applications, VCH, New York, 1991.
- [49] Y. P. M. Liang, B. Wang, Chin. Chem. Lett., 2004, 15 (2), 234.
- [50] P. V. Wright, Br. Polm. J., 1975, **7**(5), 319.
- [51] M. B. Armand, J. M. Chabagno, M. Duclot, In Fast ion Transport in Solids: Electrodes and Electrolytes, (Edited by P. Vashitshta, J. N. Mundy. North Holland Publishers, Amsterdam, 1979).
- [52] V. Chandrasekhar, V. Chandrasekhar, Adv. Polym. Sci., 1998, 135, 139–205.
- [53] J. S. Syzdek, M. B. Armand, P. Falkowski, M. Gizowska, M. Karzowicz, Y. Yukaszuk, M. Y. Marcinek, A. Zalewska, M. Szafran, C. Masquelier, J. M. Tarascon, W. G. Wieczorek, and Z. G. Zukowska, *Chem. Mater.*, 2011, 23, 1785–1797.

- [54] M. Marcinek, A. Zalewska, G. Zukowska, W. Wieczorek, *Solid State Ion.*, 2000, **136-137**, 1175–1179.
- [55] J. M. Tarascon, M. Armand, Nature, 2001, 414, 359–367.
- [56] F. Croce, S. Sacchetti, B. Scrosati, J. Power Sources, 2006, 162, 685–689.
- [57] Z. Florjanczyk, M. Marcinek, W. Wieczorek, N. Langwald, Pol. J. Chem., 2004, 78, 1279– 1304.
- [58] J. B. Goodenough, H. Y. Hong, J. A. Kafalas, *Mater. Res. Bull.*, 1976, **11**, 203–220.
- [59] F. Gray, M. Armand, Handb. Battery Mater. 1999, 499–523.
- [60] L. Sebastian, J. Gopalakrishnan, J. Mater. Chem., 2003, 13, 433–441.
- [61] J. A. Kafalas, H. Y. Hong, P. Proc. Power Sources Symp, 1978, 1-2.
- [62] A. Hooper, J. Phys. D: Appl. Phys., 1977, 10, 1487–1496.
- [63] J. Plocharski, W. Wieczorek, Solid State Ion., 1988, 28-30, 979–982.
- [64] W. Wieczorek, K. Such, H. Wycislik, J. Plocharski, Solid State Ion., 1989, 36, 255–257.
- [65] I. Villarreal, E. Morales, J. L. Acosta, *Angew. Makromol. Chem.*, 1999, **266**, 24–29.
- [66] J. Przyluski, W. Wieczorek, *Solid State Ion.*, 1989, **36**, 165–169.
- [67] W. Wieczorek, K. Such, S. H. Chung, J. R. Stevens, J. Phys. Chem., 1994, 98, 9047–9055.
- [68] B. Kumar, L. G. Scanlon, *J. Electroceram.*, 2000, **5**, 127–139.
- [69] P. Johansson, M. A. Ratner, D. F. Shriver, J. Phys. Chem. B, 2001, 105, 9016–9021.
- [70] S. Iliescu, L. Zubizarreta, N. Plesu, L. Macarie, A. Popa and G. Ilia, *Chem. Cent. J.*, 2012, 6, 132.
- [71] M. Marcinek, J. Syzdek, M. Marczewski, M. Piszcz, L. Niedzicki, M. Kalita, A. Plewa-Marczewska, A. Bitner, P. Wieczorek, T. Trzeciak, M. Kasprzyk, P. Łężak, Z. Zukowska, A. Zalewska, W. Wieczorek, *Solid State Ion.*, 2015, **276**, 107–126.

- [72] Z. Stoeva, I. M. Litas, E. Staunton, Y. G. Andreev and P. G. Bruce, *J. Am. Chem. Soc.*, 2003, **125**, 4619-4626.
- [73] C. Berthier, W. Gorecki, M. Minier, M. B. Armand, J. M. Chabagno, and P. Rigaud, *Solid State Ion.*, 1983, **11**, 91-95.
- [74] W. Gorecki, P. Donoso, C. Berthier, M. Mali, J. Roos, D. Brinkmann, and M. B. Armand, *Solid State Ion.*, 1988, **28-30**, 1018.
- [75] M. C. Wintersgill, J. J. Fontanella, Y. S. Pak, S. G. Greenbaum, A. Almudaris, A. V. Chadwick, *Polymer*, 1989, **30**, 1123.
- [76] P. G. Bruce, *Electrochim. Acta*, 1995, **40**, 2077.
- [77] P. Declerck, R. Houbertz, G. Jakopic, S. Passinger, B. Chichkov, *Mater. Res. Soc. Symp. Proc.*, 2008, **1007**, 15.
- [78] T. Flaim, Y. Wang, R. Mercado. *Proc SPIE* 2004, **5250**, 423.
- [79] L. Criante, R. Castagna, F. Vita, D. E. Lucchetta, F. Simoni, *J. Opt. A Pure Appl. Op.*, 2009, **11**, 024011. 1.
- [80] L. Liang, Y. Xu, L. Zhang, D. Wu, Y. Sun, J. Solgel Sci. Technol., 2008, 47, 173.
- [81] D. W. Mosley, K. Auld, D. Conner, J. Gregory, X. Q. Liu, A. Pedicini, *Proc SPIE*, 2008, 691017. 1-8.
- [82] V. Janicki, S. Wilbrandt, O. Stenzel, D. Gäbler, N. Kaiser, A, Tikhonravov, *J. Opt. A Pure Appl. Op.*, 2005, **7**, L9-12.
- [83] L. A. Hornak. Polymers for Lightwave and Integrated Optics: Technology and Applications, Marcel Dekker, New York, 1992.
- [84] W. F. Ho, M.A. Uddin, H.P. Chan, *Polym. Degrad. Stab.*, 2009, **94**, 158.
- [85] Y. Cheng, C. Lü and B. Yang, Recent Patents on Materials Science, 2011, 4, 15.
- [86] C. J. Yang, S. A. Jenekhe, *Chem. Mater.*, 1995, **7**, 1276.
- [87] D. W. VanKrevelen, Properties of Polymers, Elsevier, Amsterdam, 3rd edn, 1990.

- [88] O. Reisuke, O. Tsuyoshi and K. Masahisa, Eur. Pat. 530757, 1993.
- [89] T. Okubo, S. Kohmoto and M. Yamamoto, J. Appl. Polym. Sci., 1998, 68, 1791.
- [90] M. A. Olshavsky and H. R. Allcock, *Macromolecules*, 1995, 28, 6188.
- [91] M. A. Olshavsky and H. R. Allcock, *Macromolecules*, 1997, **30**, 4179.
- [92] T.Okubo, S. Kohmoto, M. J. Yamamoto, *Mater. Sci.*, 1999, **34**, 337.
- [93] Z. Cui, C. Lü, B. Yang, J. Shen, X. Su and H. Yang, *Polymer*, 2001, **42**, 10095.
- [94] C. Lü, Z. Cui, Y. Wang, B. Yang, J. Shen, J. Appl. Polym. Sci., 2003, 89, 2426.
- [95] R. Okutsu, Y. Suzuki, S. Ando, M. Ueda, *Macromolecules*, 2008, **41**, 6165.
- [96] C. Lu and B. Yang, J. Mater. Chem., 2009, 19, 2884-2901.
- [97] N. Rajeswari, S. Selvasekarapandian, S. Karthikeyan, C. Sanjeeviraja, Y. Iwai, J. Kawamura, *Ionics*, 2013, **19**, 1105.
- [98] E. M. Abdelrazek, I. S. Elashwami, A. E. Khodary, A. Yassin, *Curr. App. Phys.*, 2010, **10**, 607.
- [99] B. S. Mudigoudra, S. P. Masti, R. B. Chougale, Res. J. Recent Sci., 2012, 1 (9), 8386.
- [100] N. Hong, 1A: Introduction to WVASE Data Analysis, J. A. Woollam Co. Lincoln, 2012.
- [101] E. A. Mason, J. Membr. Sci., 1991, **60**, 125.
- [102] K. W. Böddeker, J. Membr. Sci., 1995, 100, 65.
- [103] J. A. Nollet, J. Membr. Sci., 1995, **100**, 1.
- [104] J. M. S. Henis, Commercial and Practical Aspects of Gas Separation Membranes, CRC Press Boca Raton, FL, 1994.
- [105] B. D. Freeman, *Macromolecules*, 1999, **32**,375-380.
- [106] Y. Seo, S. Kim, S. U. Hong, *Polymer*, 2006, 47, 4501–4504.
- [107] S. A. Stern, J. Membr. Sci., 1994, **94**, 1–65.

- [108] Y. Seo, S. Hong, B. S. Lee, Angew. Chem, Int. Ed., 2003, 42, 1145.
- [109] L. Robeson, J. Membr. Sci., 1991, **62**, 165.
- [110] L. M. Robeson, W. F. Borgoyne, M. Langsam, A. C. Savoca, C. F. Tien, *Polymer*, 1994, 35, 4970.
- [111] W. J. Koros, Y. H. Ma, T. J. Shimidzy, J. Membr. Sci., 1996, 120 (2), i.
- [112] P. Pandey, R. S. Chauhan, *Prog. Polym. Sci.*, 2001, **26** (6), 853.
- [113] R. Abedini, A. Nezhadmoghadam, *Petroleum & Coal*, 2010, **52**(2), 69-80.
- [114] P. Gramain, J. Sanchez, French Patent. WO 022245, March, 2002.
- [115] J. Zimmerman, Polyamide in Encyclopedia of Polymer Science and Technology, John Wiley and Sons, New York, 1984.
- [116] D. L. Ellig, F. P. Althouse, C. McCandless, J. Membr. Sci., 1980, 6, 259.
- [117] A. B. Fuertes, Carbon, 2001, **39**, 697-706.
- [118] A. F. Ismail, N. Ridzuan, and S. A. Rahman Songklanakarin, J. Sci. Technol., 2002, 24, 1025.
- [119] F. M. Gray, Solid polymer electrolytes–fundamentals and technological applications, VCH, New York, 1991.
- [120] B. Scrosati, Applications of electroactive polymers, Chapman Hall, London, 1993.
- [121] F. M. Gray, Polymer electrolytes, RSC materials monographs, The Royal Society of Chemistry, Cambridge, 1997.
- [122] J. R. MacCallum, C. A. Vincent, Polymer electrolytes reviews—I., Elsevier, London, 1987.
- [123] J. R. MacCallum, C.A. Vincent, Polymer electrolytes reviews—II., Elsevier, London, 1987.
- [124] I. Takaaki, N. Eisuke, and Y. Koike, Applied optics, 1994, 33(19), 4261.
- [125] R.W. Rousseau, Handbook of separation process technology, Wiley, New York, 1987.

[126] S. P. N. Nunes, K. V. Peinemann, Membrane Technology in the chemical industry, Wiley-VCH Weinheim, Singapore, 2001.

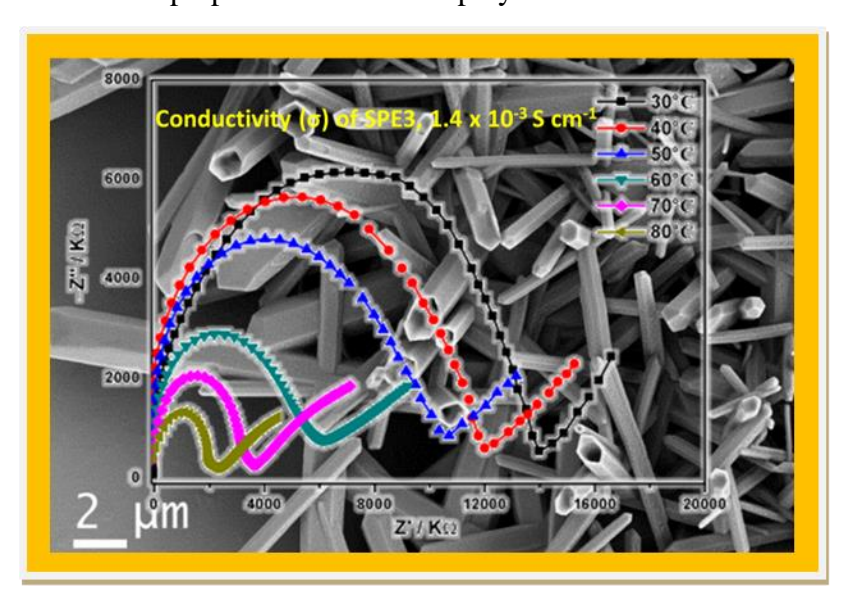
[127] S. A. Stern, J. Membr. Sci., 1994, 94, 1.

Chapter 2

Catechol based polyphosphates with tunable microstructure-assisted Li-ion conductivity as solid polymer electrolytes

Abstract:

This chapter describes the synthesis, characterization, and Li-ion conductivity of catechol based copolymer of polyphosphates (**P1-P4**) for solid polymer electrolyte (SPE) applications in Li-ion batteries. The synthesized polymers are thermally stable with high molecular weight, porous nature, and had rod-like morphology. The Li-ion conductivity of one of the SPEs produced using P3 with 20 wt% of LiTFSI was 1.4×10^{-3} S cm⁻¹ at 80°C, while P1 having 40 wt% of LiTFSI showed the conductivity of 1.2×10^{-3} S cm⁻¹ at 80 °C. Remaining all polymers (**P1- P4**) showed good conductivity at RT (~10⁻⁴ S cm⁻¹). The results demonstrate the highest Li-ion conductivities among those reported in the literature so far at 80°C. The high conductivity achieved is attributed to the microstructure of polymer molecules dictated by the bulky and rigid groups as the comonomer, which created the perpetual-voids in the polymer matrices.



2.1. Introduction

Li-ion batteries (LIBs) are used extensively in electric vehicles, energy storage solutions at grid level, home electronics, and military and aerospace applications. Such applications require high energy density and low self-discharge. Intense efforts have been there towards developing novel materials for LIBs that are economical and safe. Electrolyte plays a crucial role in a LIB since it facilitates the movement of the Li-ions between the cathode and the anode while the electrons move through the wire. The commercial LIBs use a solution of lithium hexafluorophosphate dissolved in a mixture of ethylene carbonate, ethyl methyl carbonate or dimethyl carbonate as the electrolyte. However, in large batteries used in automotive and stationary applications, the increase in temperature of batteries results in inflammability of organic solvents and instability of LiPF₆ due to its reaction with traces of protic species in the electrolyte.

Solid electrolytes surpass the conventional liquid electrolytes in terms of electronic properties such as substantial electrochemical stability, wide operating temperature range, feasible battery-package formation, and safety. 1, 4, 5 There are two classes of solid phase electrolytes for Li-ion batteries, viz. inorganic compound based electrolytes and organic polymer-based electrolytes. The solid electrolytes based on inorganic compounds are single-ion conductors, and that reduces most of the adverse side reactions and decomposition of the electrolytes. However, the operation of inorganic solid electrolytes under a high current density is delicate because the Li-ion transfer is slower than that of typical organic solvent-based electrolytes. Alternatively, organic polymer electrolytes, comprising a polymer matrix and an appropriate amount of lithium salts, form a solid-electrolyte interface and thereby restrict decomposition or other side reactions. Further, the properties such as flexibility, easy manipulation, and high-temperature use of polymer electrolytes give promises for advanced Liion secondary batteries. Solid electrolytes with a thin polymer membrane is much desirable.

Linear polyethylene oxide (PEO) added with lithium salts was the first investigated SPE. ¹¹Many other variations studied are; the attachment of oxymethylene groups in the chains of PEO, ^{12, 13}cross-linking of PEO, ¹⁶use of block copolymers, ¹⁴ and comb-branch polymers, ¹⁵ and addition of nanoparticles. ^{17,18}Polyether are generally attractive molecules as SPEs because of the presence of more numbers of oxygen atoms with lone-pair electrons in their structure and their relatively strong Lewis basicity. This structural feature results in their enhanced ability to

dissociate alkali metal salts by solvation to cations. Consequently, the polyether-based electrolytes show remarkable ionic conductivity but negligible electronic conductivity. 19 23 Despite the long known investigation, the Li-ion conductivity the polymer-lithium salts based electrolytes remain still too low $10 (< 10^{-4} \text{ S cm}^{-1})$.

Improving the safety of LIBs in terms of fire hazards is a significant challenge, especially for large battery applications in electric vehicles. Introducing the flame-retardant property to the batteries is a crucial design strategy in need to avoid thermal-runaway that may result in fire or explosion while the temperature increases in batteries. By adding flame retardant molecules, flammability of the electrolytes in LIBs can be reduced or even suppressed. For this reason, phosphorus (V) compounds are studied widely as additives in LIBs. To improve the safety of LIBs, a rather high wt% of additive is required. However, a high concentration of additives leads to increased viscosity, and a decreased ionic conductivity of the electrolyte, also result in poor anodic stability. The present strategy to realize flame-retardant property for the solid polymer electrolytes (SPE) is incorporating phosphorus-containing molecules as a repeating unit to the polymer chain. Is, 27, 28 The catechol based units have recently emerged as powerful building blocks for the preparation of a broad range of polymeric materials for critical applications like drug delivery 30 and degradable adhesives. The recent review endorsed that catechol based polymers are promising to offer more for the production of "next-generation" safe, economical, and sustainable energy storage devices. Sa

In this present work, we have described the design and study of the Li-ion conductivity of four different phosphorus-containing catechol based polymer electrolytes to find advanced functional materials for Li-ion batteries. The synthesized polymers (P1-P4) exhibited considerable thermal stability conductivity, and the electrolytes showed excellent Li-ion conductivity (~10⁻⁴ S cm⁻¹) at room temperature. Further, two SPEs reported here attained the conductivity value up to 10⁻³ S cm⁻¹ at 80°C, and this enhanced Li-ion conductivity can be attributed primarily to the porous morphology of these polymers. The presence of phosphorus in the main chain of electrolytes would give flame retardant property to the battery.

2.2. Results and discussion

2.2.1. Synthesis and characterization of polymers

The safety issues of lithium batteries are closely related to the type of electrolytes used in it. Besides safety considerations, the conductivity of Li-ions in electrolytes, which depends on the type of electrolytes, needs to be improved. To address these issues, thermally stable phosphorus-containing polymers in the form of solid polymer electrolytes (SPEs) are promising materials. To incorporate phosphorus atoms in polymers, researchers exerted several monomers based on organophosphorus compounds. However, the current interest is making polyphosphates with rigid and bulky groups for example aromatic diols. Herein, we have synthesized four polyphosphates (P1-P4) simple reactions of phosphoryl chloride with four different aromatic diols separately (Scheme 2.1). Considering on the functional groups of co-monomers, the condensation polymerization method was favored to produce the copolymers. These reactions proceeded in the presence of triethylamine as HCl scavenger.

HO OH
$$CI_{CI}^{O}$$
 CI_{CI}^{O} $CI_{CI}^$

Scheme 2.1: Schematic representation of syntheses of polyphosphates **P1-P4**.

All four polyphosphates were solids at room temperature and were soluble in dimethyl sulfoxide, dimethylformamide, and dimethylacetamide. The structure of polymers was characterized thoroughly by NMR and IR spectral data. The polymers, **P1-P4** showed a single peak in $^{31}P(^{1}H)$ NMR spectra in the region δ 81.4-83.2 ppm. The presence of the second repeating unit of comonomers was identified from the peak at the aromatic region in ^{1}H NMR spectra. The IR bands (Figure 2.1) at 3150 cm $^{-1}$ and 1489 cm $^{-1}$ and 850 cm $^{-1}$ suggested the presence of an aromatic ring in the polymers. The band at 1238 cm $^{-1}$ was owing to the symmetric and asymmetric stretching modes of the phosphodiester groups. The absorption at 1095 cm $^{-1}$ was ascribed to the P-O group. The molecular weights of various polymers (both Mw and Mn) and their PDI values are listed in Table 2.1 given below. The molecular weights of **P1**, **P2**, and **P3** were more or less similar, while **P4** was obtained with the highest Mn and Mw among all four polymers. Similarly, PDI of **P4** was 1.64 showing the better distribution of polymers of similar chain lengths compared with other polymers.

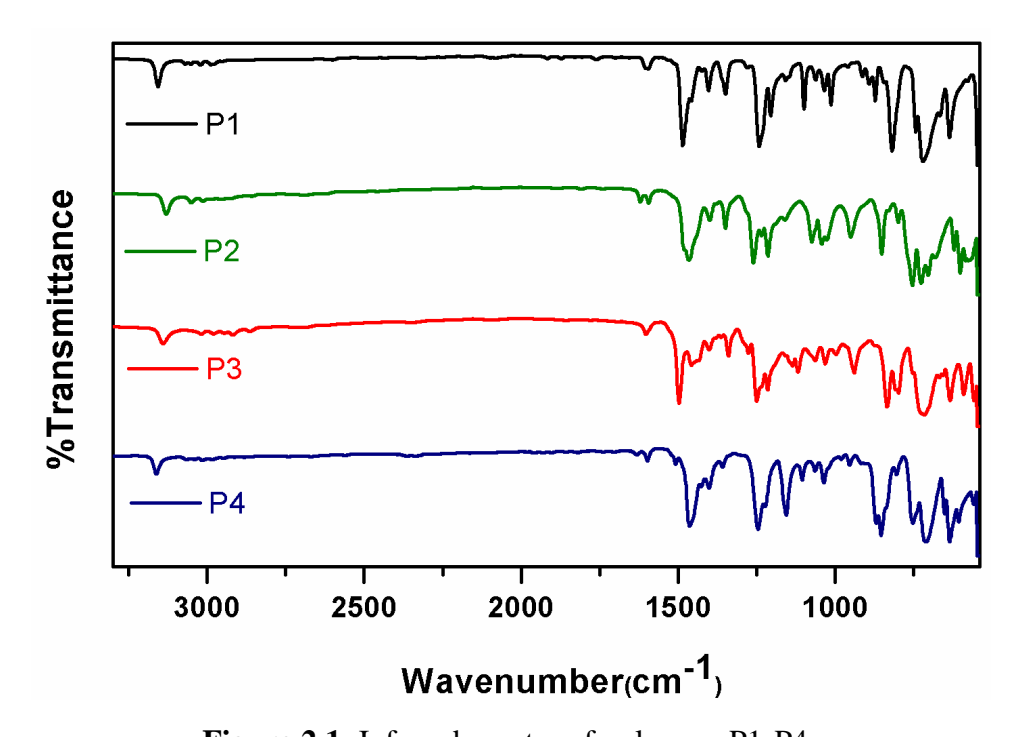


Figure 2.1: Infrared spectra of polymers P1-P4.

Table 2.1. Molecular weights of polymers P1-P4

S. No.	Polymer	Mn	Mw		
		(g mol ⁻¹)	(g mol ⁻¹)	PDI	

1	P1	113835	203564	1.78
2	P2	154068	280795	1.82
3	Р3	149055	261298	1.75
4	P4	221726	363675	1.64

2.2.2. Microstructure of polymers P1-P4

Mechanical, thermal, and conducting properties of polymers depend to a large degree on molecular orientation and chemical constitution. The presence of heteroatom like phosphorus instead of typical carbon-carbon bonds in the chain of organic polymer would introduce intrinsic deformation in the packing of chains due to the difference in the size of atoms. Further, the fifth valence of phosphorus would provide the opportunity of introducing an additional pendant group to the repeating unit and thus decide the microstructure of polymers. Variation in the structural orientation of repeating units of polymer molecules directed by the difference in the hybridization of phosphorus and carbon atoms could provide a disordered framework in the polymer matrix. All these modifications would afford interesting chemical and physical properties to the polymers such as the stability at high temperatures, flame-retardant property, and amorphous nature. $^{20, 25, 26}$ In the same way, due to the presence of atoms of dissimilar sizes in the chains of inorganic polymers polyphosphazenes and polysiloxanes exhibited Li-ion conductivities of 4.5×10^{-4} S cm⁻¹ and 5.0×10^{-5} S cm⁻¹ respectively. 20

The focus of this work is to tune the microstructure of the polymer molecules by introducing bulky and rigid groups and enlarging the amorphous region, and then study the Tg, crystallinity, and Li-ion conductivity of the polyphosphates. Perhaps, the asymmetrical sizes and shapes of these bulky groups expected to enlarge the amorphous region and introduce intrinsic porosity. The energy minimized structure of polymer P3 is shown in Figure 2.2(a) to visualize the microstructure of the polymer chain. The structure consisted of 6 polymer chains of 20 repeat units each and was constructed using the MM2 force field by Chem3D software. The figure visualizes the possibility of perpetual voids in the microstructure of polymer through which lithium ions can move ease. Figure 2.2(b) depicts slack chain packing caused by the molecular structure of chains that can create voids in the superstructure of the polymers matrix. The

aromatic rings would prevent the close packing of polymeric chains and create voids within the system, which ultimately will enhance ionic conductivity.

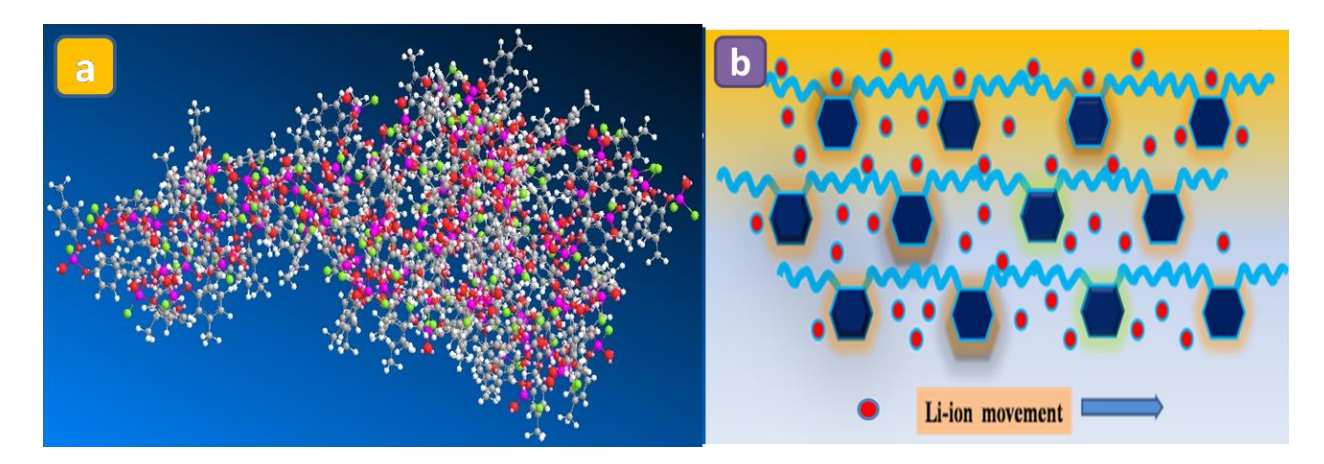


Figure 2.2: (a) The energy minimized structure of P3 obtained using MM2 force field by Chem3D software (b) A schematic illustration of structural framework of polymer matrices that can support the movement of Li-ions through solid polymer electrolytes

Cooperative self-organization of macromolecules is known to influence the structure and application of materials.³⁴ Self-assembling polymers tend to form large aggregates such as spherical, cylindrical, or tubular-shaped macro assemblies as a consequence of specific, intermolecular interactions among themselves. These assemblies may, in turn, effectively behave as huge polymers. The strategy of self-assembly was used to fabricate free-standing, flexible nanocomposite films, and electrodes by mixing with conducting species. Thus the investigation of FESEM images of P1-P4 (Figure 2.3) showed interesting self-aggregation of polymer molecules and the formation of stable and ordered architecture. This aggregation resulted in the formation of hollow tubular morphology for P1, P2, and P3. However, the molecules of P4 formed human-backbone like morphology, probably because of the bulky nature of the catechol unit. The possibility of hydrogen bonding interaction in the repeating units facilitated the self-assembly of polymer chains, while the bulky nature of the repeating units construct the superstructure. These shreds of evidence supported the conceived model of formation of the endless void, which is expected to facilitate the Li-ion conductivity.

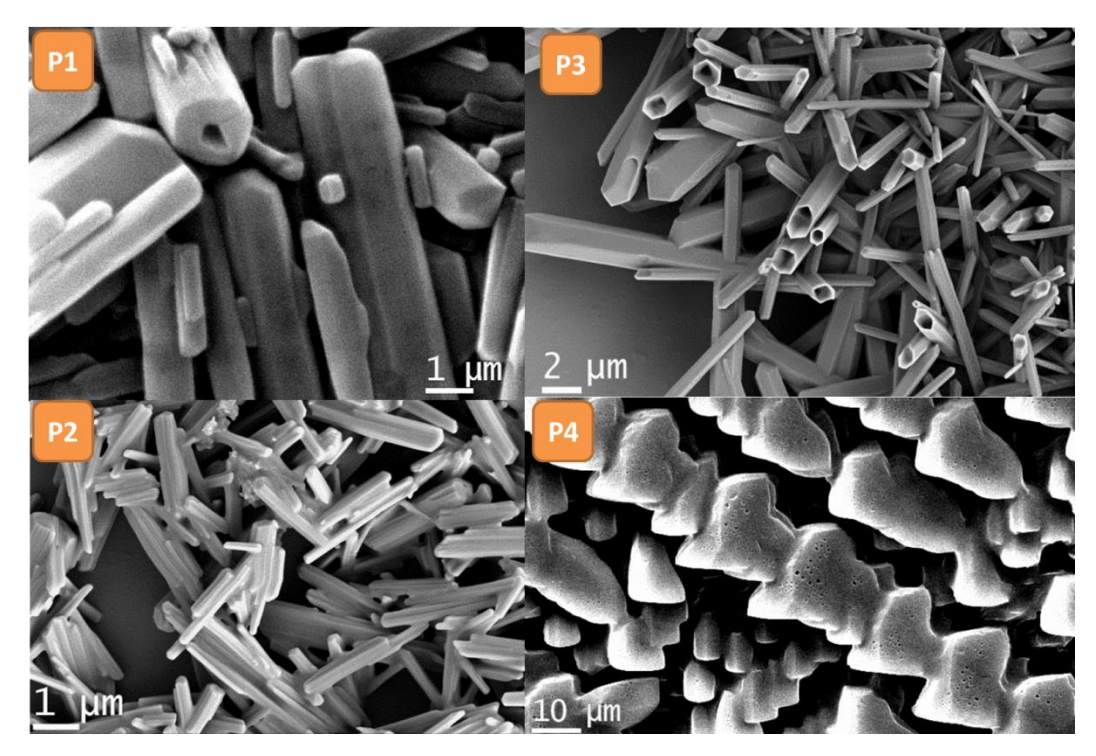


Figure 2.3: FESEM images of polymers P1-P4.

2.2.3. Thermal properties of P1-P4

As mentioned earlier, the thermal stability is one of the crucial parameters of a polymer to be considered for solid polymer electrolytes. Contemporary density functional theory (DFT) based ab initio calculation revealed the significant charge separation in the P-C and P-O bonds ascribing to arise in their bond dissociation energies. This observation explains the increased stability of the polymer with P-C and P-O bonds in the primary polymer chain. Many phosphorus-containing polymers are reported to be thermally stable at higher temperatures authenticating the thermal stability of such hybrid polymers. Thus, the thermogravimetric analyses showed that the polymers P1-P3 were stable up to 200°C, while polymer P4 was stable until 270°C (Figure 2.4(a)). This observation correlates with the high molecular weight observed for P4. Further, the presence of two phenyl rings in the structure could also cause enhanced thermal stability to P4 compared to other polymers. The methyl group in P2 and P3 accounts for the early decomposition of those polymers, and the columnar stacking of phenyl groups in P1 and P4 renders them extra stability.

The glass transition temperature (Tg) dictates the working range of polymer for various applications. The Tg value of P1 is around 298 °C, P2, and P3, around 212 and 252 °C, and that

of P4 around 343°C (Figure 2.4(b)). DSC thermogram (Figure 2.4(d)) showed that all SPEs have considerably low Tg compared with their polymer counterparts. This observation means that the addition of Li salt decreased crystallinity. This change, in turn, makes it more amorphous and increased the flexibility of the chain of polymer.³⁶ Within the SPEs of the same polyphosphate, the Tg was increasing with increasing Li-ion content. For instance, Tg of SPE3 increased from 38°C to 63°C as the Li-ion percentage increased from 10 to 40%.

Table 2.2. Thermal stability analysis of polymers P1-P4 and SPEs

Polymer	Td	Tg	SPE	Td	Tg
P1	388	298	SPE3(10%)	50	38
P2	324	212	SPE3(20%)	65	48
Р3	328	252	SPE3(30%)	67	47
P4	395	343	SPE3(40%)	84	63

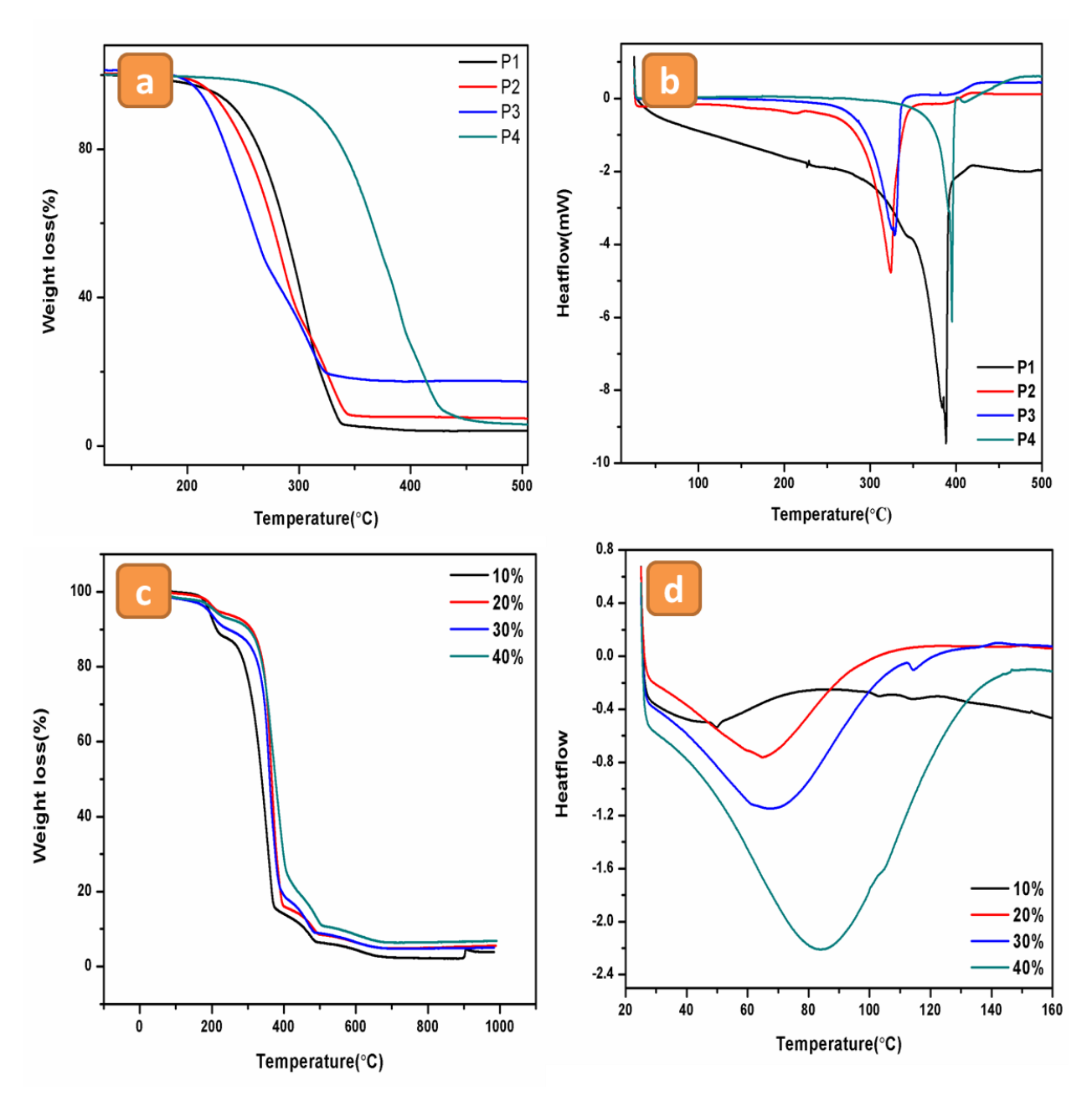


Figure 2.4: TGA and DSC plots of polyethers P1-P4 (a and b), SPE3 (c and d).

2.2.5. Conductivity studies

The polyphosphates (P1-P4) were blended with lithium bis(trifluoromethane sulfonyl)imide (LiTFSI) in weight proportions of 10%, 20%, 30%, and 40% to produce series of solid polymer electrolytes, SPE1-SPE4 respectively. The Li-ion conductivities of SPEs were determined using SS|electrolyte|SS cell configuration at various temperatures. The pure polyphosphates alone showed the Li-ion conductivities of about 10⁻¹¹ S cm⁻¹ to 10⁻¹² S cm⁻¹, demonstrating the absence

of protonic or electronic conductance. The bulk resistances followed by the conductivities were calculated from complex impedance spectra of polymers and their series of SPE1, SPE2, SPE3, and SPE4. The Li-ion conductivities of SPEs determined at 30°C, as well as at 80°C, are presented in Table 2.3.

SPEs presented very high Li-conductivities compared to their polymers. Figures 2.5 to 2.8 display the temperature-dependent Nyquist plots of the solid polymer electrolytes SPE1-SPE4 (10%-40% Li salt) covering the temperature range of 30-80 °C with an increment of 10 °C. Nyquist plots obtained as a clear semicircle attributed total observed conductivity to Li-ions only; the plots could have been complicated if some other contaminants were added to the conductivity measured. Among all combinations studied, the SPE3 (20%) exhibited the best conductivity of 4.1× 10⁻⁴S cm⁻¹at room temperature and 1.4× 10⁻³S cm⁻¹at 80°C. Figure 2.9 represents the Arrhenius plots for conductivities of SPE1 to SPE4 (10% - 40%). A general trend of increasing conductivity upon increasing temperature is observed in all the polymers.

Table 2.3. Li-ion conductivities of SPE1- SPE4 (10% - 40%) at various temperature

	Conductivity (σ) of SPEs (S cm ⁻¹)							
SPEs	SPE1		SPE2		SPE3		SPE4	
(wt% of LiTFSI)	30 °C	80°C	30 °C	80°C	30 °C	80°C	30 °C	80°C
(10%)	1.9× 10 ⁻⁶	6.6× 10 ⁻⁶	2.2×10^{-5}	4.6× 10 ⁻⁵	2.8×10^{-5}	1.7× 10 ⁻⁴	9.8× 10 ⁻⁶	1.9× 10 ⁻⁵
(20%)	1.2× 10 ⁻⁵	1.4×10 ⁻⁴	5.8× 10 ⁻⁵	4.8×10^{-4}	4.1×10^{-4}	1.4×10^{-3}	6.0× 10 ⁻⁵	9.6× 10 ⁻⁶
(30%)	1.7×10^{-4}	4.7×10^{-4}	8.1× 10 ⁻⁵	1.2×10^{-4}	5.5×10^{-5}	2.5×10^{-4}	2.8×10^{-5}	3.1×10^{-5}
(40%)	4.9× 10 ⁻⁴	1.2×10^{-3}	8.1× 10 ⁻⁵	4.3× 10 ⁻⁴	3.9× 10 ⁻⁴	1.0×10^{-3}	7.2× 10 ⁻⁵	9.2× 10 ⁻⁴

The local segmental motion of the chains in amorphous polymers facilitates the Li-ionic conductivity at a temperature beyond their Tg value. The polymer chains are quite flexible at temperatures above Tg, and in this stage, the chains are in constant motion. This segmental motion of chains will create voids that simultaneously change its position as the ion gradually moves its way along.³⁷ However, the conductivity of polymers P1-P4 at temperatures below their Tg can be explained using intrinsic disorder in the microstructure of polymers. The stearic

hindrance introduced by the bulky groups like benzyl or naphthyl will possibly avoid close contact between the polymer chains and thereby maintaining the essential criteria for ion movement intact. Also, the rotational motion is hindered considerably. Altogether, these factors resulted in more significant disordered packing of chains and created channels for Li-ion mobility. To the best of our understanding, the SPE3 produced in this work exhibited the highest conductivity achieved for any solid polymer electrolytes reported in the literature so far.

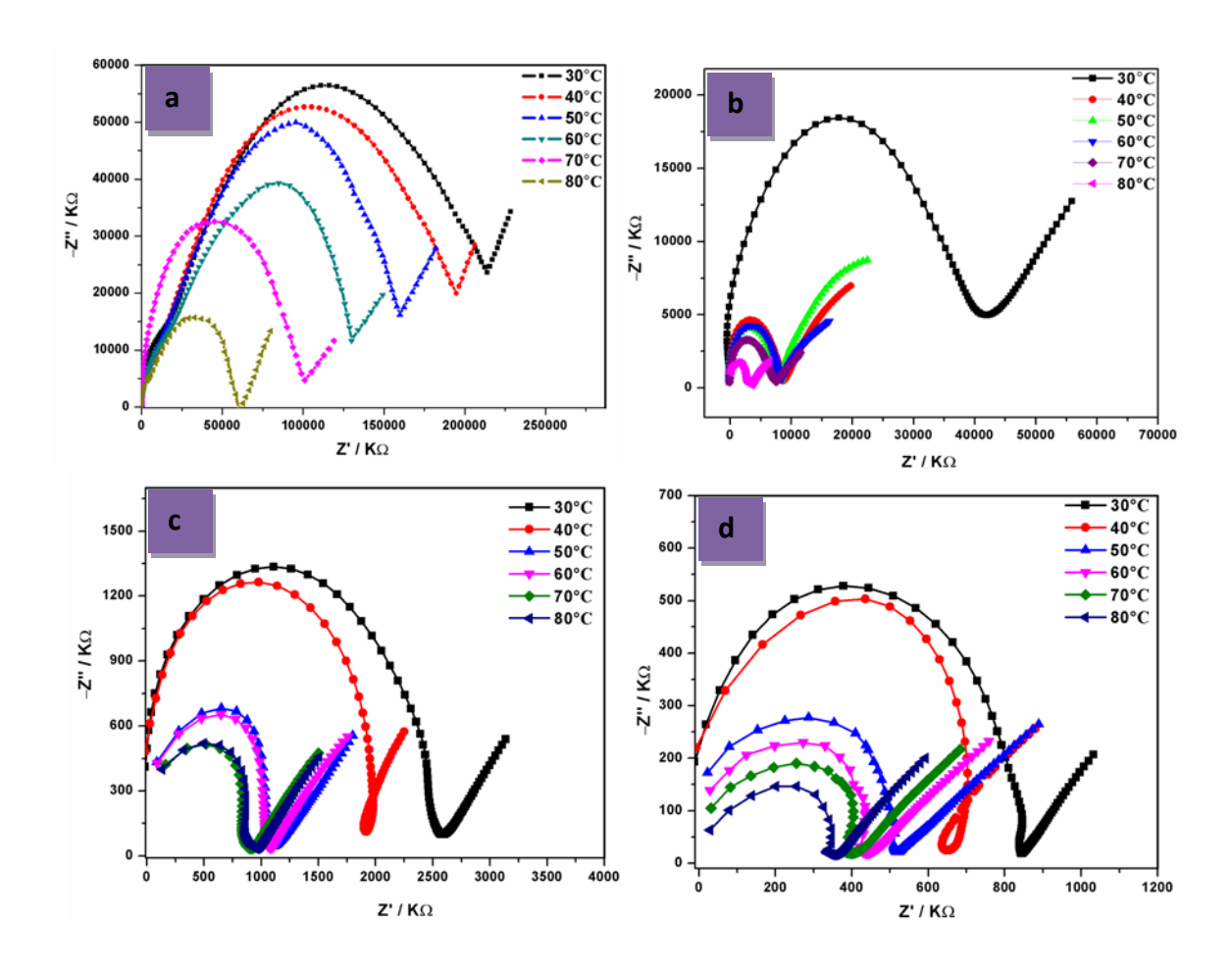


Figure 2.5: Temperature dependent Nyquist plots of SPE1 with different percentages of lithium salt (a) 10% (b) 20% (c) 30% (d) 40%

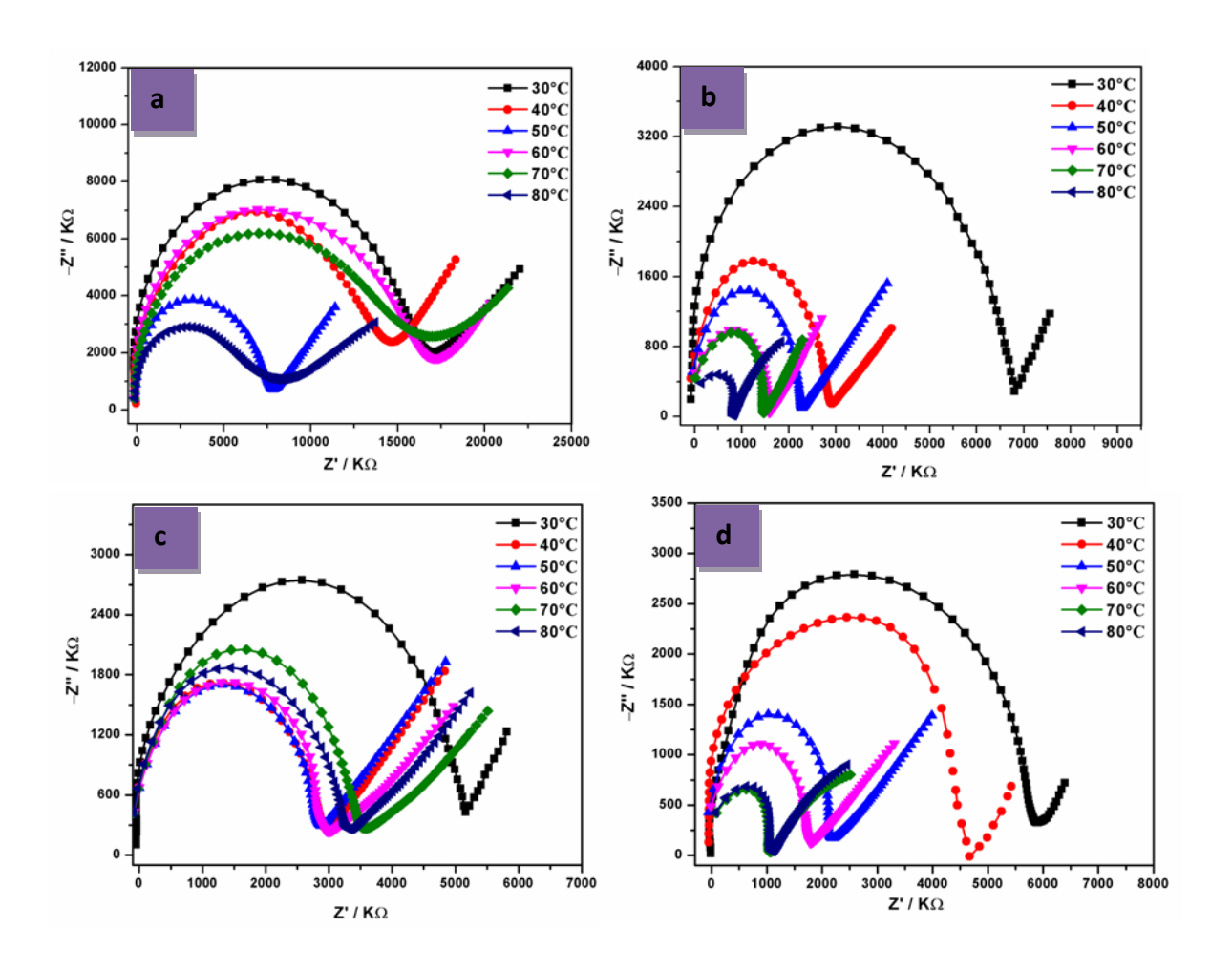


Figure 2.6: Temperature dependent Nyquist plots of SPE2 with different percentages of lithium salt (a) 10% (b) 20% (c) 30% (d) 40%

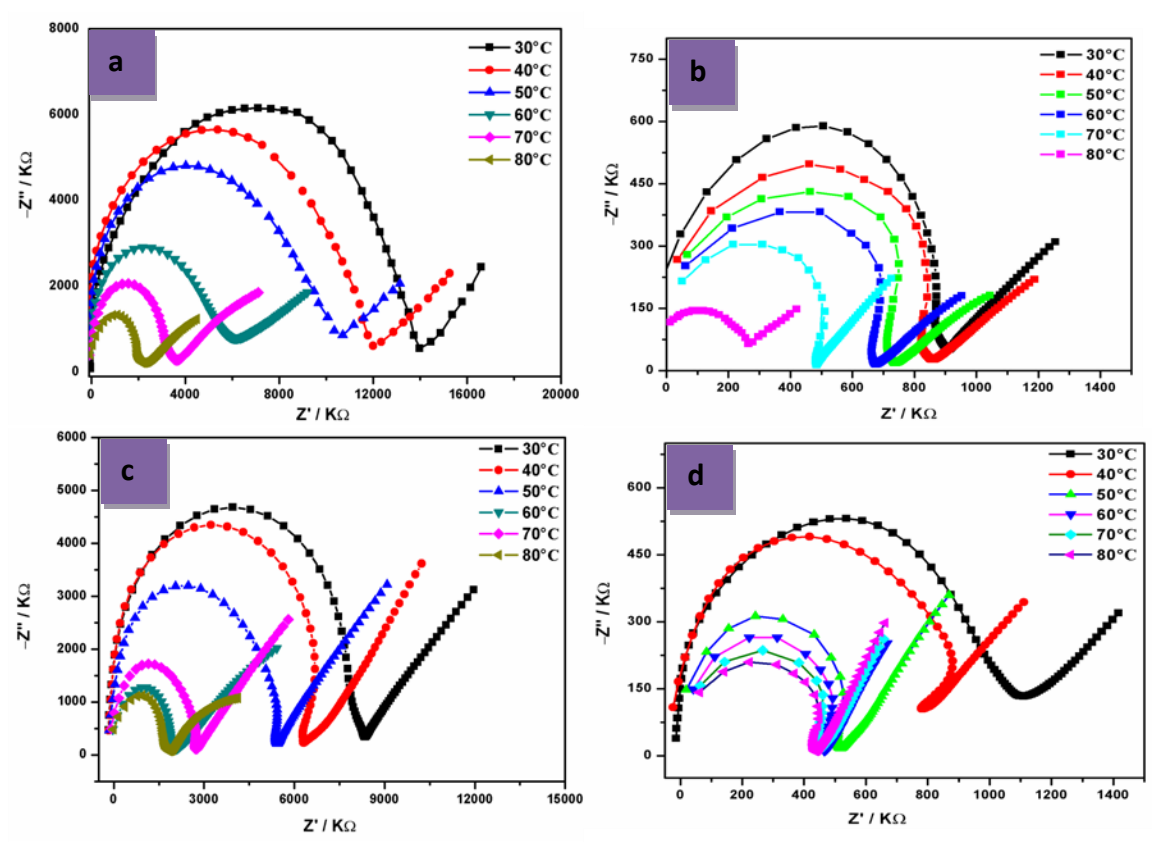


Figure 2.7: Temperature dependent Nyquist plots of SPE3 with different percentages of lithium salt (a)10% (b) 20% (c) 30% (d) 40%

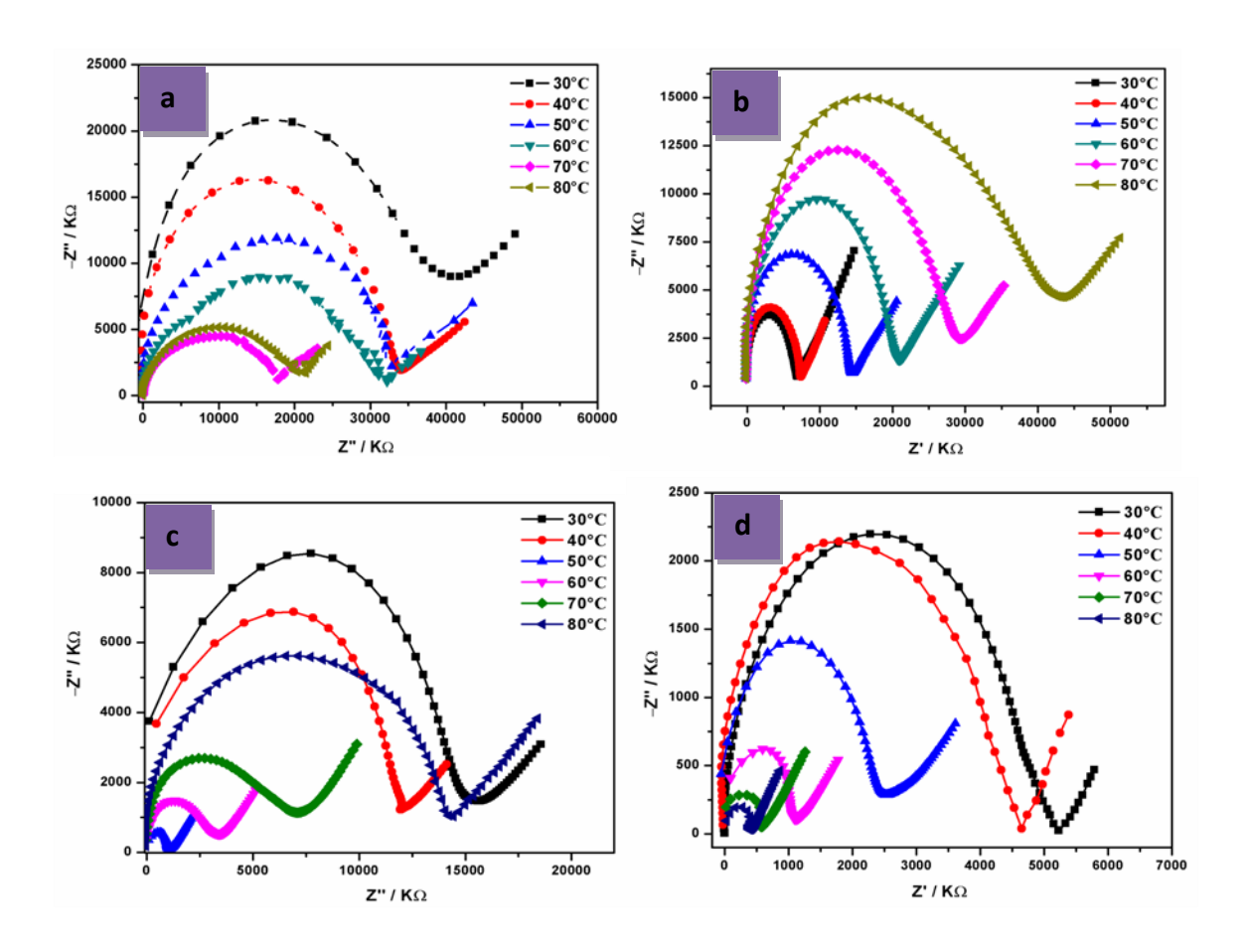


Figure 2.8: Temperature dependent Nyquist plots of SPE4 with different percentages of lithium salt (a)10% (b) 20% (c) 30% (d) 40%

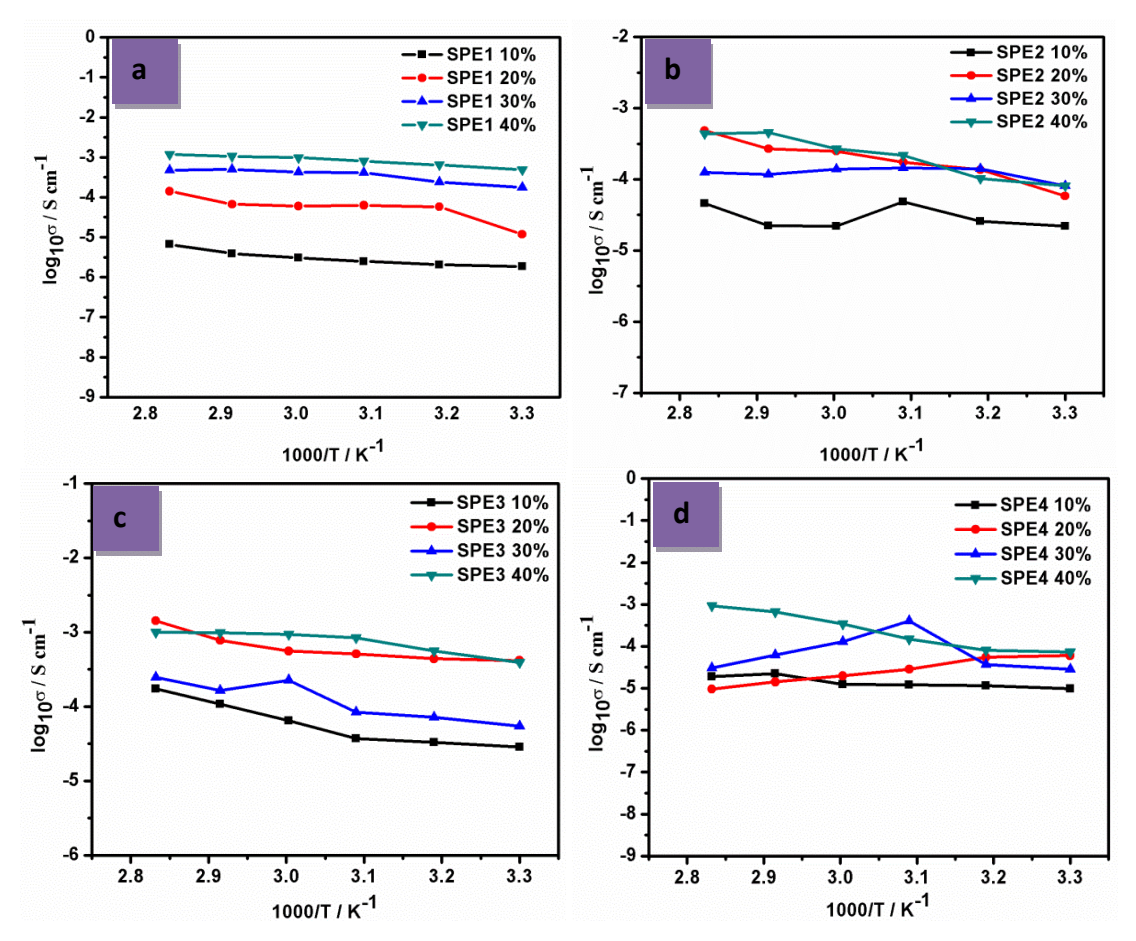


Figure 2.9: Arrhenius plots of temperature dependent conductivities of (a) SPE1 (b) SPE2 (c) SPE3 (d) SPE4

2.2.6. Fabrication of coin cell

A preliminary experiment was performed with polymer **P1** to identify the potential of the synthesized polymers towards battery fabrication. The lithium-lithium symmetric cell was fabricated, as shown in figure 2.10. The first step towards this was making the slurry by mixing 20 mg of polymer, P1 with 1 mL of DMSO solvent. Further, the slurry was drop-casted onto a lithium foil and dried. Commercially available electrolyte, which is 1M LiPF₆ in EC/DEC solvent, was used for the fabrication.

Galvanostatic charge-discharge cycling studies were performed at a current density of 20 mA.cm⁻² and a cycling capacity of 10 mAh.cm⁻². The overpotential values were found to vary as follows: 180 mV (10th cycle), 116 mV (25th cycle), 106 mV (50th cycle), 109 mV (75th cycle) and 109 mV (100th cycle). These values are significantly lower and constant compared to pristine Li-Li cells that show rapid fluctuation in overpotential values. Constant variation of

overpotential indicates controlled lithium dendrite growth on polyphosphate coated lithium foil. This observation indirectly indicates the presence of lithiophilic sites of polyphosphate polymer is responsible for the controlled Li electro deposition during electrochemical cycling. Also, the coating of polyphosphate on lithium foil renders a stable cycling behaviour of about 2000 cycles. Further studies in this direction are in progress, and the result obtained so far indicates the potential of these polymers as potential candidates in regulating controlled Li electro deposition.

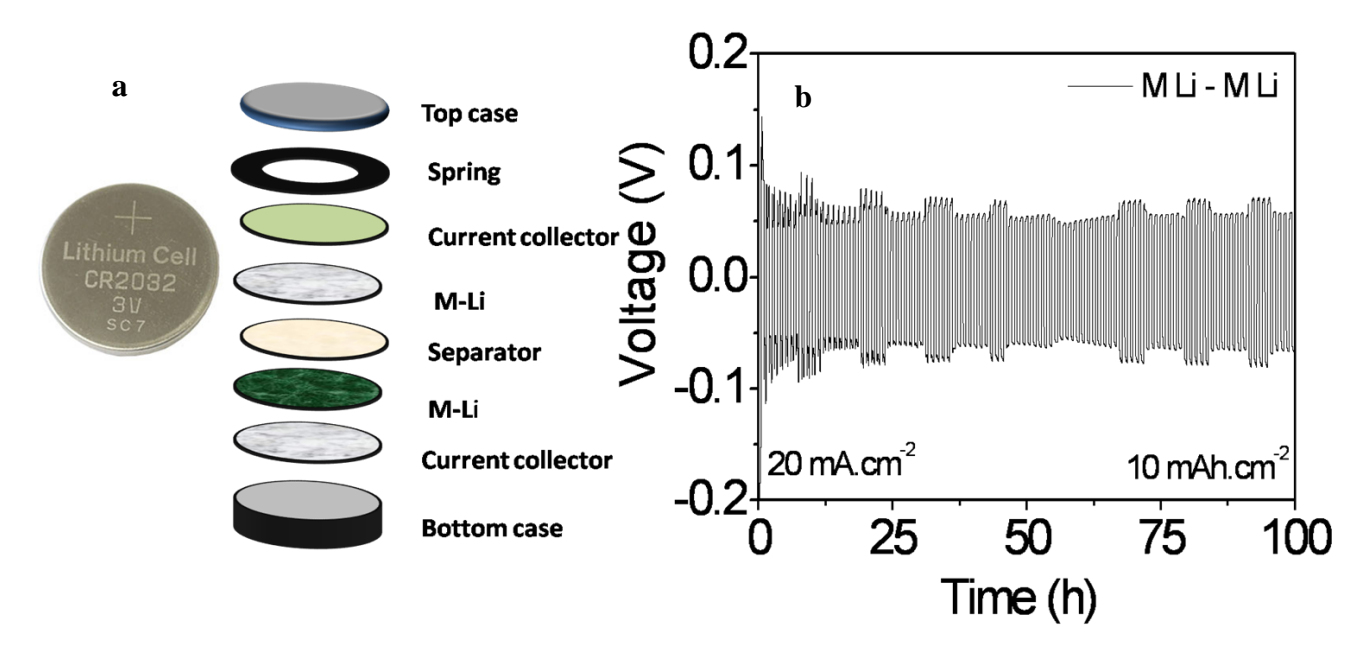


Figure 2.10. (a) The assembly of various components making up a coin cell (b) Voltage-time graph obtained by the charge discharge cycling studies.

2.3. Conclusions

In conclusion, we have successfully produced four different polyphosphates by condensation polymerization and studied their Li-ion conductivities. The synthesized polyphosphates P1-P4 are greatly stable solids at room temperature. The increase of Tg value of SPEs showed that the addition of lithium salt increased the flexibility of the polymer. All the polymers showed good conductivity, especially, the SPE3 (20%) which showed the highest conductivity of 1.4× 10⁻³ S cm⁻¹ at 80 °C and SPE1 (40%) of 1.2× 10⁻³ S cm⁻¹ at 80°C. The higher Li-ion conductivities observed are attributed to the microstructure of polymer molecules dictated by the bulky and

rigid groups as the co-monomer, which created the endless voids in the polymer matrices. These voids facilitated the smooth movement of Li-ions apart from the well-known hopping mechanism. The presence of phosphorus in the main chain of these polyphosphates would bring the flame-retardant characteristic to the SPEs. Randomized trials earlier in our lab predicted the tunability of microstructure assisted Li-ion conductivity while the present study validated the model, which can initiate more research in this direction. The polymers synthesized being stable solids and showing excellent Li-conductivity values are quite promising for solid state Li-ion batteries.

2.4. Experimental section

2.4.1. Materials and instrumentation

Standard Schlenk technique was used to handle air and moisture sensitive compounds under a dry nitrogen atmosphere. The solvents were purified and dried by refluxing over an appropriate drying agent followed by distillation under inert atmosphere. All the solvents utilized under inert atmosphere were deoxygenated methodically by freeze- pump- thaw method before use. The compound LiN(SO₂CF₃)₂ is procured from Acros and used to make electrolytes without any further processing.

The chemical structures of polymer chain were confirmed using ^{31}P and ^{1}H NMR spectral data. The NMR spectra of polymers were acquired at room temperature using the Bruker Avance FT NMR (500 MHz) spectrometer. Chemical shifts in spectra were reported in δ ppm and referenced to 85% $H_{3}PO_{4}$ for ^{31}P and tetramethylsilane for ^{1}H . The number and weight average molecular weights of polymers produced in this work were ascertained using polystyrene as the standard in a Gel Permeation Chromatography (Make: Shimadzu 10AVP). The separation of polymer chains was realized in the Phenogel mixed bed column (300 × 7.80 mm), which was run with tetrahydrofuran (THF) as the eluent at 30°C (flow rate = 0.5 mL/min).

The Perkin Elmer (Pyris STA 6000 model) thermogravimetric analyzer was used to study the thermal stability of polymers. The decomposition behavior of polymers in the temperature range of 50 $^{\circ}$ C – 995 $^{\circ}$ C with a heating rate of 20 $^{\circ}$ C/min was tested under the flow of nitrogen. The temperature at which 5 % weight lost was considered as the onset point of decomposition (Td). The glass transition temperature (Tg) was determined by operating the Differential Scanning Calorimeter (Mettler Toledo - DSC 1) in the temperature range of 25 $^{\circ}$ C – 240 $^{\circ}$ C and

heating rate of 10°C/min. FESEM images were obtained using an Ultra 55 Carl Zeiss instrument. The samples were dispersed in dimethylacetamide solvent and drop cast on a glass plate.

2.4.2. General synthetic procedure of polyphosphates (P1-P4)

A solution of phosphoryl chloride (0.56 g, 3.6 mmol) in THF (20 mL) was placed in a 250 mL RB flask (two-necked) under the flow of nitrogen gas. The reaction mixture was cooled down to 0°C, and then one of the aromatic diols (9.08 mmol) dissolved in dry THF was added followed by drop-wise addition of dry triethylamine (10 mL) using an additional funnel under a nitrogen atmosphere with stirring (scheme 1). The resulting reaction mixture was maintained at the same conditions for 4 h. The mixture was filtered off by using the frit, and the byproduct [NHEt₃]Cl was removed by washing several times with dichloromethane and applying a vacuum for 2 h. The polymers were purified further by washing in a Soxhlet apparatus for 24 h using dichloromethane to get pure polyphosphates (**P1-P4**).

NMR Spectral data (500 MHz, DMSO).Polymer **P1**: 1 H δ 6.56(d, 2H), 6.57(d, 2H) ppm. 31 P{ 1 H} δ -82.84ppm.Polymer**P2**: 1 H δ 6.45-6.47(dd, 1H), 6.41-6.42(dd, 1H), 6.35-6.37(dd, 1H), 2.03(s,3H) ppm. 31 P{ 1 H} δ -83.23ppm.Polymer**P3**: 1 H δ 6.37(dd, 1H), 6.35(dd, 2H), 2.1(s, 3H) ppm. 31 P{ 1 H} δ -81.47ppm.Polymer**P4**: 1 H δ 7.61-7.63(dd, 2H), 7.21-7.22 (dd, 2H),7.02 (d, 2H) ppm. 31 P{ 1 H} δ -82.85 ppm.

2.4.3. Preparation of solid polymer electrolytes SPE1-SPE4

The films of polyphosphates were prepared to measure the conductivity by dissolving assynthesized polymers in DMAc/DMSO solvents; however the films obtained were brittle. Hence, SPEs in the form of pellets were made to measure the conductivity. Different ratios of SPEs were prepared as follows. Initially, all the polyphosphates (P1-P4) were dried for 6 h at 60°C and LiN(SO₂CF₃)₂ was dried for 8 h at 150°C under vacuum, after that, they were mixed inside a glove-box filled with ultrapure nitrogen. The polymer-lithium salt mixture was stirred in THF overnight at room temperature for homogeneity between polymer and salt. Then, the solvent was evaporated and dried under vacuum for 10 h to get SPE1 - SPE4, respectively. The obtained solids were filled into a die and then it was compressed with 3 ton pressure to obtain pellets of about 2 mm thickness and 1.07 mm diameter. The prepared pellets (SPEs) were kept between two gold plated SS electrodes in a homemade cell and the cell was sealed to avoid contamination.

2.4.4. Measurements of impedance of solid polymer electrolytes

The cell was constructed, ensuring proper interfacial contacts between the electrolyte (pellet) and electrodes. The impedance of polymers and SPEs was determined in an electrochemical workstation (Zahner-Zennium loaded with the Thales data acquisition software). The impedance is measured in the frequency range of 1 Hz - 4 MHz for all samples. The conductivities were calculated 25,26 using the equation, $\sigma = d/(A R_b)$. In this equation, d = thickness of the pellet, A = thickness of the pellet, and $R_b = thickness$ of the pellet, and thickness of the curve with the real axis. The entire measurements were repeated three times to ensure reproducibility of results.

Supporting information: ¹H NMR and ³¹P NMR of P1-P4 are provided at the end of the chapter.

2.5. References

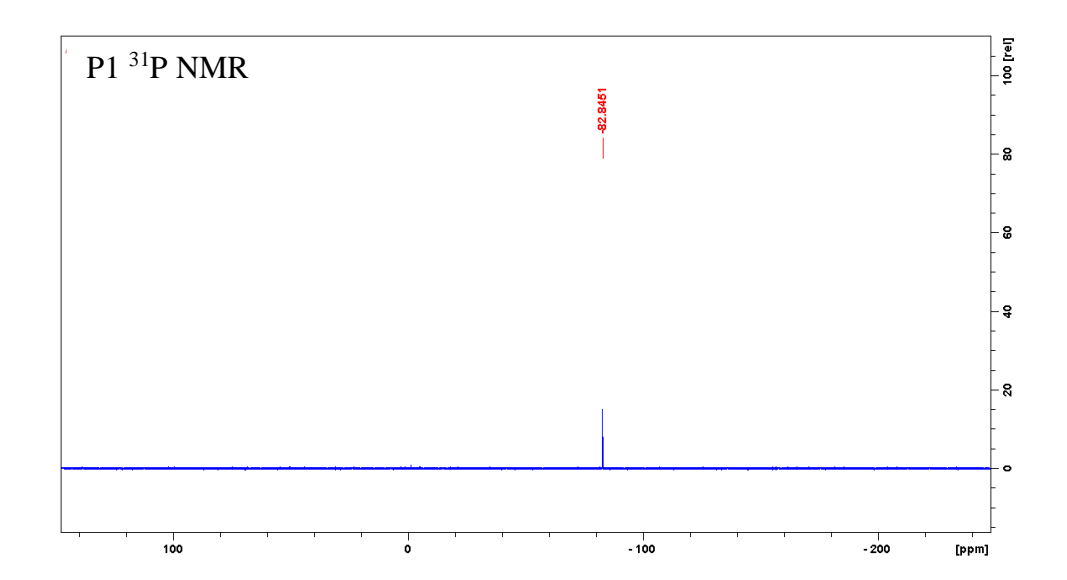
- [1] I.Villaluenga, K. H. Wujcika, W. Tonga, D. Devauxa, D.H.C. Wong, J. M. De Simone, N. P. Balsaraa, *Proc. Natl. Acad. Sci.*, 2016, **113**(1), 52–57; (b) M. H. Braga, N. S. Grundish, A. J. Murchisona, J. B. Goodenough, *Energy & Environmental Science*, 2017, **10**, 331-336; (c) Y. Meesala, A. Jena, H. Chang, and R. S. Liu, *ACS Energy Lett.*, 2017, **2**, 2734-2751; (d) M. S. Whittingham, *Chem. Rev.*, 2004, **104**(10), 4271-4302; (e) A. Yoshino, *Angew. Chem. Int. Ed.*, 2012, **24**, 5798-5800; (f) K. J. Stevenson, *J. Solid State Electrochem.*, 2012, **16**, 847–855.
- [2] (a) A.Varzi, R. Raccichini, S. Passerini, B. Scrosati, J. Mater. Chem. A, 2016, 4, 17251-17259; (b) M. Nie, D. P. Abraham, D. M. Seo, Y. Chen, A. Bose, B. L. Lucht, J. Phys. Chem. C, 2013, 117(48), 25381-25389; (c) P.G. Bruce, B. Scrosati, J.M. Tarascon, Angew. Chem. Int. Ed., 2008, 47, 2930-2946; (d) A.S. Arico, P.G. Bruce, B. Scrosati, J.M. Tarascon, W.V. Schalkwijk, Nat. Mater., 2005, 4, 366-377.
- [3] (a) B. Kurc, *Int. J. Electrochem. Sci.*, 2018, 13, 5938 5955, doi: 10.20964/2018.06.46; (b) J.
 S. Gnanaraj, E. Zinigrad, M. D. Levi, M. D. Aurbach, M. Schmidt, *J. Power Sources*, 2003, 119–121, 799-804.
- [4] S. Iliescu, L. Zubizarreta, N. Plesu, L. Macarie, L. Popa, G. Ilia, *Chem. Cent. J.*, 2012, **6**, 132-145.

- [5] T. Lestariningsih, Q. Sabrina, E. M. Wigayati, J. Phy.: Conf. Ser., 2018, 985, 012049.
- [6] P. B. Balbuena, AIP Conference Proceedings, 2014, 1597, 82.
- [7] T. Famprikis, P. Canepa, J. A. Dawson, M.S. Islam, C. Masquelier, *Nature Materials*, 2019, **18**, 1278–1291.
- [8] (a) F. Ma, Z. Zhang, W. Yan, X. Ma, D. Sun, Y. Jin, X. Chen, K. He, ACS Sustainable Chem. Eng., 2019, 7 (5), 4675-4683; (b) Q. Zhang, K. Liu, F. Ding, X. Liu, Nano Research, 2017, 10, 4139–4174; (c) A. Arya, A. L. Sharma, Ionics, 2017, 23, 497–540; (d) N. Rajeswari, S. Selvasekarapandian, M. Prabu, S. Karthikeyan, C. Sanjeeviraja, Bull. Mater. Sci., Indian Academy of Sciences, 2013, 36, 333–339; (e) J. Vatsalarani, S. Geetha, D.C. Trivedi, P.C. Warrier, J. Power Sources, 2006, 158, 1484-1489; (f) B. Sun, J. Mindemark, K. Edström, D. Brandell, Solid State Ion., 2014, 262, 738-742; (g) J. Mindemark, M. J. Lacey, T. Bowden, D. Brandell, Prog. Polym. Sci., 2018, 81, 114-143; (h) R. C. Agrawal, G. P. Pandey, J. Phys. D: Appl. Phys., 2008, 41, 223001-223019.
- [9] (a) D. P. Gates, Annu. Rep. Prog. Chem. Sect. A Inorg. Chem., 2004, 100, 489-508; (b) R.D. Archer, Inorganic and Organometallic Polymers, Wiley-VCH, New York, 2001; (c) T. Vlad-Bubulac, C. Hamciuc, O. Petreus, High. Perform. Polym., 2006, 18, 255-264.
- [10] E. Staunton, Y. G. Andreev, P. G. Bruce, J. Am. Chem. Soc., 2005, 127, 12176-12177.
- [11] O. Borodin, and G. D. Smith, *Macromolecules*, 2006, **39**, 1620-1629.
- [12] D. J. Wilson, C. V. Nicholas, R. H. Mobbs, C. Booth, J. R.M. Giles, *Polym. J.*, 1990, 22, 129-135.
- [13] O. Buriez, Y. B. Han, J. Hou, J. B. Kerr, J. Qiao, S. E. Sloop, M. Tian, S. Wang, *J. Power Sources*, 2000, **89**, 149.
- [14] P. P. Soo, B. Huang, Y. I. Jang, Y.M. Chiang, D. R. Sadoway, A. M. Mayes, *J. Electrochem. Soc.*, 1999, **146**, 32.
- [15] H. R. Allcock, M. E. Napierala, D. L. Olmeijer, C. G. Cameron, S. E. Kuharcik, C. S. Reed, S. J. M. O'Connor, *Electrochim. Acta*, 1998, 43, 1145.

- [16] P. G. Bruce, P. G. Vincent, J. Chem. Soc. Faraday Trans, 1993, 89, 3187.
- [17] F. Croce, R. Curini, A. Martinelli, L. Persi, F. Ronci, B. Scrosati, R. Caminiti, *J. Phys. Chem. B*, 1999, **103**, 10632.
- [18] (a) B. Scrosati, F. Croce, L. Persi, J. Electrochem. Soc., 2000, 147, 1718; (b) J. J. Qiu, Q. Xue, Y.Y. Liu, M. Pan, C.M. Liu, Phosphorus, Sulfur, and Silicon, 2014, 189(3), 361-373, DOI: 10.1080/10426507.2013.819869; (c) F. Marquardt, H. Keul, M. Möller, Eur. Polym. J., 2015, 69, 319-327.
- [19] M. B. Armand, J.M. Chabagno, M. J. Duclot, Fast Ion Transport in Solids; Elsevier, New York, 1979, 131.
- [20] J.R. Mac Callum, C.A. Vincent, Eds. Polymer Electrolyte Reviews-1 and 2, Elsevier Applied Science, London, 1987 and 1989.
- [21] A. Nishimoto, K. Agehara, N. Furuya, T. Watanabe, M. Watanabe, *Macromolecules*, 1999, **32**, 1541.
- [22] A. Nishimoto, M. Watanabe, Y. Ikeda, S. Kojiya, *Electrochim. Acta*, 1998, 43, 1177.
- [23] R. Chen, X. Huang, R. Zheng, D. Xie, Y. Mei, R. Zou, *Chem. Eng. J.*, 2020, **380**, 122500–122510.
- [24] a) N.V. Aspern, S. Röser, B. R. Rad, P. Murmann, B. Streipert, X. Mönnighoff, S. D. Tillmann, M. Shevchuk, O. S. Kazakova, G. V. Röschenthaler, Nowak, S. M. Wintera, I. C. Laskovic, *Journal of Fluorine Chemistry*, 2017, **198**, 24–33 b) C. C. Su, M. He, C. Peebles, L. Zeng, A. Tornheim, C. Liao, L. Zhang, J. Wang, Y. Wang, Z. Zhang, *ACS Appl. Mater. Inter.*, 2017, **9**, 30686–30695
- [25] A. Nishimoto, M. Watanabe, Y. Ikeda, S. Kojiya, *Electrochim. Acta*, 1998, 43, 1177.
- [26] (a) K.H. Lee, J.K. Park, W. J. Kim, *Electrochim. Acta*, 2000, **45**, 1301-1306; (b) E. Morales, J. L. Acosta, *Electrochim. Acta*, 1999, **45**, 1049-1056; (c) S.Y. An, I. C. Jeong, M. S. Won, E.D. Jeong, Y.B. Shim, *J. Appl. Electrochem.*, 2009, **39**, 1573-1578; (d) K.M. Abraham, Z. Jiang, B. Carroll, *Chem. Mater.*, 1997, **9**, 1978-1988; (e) J. Britz, W.H. Meyer, G. Wegner,

- Macromolecules, 2007, **40**, 7558-7565. (f) K. M. Abraham, Z. Jiang, B. Carroll, Chem. Mater., 1997, **9**, 1978-1988;(g) K. Yoshida, M. Nakamura, Y. Kazue, N. Tachikawa, S. Tsuzuki, S. Seki, et al. J. Am. Chem. Soc., 2011, **133**, 13121-13129;(d) J. Britz, W. H. Meyer, G. Wegner, Macromolecules, 2007, **40**, 7558-7565.
- [27] X. Cao, Y. Li, X. Li, J. Zheng, J. Gao, Y. Gao, X. Wu, Y. Zhao, Y. Yang, *ACS Appl. Mater. Inter.*, 2013, **5**, 11494–11497.
- [28] S. Monge, B. Canniccioni, A. Graillot, J. J. Robin, *Biomacromolecules*, 2011, **12**, 1973–1982.
- [29] E. Faure, C. F. Daudré, C. Jérôme, J. D. Fournier, P. Woisel, C. Detrembleur, *Prog. Polym. Sci.*, 2013, **38**, 236-270.
- [30] J. Su, F. Chen, V. L. Cryns, P. B. Messersmith, *J. Am. Chem. Soc.*, 2011, **133**, 11850–11853.
- [31] G. Becker, L. M. Ackermann, E. Schechtel, M. Klapper, W. Tremel, and F. R. Wurm, *Biomacromolecules*, 2017, **18**(3), 767-777.
- [32] P. K. Forooshani, B. P. Lee, J. Polym. Sci., Part A: Polym. Chem., 2017, 55, 9–33.
- [33] N. Patil, C. Jérôme, C. Detrembleur, *Prog. Polym. Sci.*, 2018, **82**, 34-91.
- [34] (a) D. Wang, R. Kou, D. Choi, Z. Yang, Z. Nie, J. Li, L.V. Saraf, D. Hu, J. Zhang, G.L. Graff, J. Liu, M. A. Pope, and I. A. Aksay, *ACS Nano*, 2010, **4**(3), 1587-1595. (b) D. Wang, D. Choi, J. Li, Z. Yang, Z. Nie, R. Kou, D. Hu, C. Wang, L. V. Saraf, J. Zhang, I. A. Aksay, and J. Liu, *ACS Nano*, 2010, **3**(4), 907-914.
- [35] K. Hemelsoet, F.V. Durme, V.V. Speybroeck, M.F. Reyniers, M. Waroquier, *J. Phys. Chem.*, 2010, **114**, 2864–2873.
- [36] K.A. Francis, C.W. Liew, S. Ramesh, K. Ramesh, S. Ramesh, *Mater. Express*, 2016, **6**, 252-258.
- [37] (a) H.V. Babu, K. Muralidharan, *Polymer*, 2014, **55**, 83-94. (b) H.V. Babu, B. Srinivas, K.P.K. Naik, K. Muralidharan, *J. Chem. Sci.*, 2015, **127**, 635-641. (c) H.V. Babu, B. Srinivas, K.

Muralidharan, *Polymer*, 2015, **75**, 10-16.(d) Z. Stoeva, I. M. Litas, E. Staunton, Y. G. Andeev, P.G. Bruce, *J. Am. Chem. Soc.*, 2003, **125**, 4619-4626; (e) P.G. Bruce, S.A. Campbell, P. Lightfoot, M. A. Mehta, *Solid State Ion.*, 1995, **78**, 191-198.



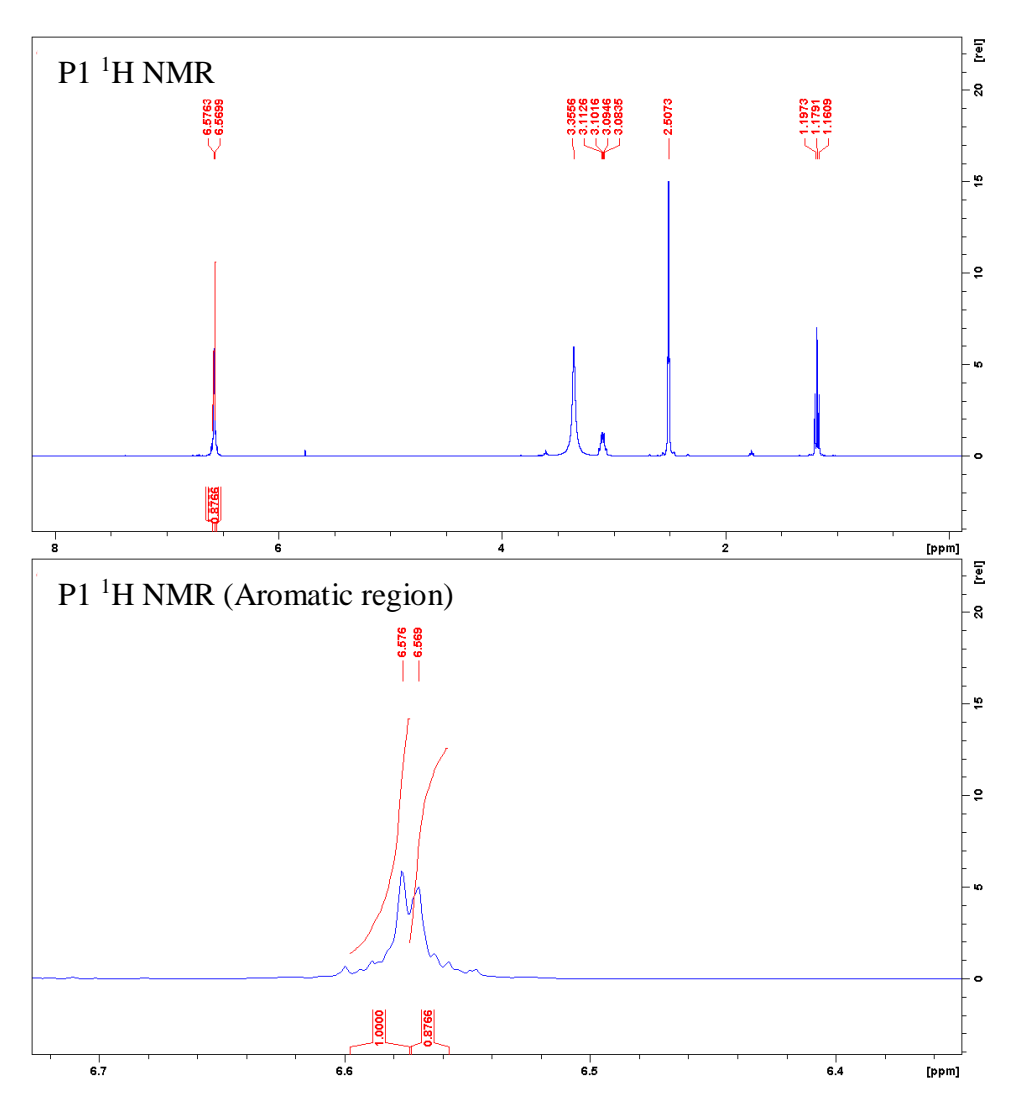
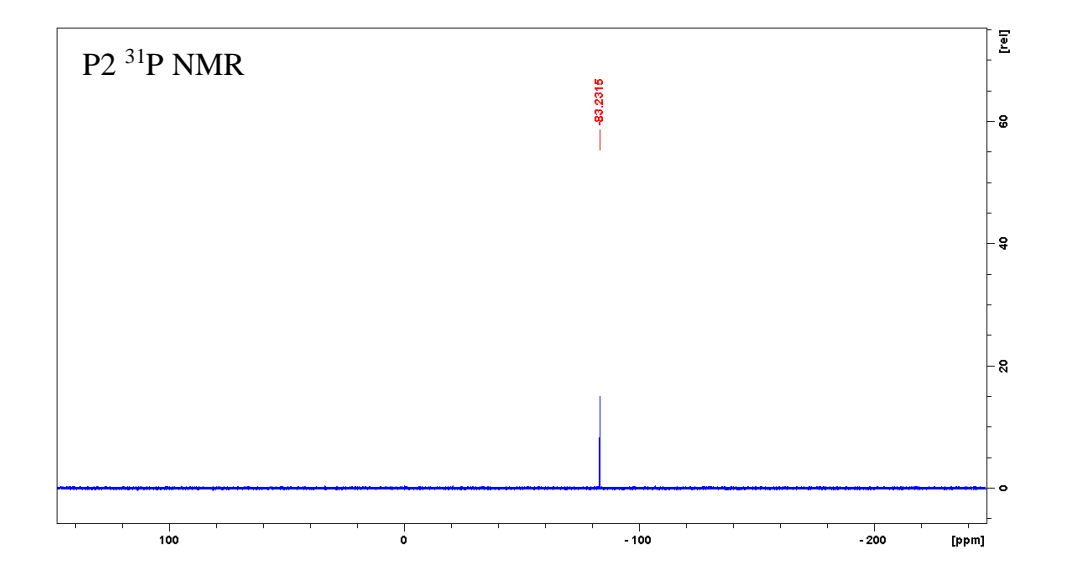


Figure 2.S1: NMR spectra of polymer P1:³¹P NMR (top), ¹H NMR (bottom)



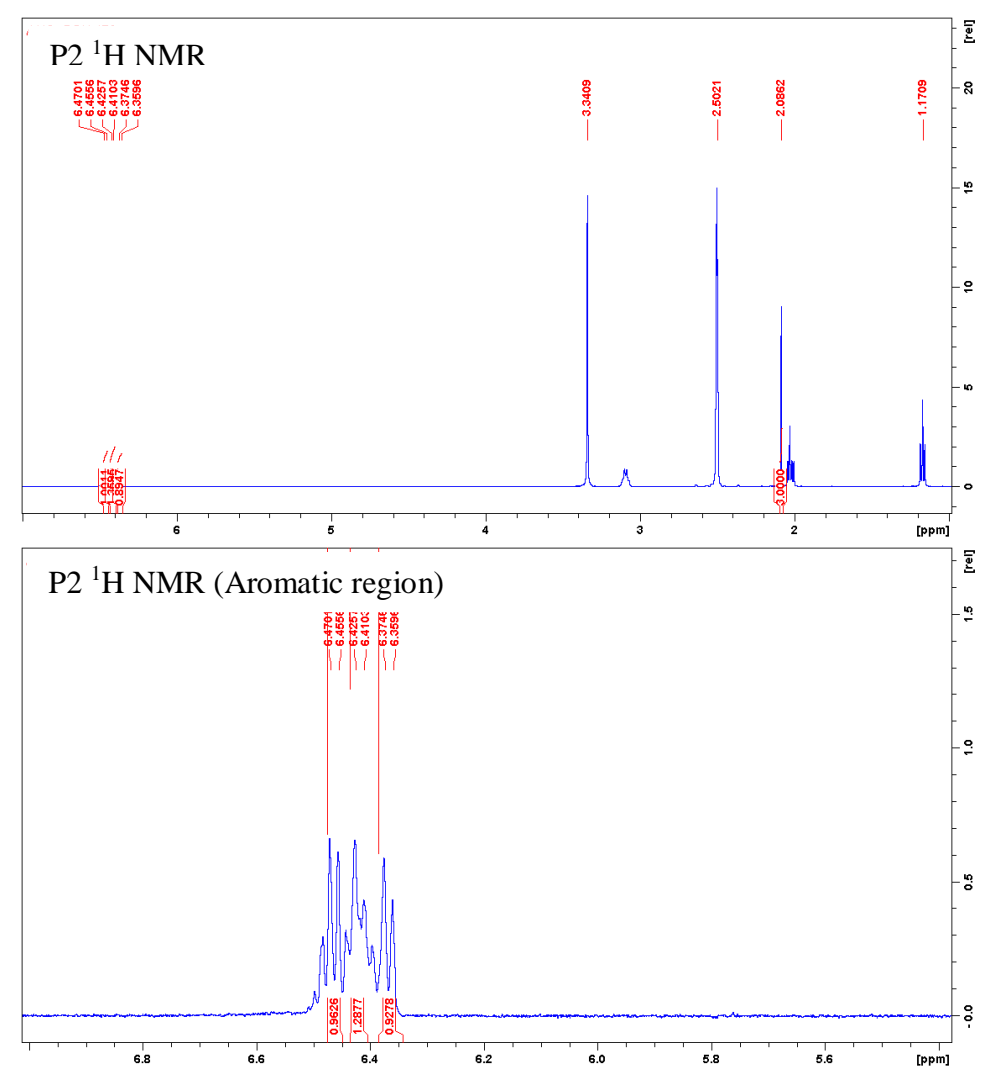
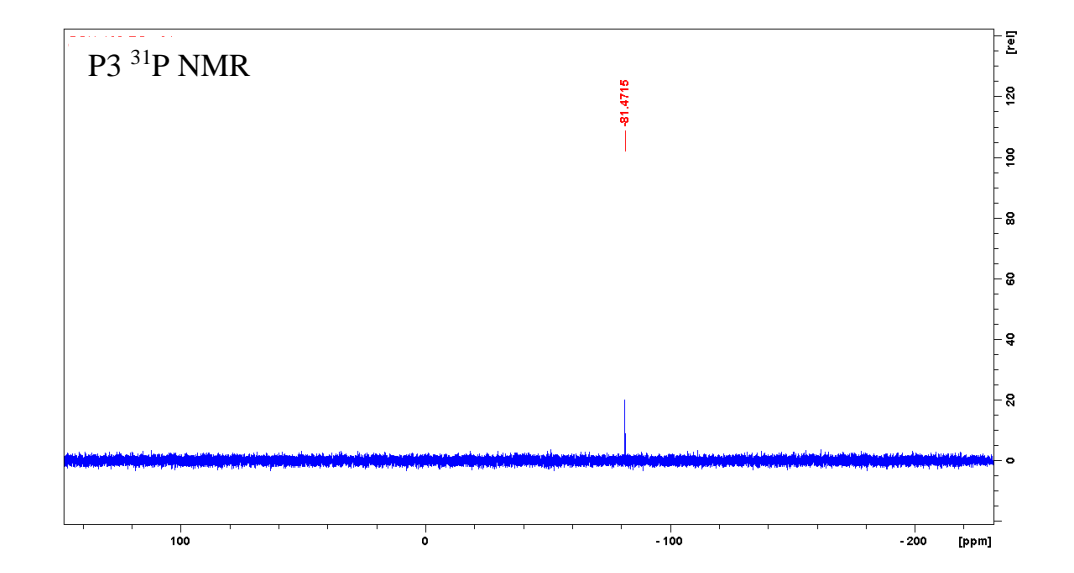


Figure 2.S2: NMR spectra of polymer P2:³¹P NMR (top), ¹H NMR (bottom)



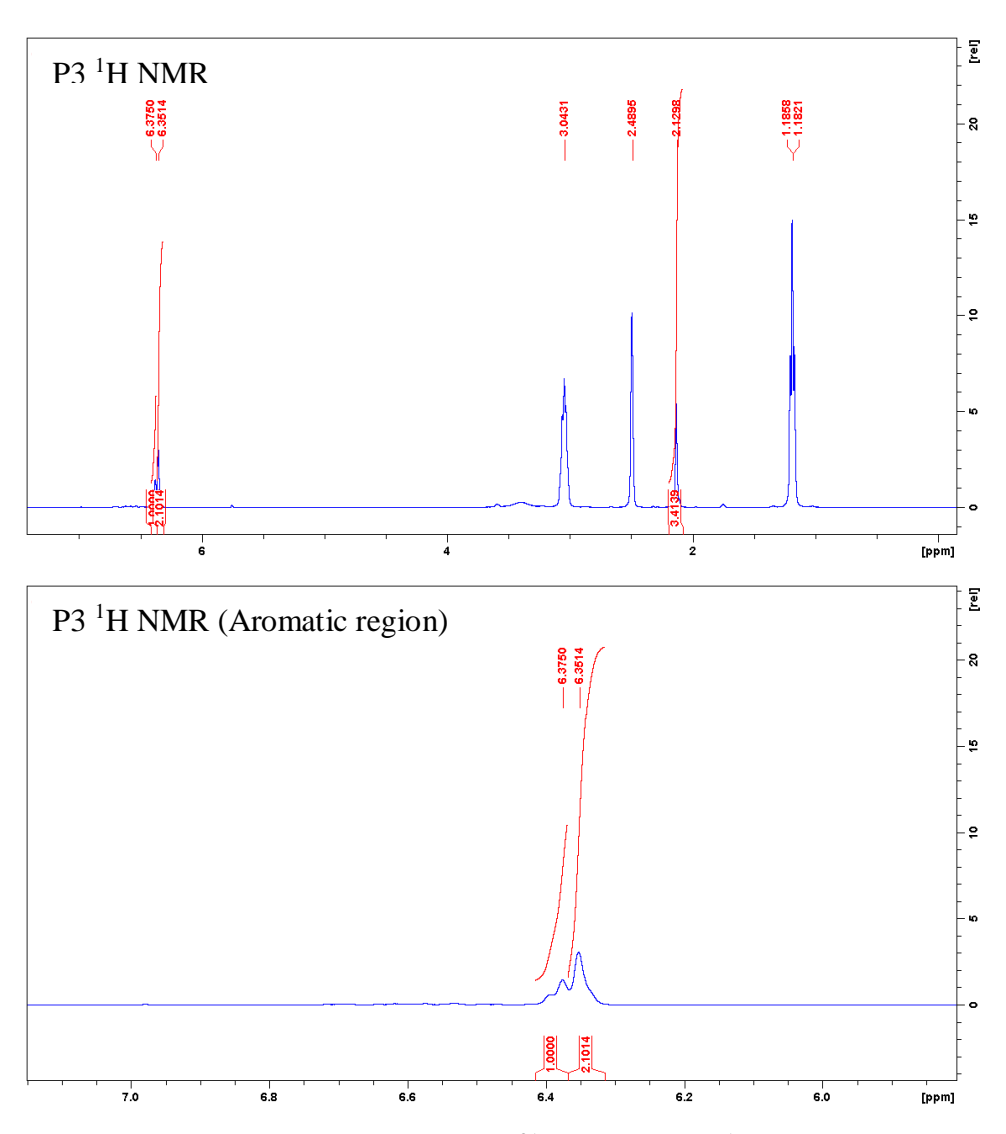
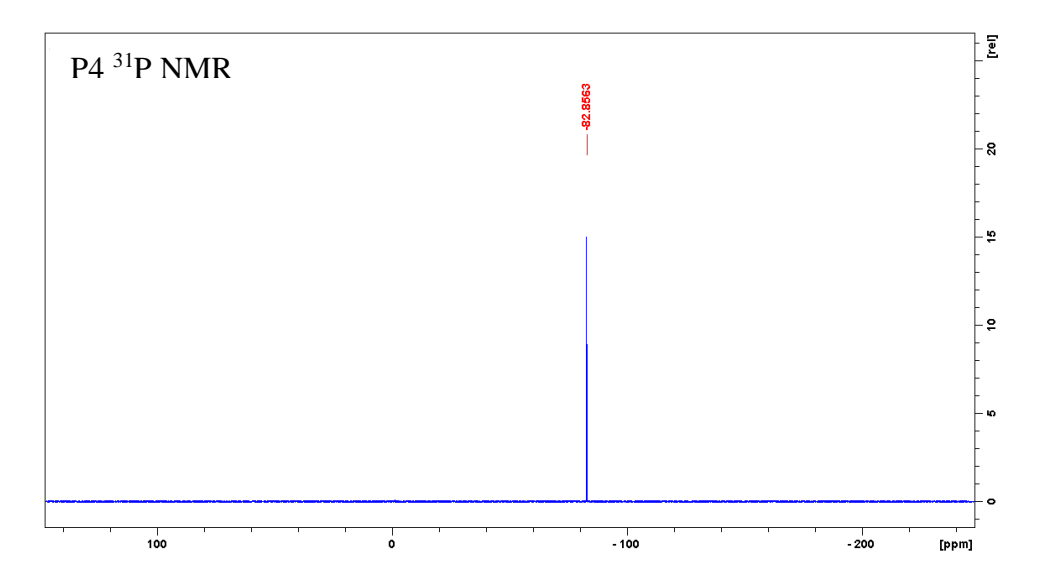


Figure 2.S3: NMR spectra of polymer P3:³¹P NMR (top), ¹H NMR (bottom)



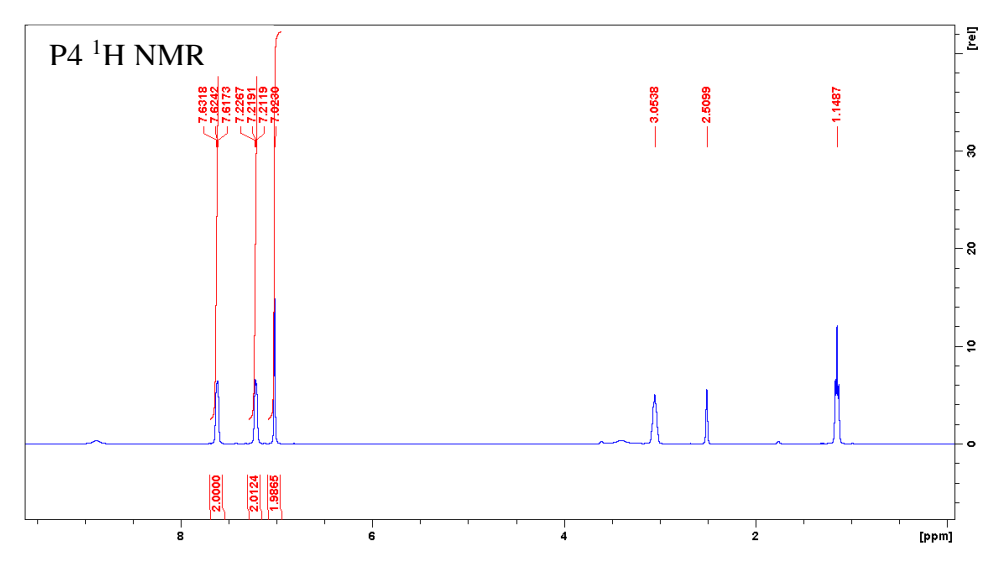


Figure 2.S4: NMR spectra of polymer P4: ³¹P NMR (top), ¹H NMR (bottom)

Chapter 3

Poly(methyl methacrylate)/polyphosphate blends with tunable refractive indices for optical applications

Abstract:

Tuning the refractive index of the transparent materials is essential for optical applications. Herein, we report novel materials with a tunable refractive index that are prepared by blending poly(methyl methacrylate) (PMMA) with different concentrations of two polyphosphate hybrid polymers having phosphorus in the main chain (P5 and P6). The refractive indices and associated optical parameters of these polymers and hybrid materials (PB5 and PB6 series) are investigated using ellipsometry and optical modeling method to find their applicability in optics. Refractive indices of these materials are fine-tuned by altering the ratio of PMMA to P5 or P6. This approach is simple and ideal for obtaining homogeneous blends. Refractive index tunability of 0.05 and 0.1 are achieved for PB5 and PB6 series respectively by this approach. Also, Abbe numbers of these blends are reasonable for PB5 series compared to the conventional lens materials, with a maximum value of 56 achieved in the case of PB520 blend. Also, the trend in variation of extinction coefficient with wavelength for blends PB650, PB660 and PB680 seem promising for optical filter kind of applications. These results show that the synthesized polymer blends are promising as optical materials with refractive index tunability.



Optical Materials, 2020, 104, 109841

3.1. Introduction:

Functional materials with excellent optical properties such as high refractive index (RI) and good transparency are useful for a variety of applications, including anti-reflection coatings, optical waveguides, ¹ ophthalmic lenses, ² and adhesives for optical components. A few polymers such as aromatic heterocyclic polymers, ³polythiophene, ⁴ and conjugated polymers, ⁵ were reported to show the RI value higher than 1.7, so far. If the RI value of the polymer is high, the thickness of the materials required for lens manufacture is less. Further, solubility, optical dispersion, and optical transmittance in the visible region are properties that decide the practical use of a polymer. Thus, the development of high-refractive-index polymers (HRIP) with worthy optical properties is still a hot topic.

Much-dedicated efforts are on to produce polymer-inorganic hybrid materials,⁶ because they have enhanced thermal, mechanical, magnetic, optical, electronic, and optoelectronic properties compared with their corresponding individual polymer or inorganic component. Nanoparticles can considerably increase the RI but may affect the transparency of the material due to agglomeration.⁷ Further, these particles tend to agglomerate during dispersion in a solvent or a polymer matrix, which ultimately hinders the application. Therefore, obtaining hybrid materials with useful RI value overcoming all issues is a challenge.

RI of a material is related to molar volume and mean polarizability by the Lorentz - Lorenz equation.^{3, 8-10}The equation gives an estimation of the refractive index of the material from the individual molar refractions of functional groups and the repeating units.

$$\frac{n^2 - 1}{n^2 + 1} = \frac{4\pi}{3} N\alpha = \sum_{i} (R_{LL})_{i}$$

where N is the number of molecules per unit volume, α is the mean polarizability and R_{LL} is the individual molar refraction values. Therefore, as per the equation, the introduction of phosphorus, sulphur, and halogen with high molar refraction values will increase the RI of the material. Phosphorus has higher polarizability due to its electronic structure. Unlike nitrogen, which has a 3s-3d energy gap of 23eV, phosphorus has an energy gap of 17eV and is, therefore, more polarisable. 17

Organic-inorganic hybrid polymers with phosphorus as one of the atoms in the main-chains have exceptional advantages owing to their conformational flexibility introduced by the size and the fifth valence of phosphorus atoms. These properties of the phosphorus-

containing polymers help in designing polymers for various applications¹⁸⁻²⁰ with tuneable properties. Considering these advantages, Olshavsky and Allcock prepared a series of polyphosphazenes with high RIs and optically transparent in the visible region.^{21, 22}These polymers possessed moderate to high Abbe numbers and RI as high as 1.75. McGrath and coworkers synthesized aromatic polyphosphonates and studied for their use as HRIPs.^{23, 24} In 2001, H. K. Shobha et al. have synthesized a variant of polyphosphonates starting from phenyl phosphonic dichloride and the diol using triethyl amine as the base and phenol as an end capper.²⁴Recently in 2017, Macdonald et al. have synthesized a series of similar high refractive index polymers starting from phenyl and methyl phosphonic dichloride using triethyl amine and n-methyl imidazole as bases and end capped the polymers with various endcappers.²⁵ The highest reported RI for a polyphosphonate is 1.64.

Mostly polyphosphonates have been explored as high refractive materials, and polyphosphates are less explored in this regard. Polyphosphates are similar to the polycarbonates by the structure, and they are the materials of commercial importance because of their excellent flame-retarding characteristics. Moreover, polyphosphates can be degradable biomaterials. Bisphenol A-bis(diphenyl phosphate) commercially known as Fyrolflex BDP is a well-known fire retardant. In this work, we have explored the refractive index tunability of PMMA, a well-known polymer for optical applications, using two polyphosphate polymers, one of which is a polymer of bisphenol A diphenyl phosphate and the other is a biphenyl variant of the same.

One of the intriguing strategies of increasing the RI of a polymer is making hybrid materials by combining a typical organic polymer with the hybrid polymer having phosphorus atoms. Therefore, we have synthesized two polyphosphates (Scheme 3.1), and the present work describes a novel approach of tailoring the refractive index of PMMA by mixing with varied weight ratios of synthesized polyphosphates. PMMA is a ubiquitous amorphous polymer in various optical components. Further, PMMA finds a wide variety of applications because of its several desirable qualities, including toughness, durability, transparency, and biocompatibility. Nevertheless, it is not just the value of the refractive index; the flexibility of tuning of optical properties is also crucial for the practical use of material. Consequently, polyphosphates described here are blended with PMMA by simple solution mixing to ensure homogeneous mixing of composition. The RI values and Abbe's number (V_D) of these blends were tunable

compared to that of individual polymers showing the advantages of the present study described here.

Scheme 3.1: Schematic representation for the syntheses of polymers P5 and P6.

3.2. Results and discussion

Table 3.1. NMR data and molecular weight distribution of P5 and P6

Doleman	³¹ P NMR in CDCl ₃	¹ H NMR in CDCl ₃	Mr. (Da)	May (Da)	PDI
Polymer	Δ	δ	Mn (Da)	Mw (Da)	
P5	-17.2 (s) and -18.9 (s)	7.2-7.4 (m, 14H), 1.6	32372	64331	1.98
		(s, 6H)			
P6	-17.46 (s)	7.2-7.5 (m, 14H)	6639	10983	1.65

The NMR spectral data confirmed the structure of repeating units in the polymers. The two signals in the ³¹P NMR spectrum of the polymer P5 are assigned to the phosphorus in the repeat unit and the phosphorus at the end chain. The polymers P5 and P6 were purified by repeated precipitation from chloroform into hexane, and therefore there is no possibility of any unreacted phosphorous source used in the reaction. Usually, if chain length is small, it is expected to show two distinguishable peaks in the ³¹P NMR spectrum. Similar observations of two phosphorus peaks in ³¹P NMR have been reported by many researchers. ^{18, 26-30} However, in our case, the

higher molecular weight polymer P5 showed two ³¹P signals. The reason for this observation is explained, presumably based on the high polydispersity index (PDI). In general, higher PDI value reflects the heterogeneity in chain length, *i.e.*, the presence of more random arrangement. As PDI is more for P5, there should be a considerable variation in molecular weights of each chain of the polymer whose average is given as 32,372 Da (Mn). So the presence of smaller chains where the two phosphorus environments are distinguishable may be resulting in two ³¹P NMR peaks in P5. The chain length of P6 could be longer than these smaller chains in P5 and hence cannot differentiate the two phosphorus environments.

Also both these polymers possessed interesting film forming nature as depicted in figure 3.1. All the more, the film was formed by simple solvent casting in chloroform and drying at room temperature. The images of these films coated on the soda lime glass are shown in figure 3.3 and a schematic representation of the same is shown in figure 3.2.

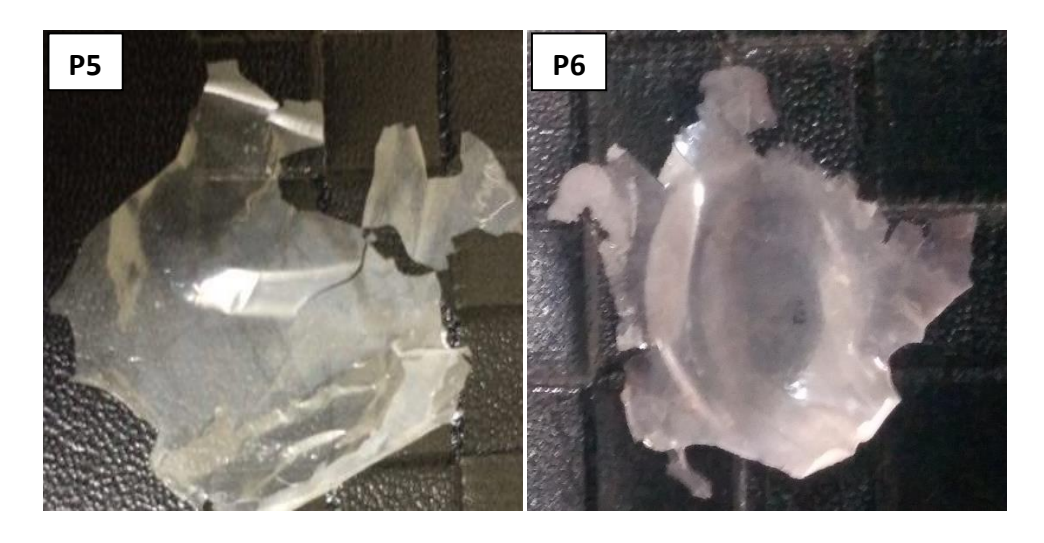


Figure 3.1: Polymers P5and P6casted into films by solvent casting.

Table 3.2. Phosphates (P5 or P6) and PMMA blends and their weight ratio*

Name of the	Polyphosphate	Percentage of P5 or	Weight ratio
polymer blend	(P5 or P6)	P6 in the blend	PMMA : P5 or P6
PB510	P5	10	4:1
PB520	P5	20	3:2
PB550	P5	50	1:1
PB560	P5	60	2:3

PB580	P5	80	1:4
PB610	P6	10	4:1
PB620	P6	20	3:2
PB650	P6	50	1:1
PB660	P6	60	2:3
PB680	P6	80	1:4

^{*}The nomenclature of polymer blends based on weight percentage of PMMA and polyphosphate (P5 or P6) and their weight ratios are given.

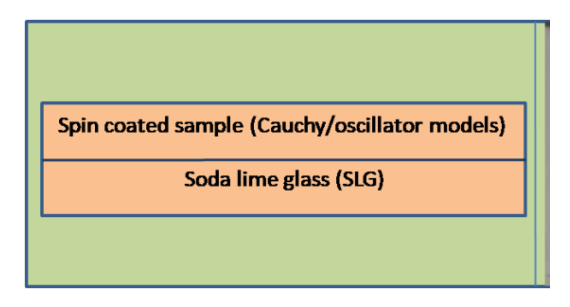


Figure 3.2: A schematic representation of the sample coated on SLG.

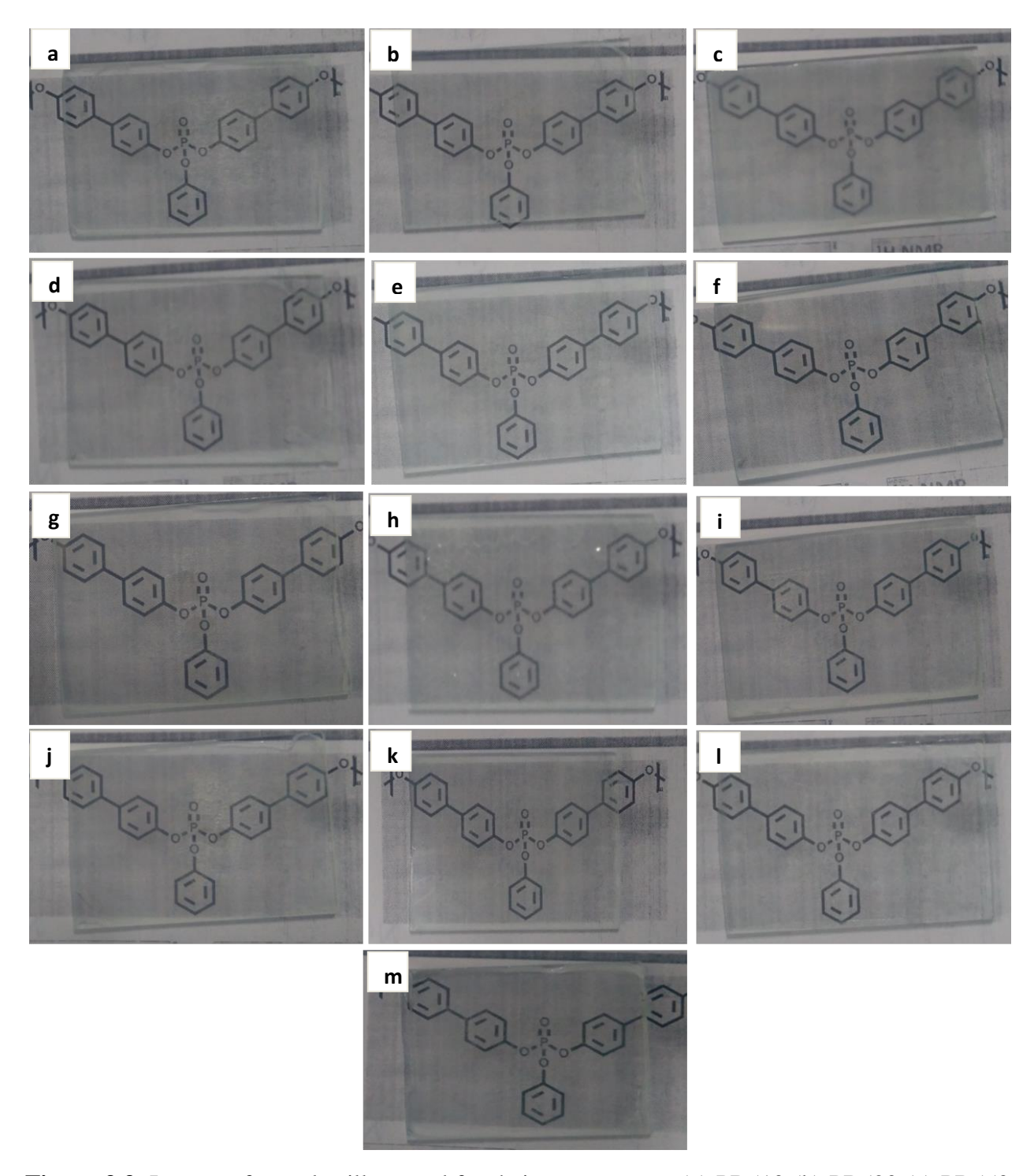


Figure 3.3: Images of samples illustrated for their transparency (a) PB510 (b) PB520 (c) PB550 (d) PB560 (e) PB580 (f) P5 (g) PB610 (h) PB620 (i) PB650 (j) PB660 (k) PB680 (l) P6 (m) PMMA

3.2.1. FT-IR spectra and interaction between polymers in blend

The infrared spectra of the polymers and their blends are shown in Figure 3.4. The characteristic FT-IR bands of PMMA are observed at 1386 cm⁻¹ and 750 cm⁻¹ corresponding to vibrations of the α-methyl group while the 1141 cm⁻¹ and 1188 cm⁻¹ bands correspond to the C-O-C stretching (Figures 4(a) and (b)). C-H bending is observed at 1434 cm⁻¹, and the carbonyl stretching band is observed at 1721 cm⁻¹. At 2949 cm⁻¹ and 2992 cm⁻¹, the C-H stretching of CH₂ and CH₃ are observed respectively.^{31, 32}

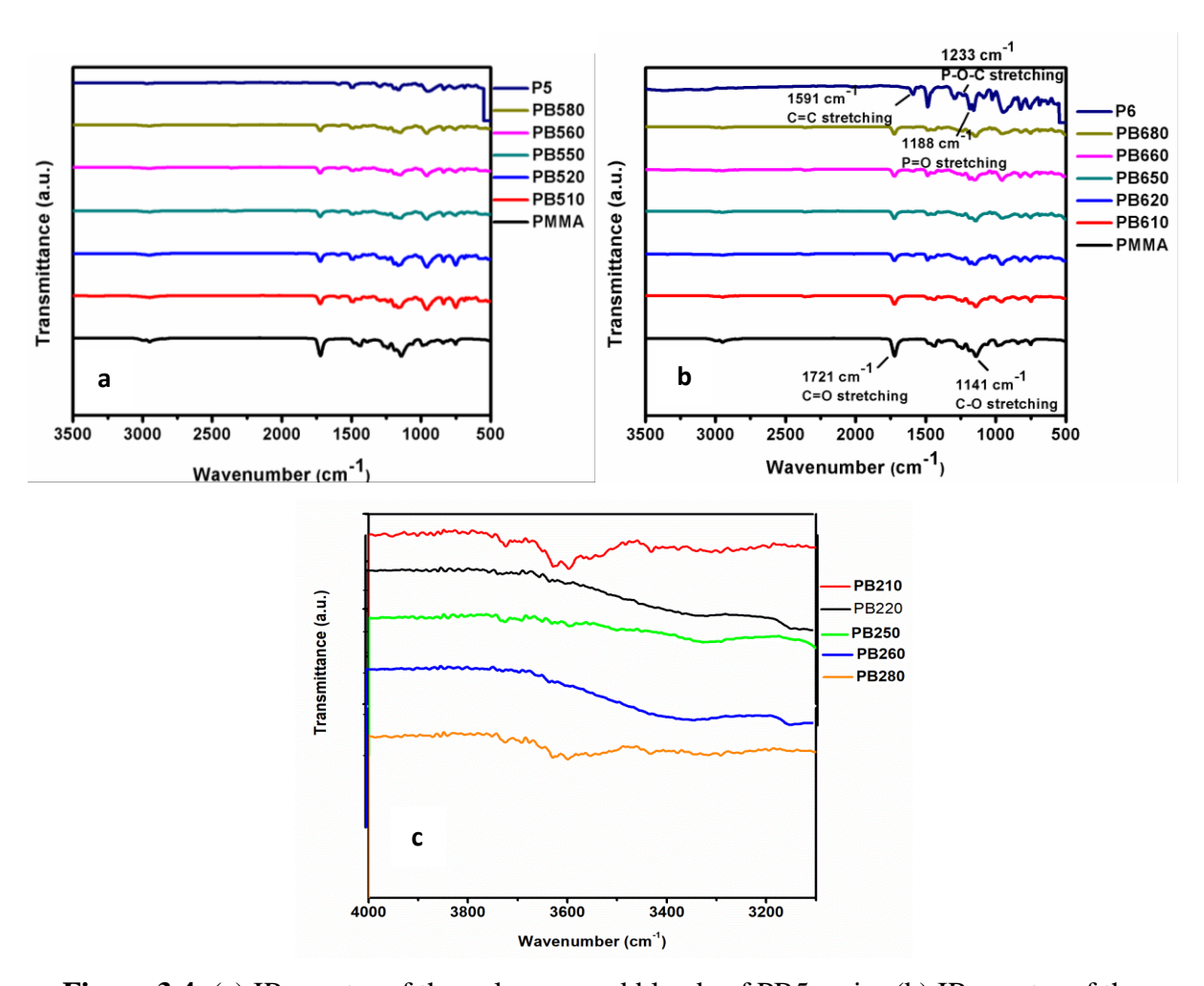
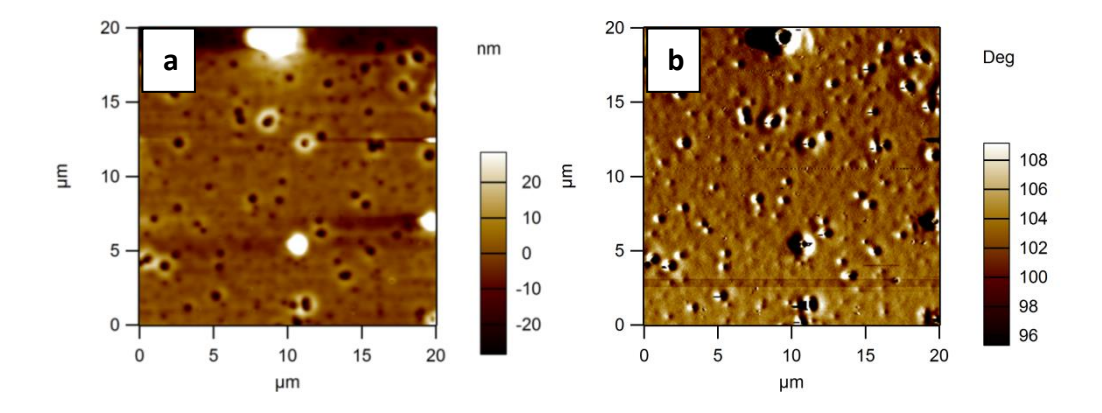


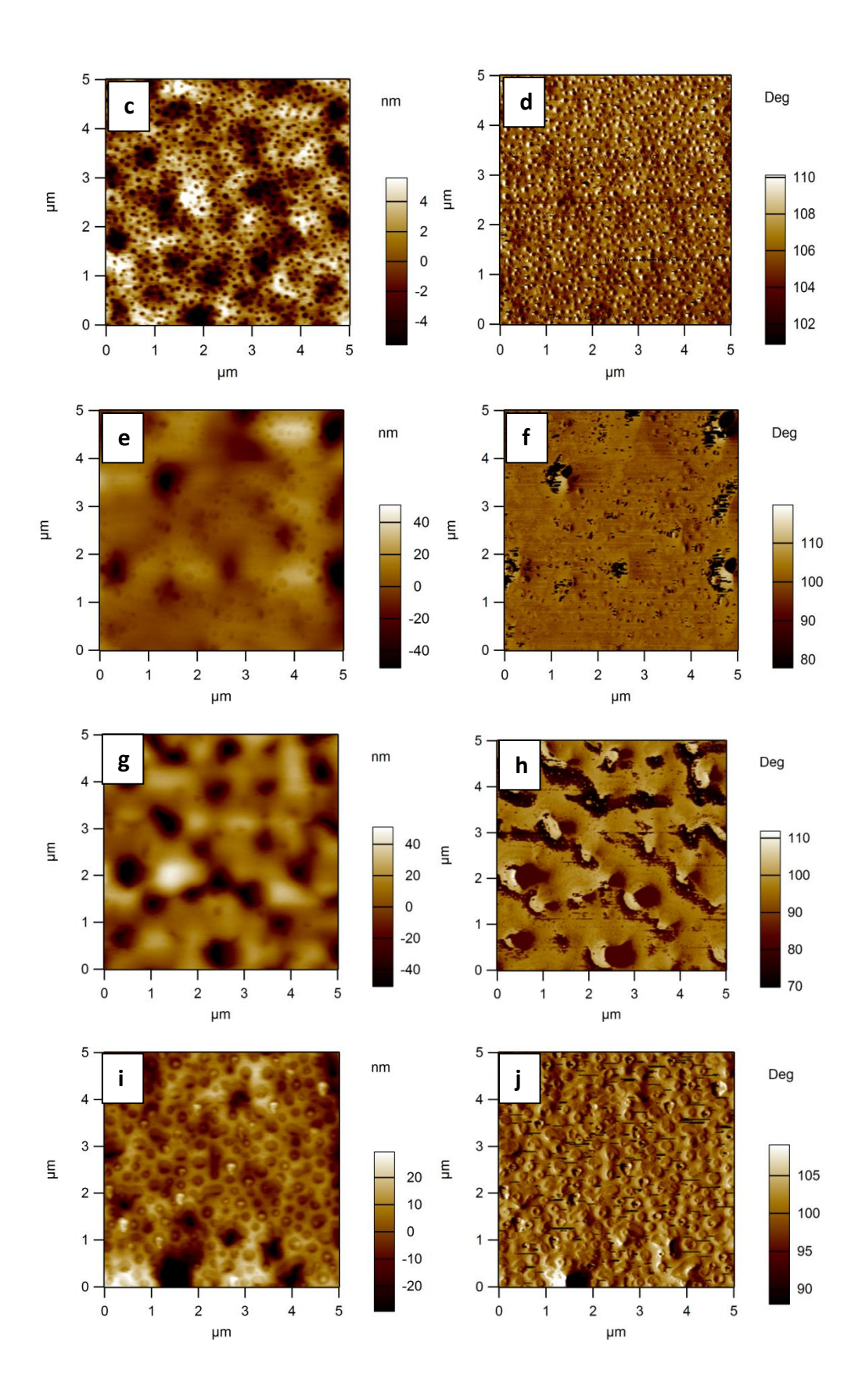
Figure 3.4: (a) IR spectra of the polymers and blends of PB5 series (b) IR spectra of the polymers and blends in PB6 series(c) IR spectra of the blends of PB6 series showing the region 3200-3550 cm⁻¹illustrating intermolecular hydrogen bonding.

After blending with the polyphosphates, the characteristic phosphate bands at 1233 cm⁻¹ and 1191 cm⁻¹ corresponding to P-O-C and P=O stretching are observed in the blended samples along with the C=C stretching at 1591 cm⁻¹. This observation confirms the formation of the blend. The nature of interactions between the polyphosphates and PMMA is explained from the evidence of hydrogen bonding in blends. The presence of broad peaks in the region 3200-3500 cm⁻¹ is indicative of the intermolecular hydrogen bonding between polyphosphates and PMMA (Figure 3.4.(c)). Hydrogen bonding could take place between the carbonyl oxygen of PMMA and methyl groups of P1.³³Similarly, phosphoryl oxygen of P5 and P6 can interact with methyl of PMMA. However, since the hydrogen bonding is quite weak, there is no considerable red-shift observed in the IR frequencies corresponding to those hydrogen-bonded groups.

3.2.2. AFM topography and uniformity of the blends:

Herein, the AFM topography and phase images of two representative blends from either series are shown in figure 3.5 along with the pure polymers P5 and P6. The images of blends with lower percentages of polyphosphates, P5 or P6 show a more uniform morphology compared to the blends with higher percentages of polyphosphates.





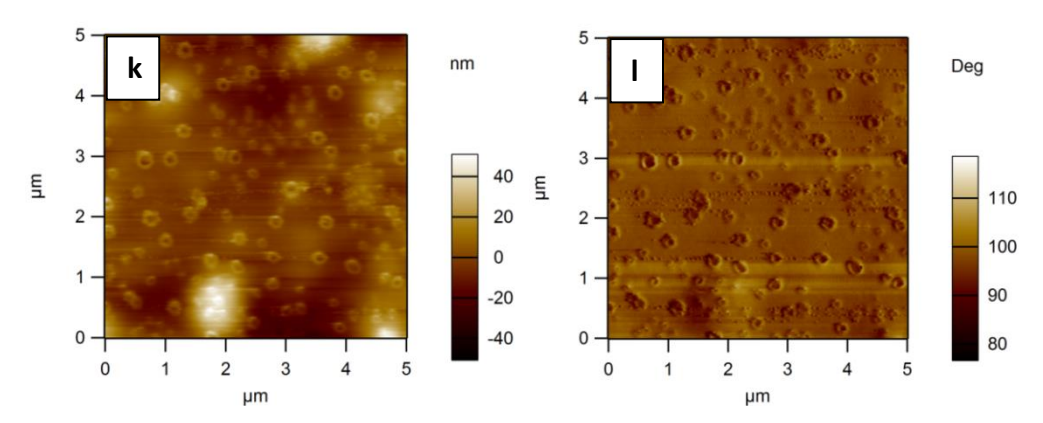


Figure 3.5: AFM topography (right) and phase (left) images of P5 (a and b), PB510 (c and d), PB580 (e and f), PB660 (g and h), PB620 (i and j), P6 (k and l).

3.2.3. Absorption behavior of polyphosphates

In order to understand the optical absorption of polyphosphates and their blends with PMMA, the polyphosphates were subjected to UV-Vis-NIR optical absorption studies. As the optical absorption of PMMA was well studied and reported elsewhere, 34, 35 it was not presented here. The spectra of P5 and P6 recorded from 1400 nm to 200 nm are presented in figure 3.6(a). The absorption of P5 in visible and NIR region is almost zero from 1400 nm to 370 nm compared to base line. In case of P6, in the visible region, an additional absorption peak shows broadband centered at 480 nm with an onset absorption of 520 nm (see figure 3.6(b)). It has been reported that the visible light absorbance has several contributions such as intrinsic absorbance (actual absorbance due to electronic excitation), scattering (apparent absorption due to scattering with respect to particle or grain size) and the dopant effect.³⁶In this case, the addition absorption in P6 at λ_{max} around 480 nm is probably due to inter band transition. On the other hand, in the UV region (300 -200 nm, inset) multiple oscillations were observed in the sample P5 (λ_{max} 240, 260, 270 and 285 nm) whereas P6 shows only a single oscillation having λ_{max} 250 nm. These peaks are mainly due to π - π * band of benzene ring.³⁷ All the above peaks in the UV region are characteristic absorption of biphenyl derivatives with phosphorus in the main chain as reported by Freedman.³⁸

Figure 3.6(c) shows the extinction co-efficient of the P6 blended samples. The PB5 polymer blends, on the other hand, showed negligible or zero extinction coefficients and hence not explicitly plotted. The samples PB610 and PB620 are not showing any additional characteristic absorption in the range 1400 to 370 nm similar to P6. Upon increasing the P6

weight % further, the sample PB650 shows the characteristic absorption around 590 nm. Similarly, further increasing the P6 concentration, shifts the absorption peak to lower energy side. The heavily doped sample PB680 shows multiple oscillations in the range 400 to 1000 nm. From this observation, it is clear that the processing conditions and the addition of polyphosphates into PMMA changes the optical properties by entering into the basic network of the PMMA. Doping basically affects the overall film absorption and the band gap of the film depending upon the concentration. ³⁶Such controllable absorption behavior depending upon the weight % of polyphosphates are highly recommended for tuning the optical properties depending upon the applications.

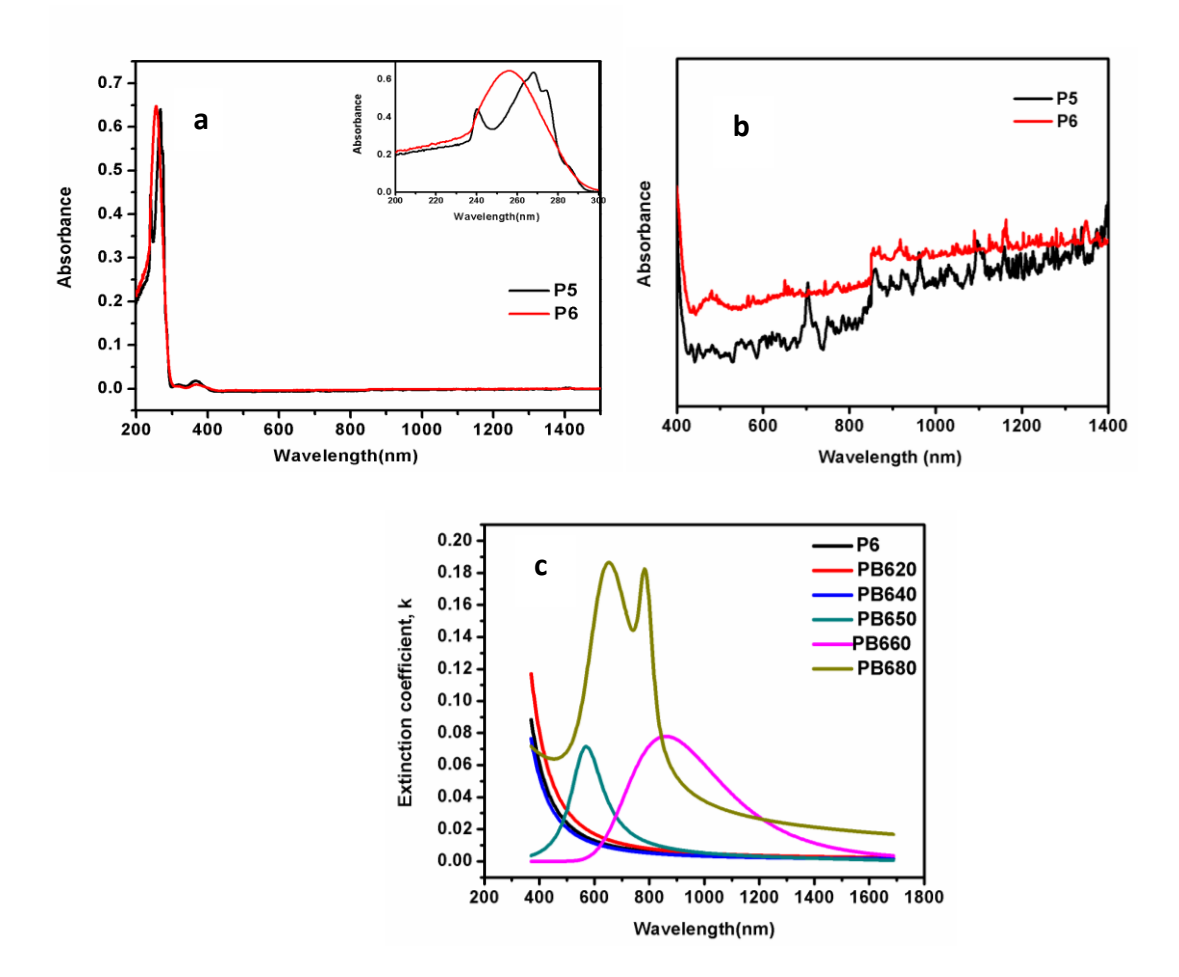


Figure 3.6: (a) Absorption spectra of P5 and P6 (b) Absorption spectra of P5 and P6 (c) Extinction coefficients of blends of P6.

3.2.4. Thermal analysis of the polyphosphates and their blends

All the blends in PB5 and PB6 series showed a thermal stability of about 100 °C on an average, which is quite reasonable for a variety of optical applications (Figure 3.7(a) and b). Analysis of glass transition temperatures of the blends in PB5 series indicate that they are completely miscible blends since their Tg lie in between the parent polymers as shown in figure 3.7(c). In case of PB6 series also, the Tg of the blends lie almost in the same range as the blends of PB5 series and is all below that of parent polymer PMMA (Figure 3.7(d)). However, since the polymer P6 shows a gradual weight loss starting from around 45 °C itself, the DSC analysis of the polymer could not be performed.

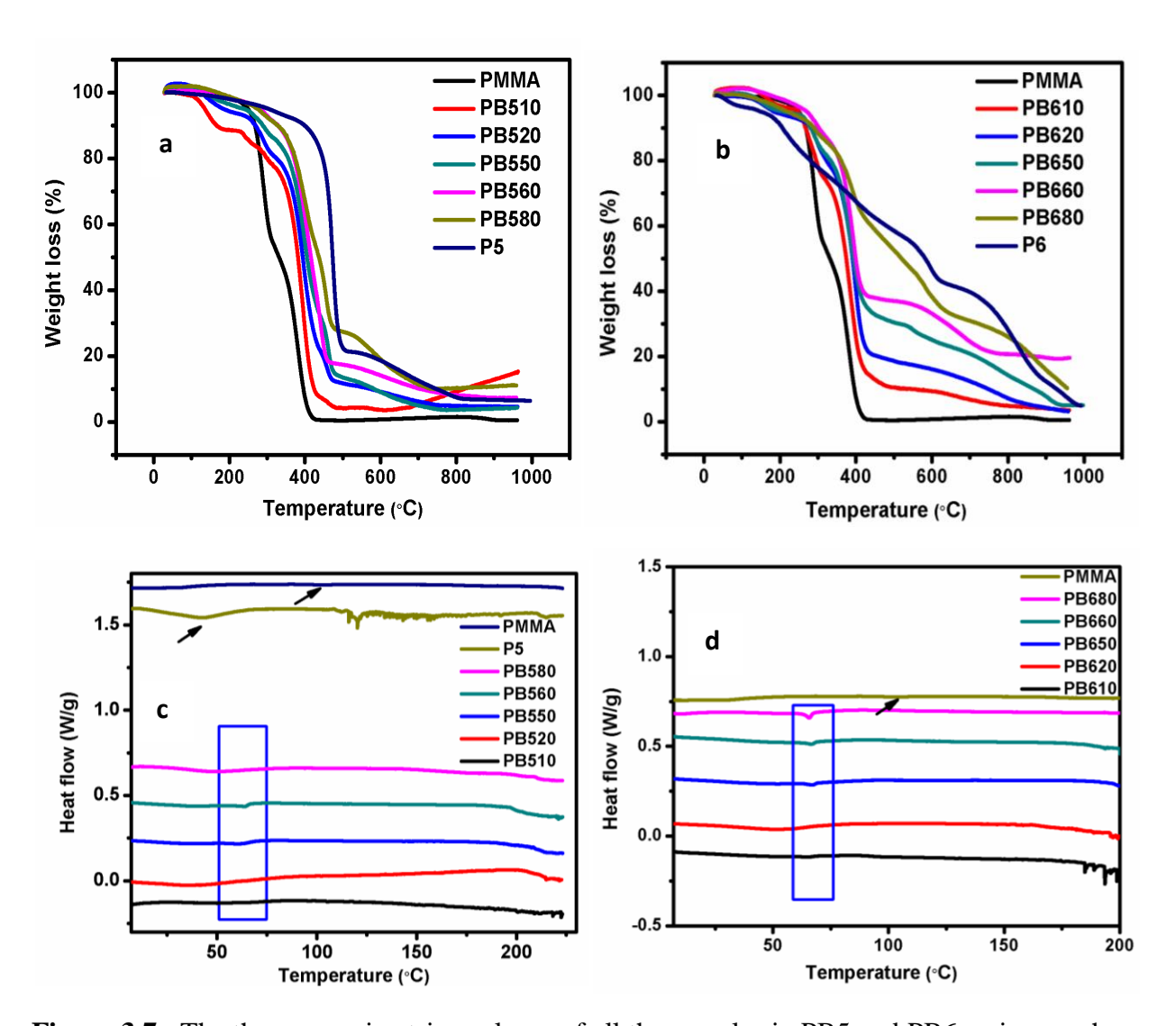
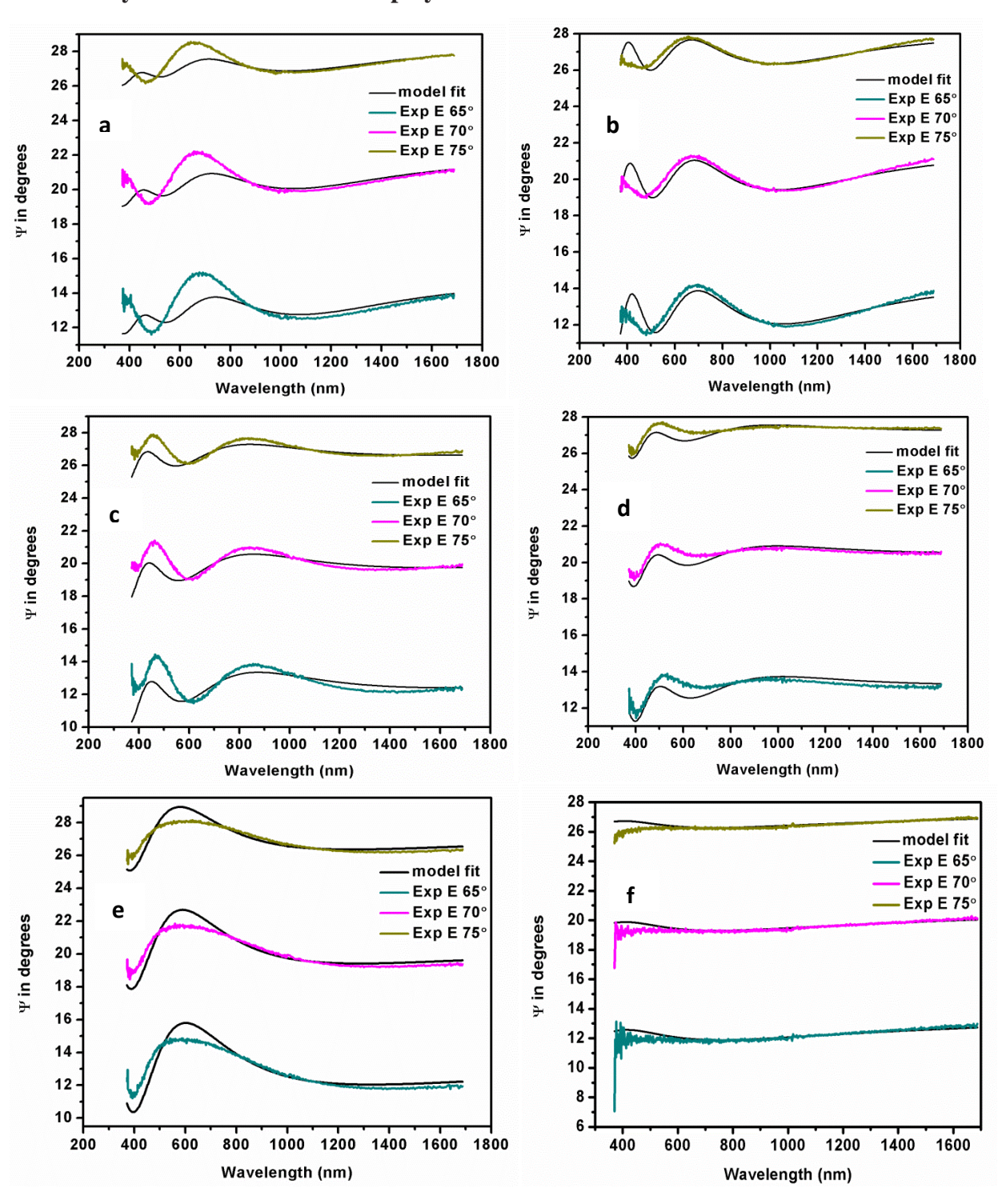
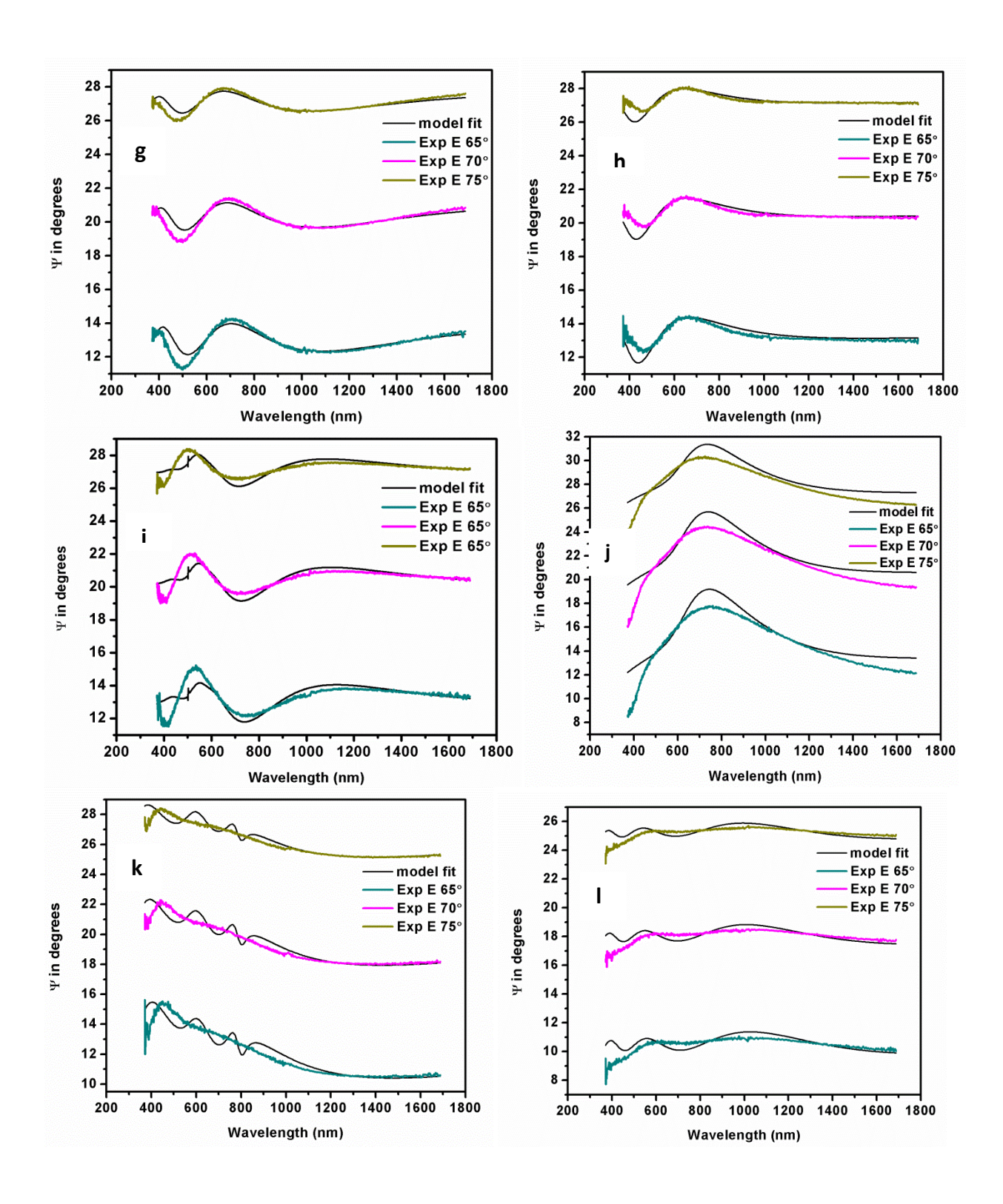


Figure 3.7: The thermogravimetric analyses of all the samples in PB5 and PB6 series are shown in figure (a and b). In both PB5 and PB6 series, all the blends are stable upto 180 °C. However, in

case of PB6 series, the polymer P6 shows a gradual decay in thermal stability, because of which the DSC measurement could not be undertaken for the parent polymer P6. The boxes and arrows in the figure indicate the Tgs of various samples denoted.

3.2.5. Study of refractive indices of polymer blends





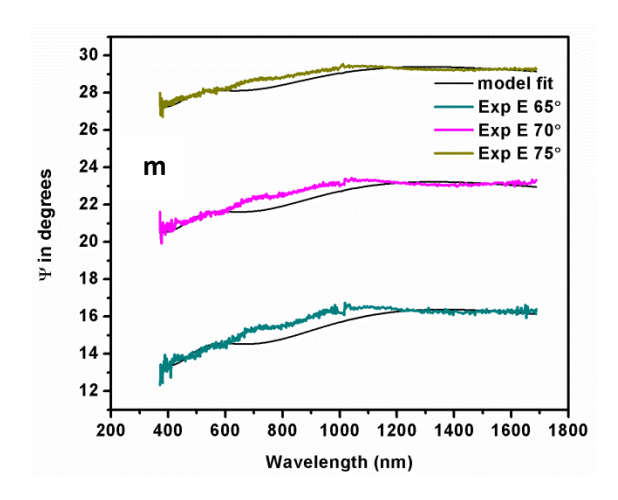


Figure 3.8: Ellipsometric spectra for the samples spin-coated on a glass substrate (experimental data and model fit are shown) (a) PB510 (b) PB520 (c) PB550 (d) PB560 (e) PB580 (f) P5 (g) PB610 (h) PB620 (i) PB650 (j) PB660 (k) PB680 (l) P6 (m) PMMA

3.2.5.1. PB5 series:

The refractive indices of the polymer blends listed in the table 2 were determined using ellipsometer and values were deduced from theoretical model fitting. The data was measured at three different wave lengths (486, 589 and 656 nm). A representative sequence of graphs showing how the data is obtained is given below. The experimental data which was found to be in close agreement with the theoretical model as is evident from the representative figure 3.9(a) is used to get the refractive index data shown in figure 3.9(b) and the uniqueness of the fit was analyzed for each sample by the uniqueness fit as is represented in figure 3.9(c). The fit was obtained employing minimum MSE and Kramers-Kronig consistency.

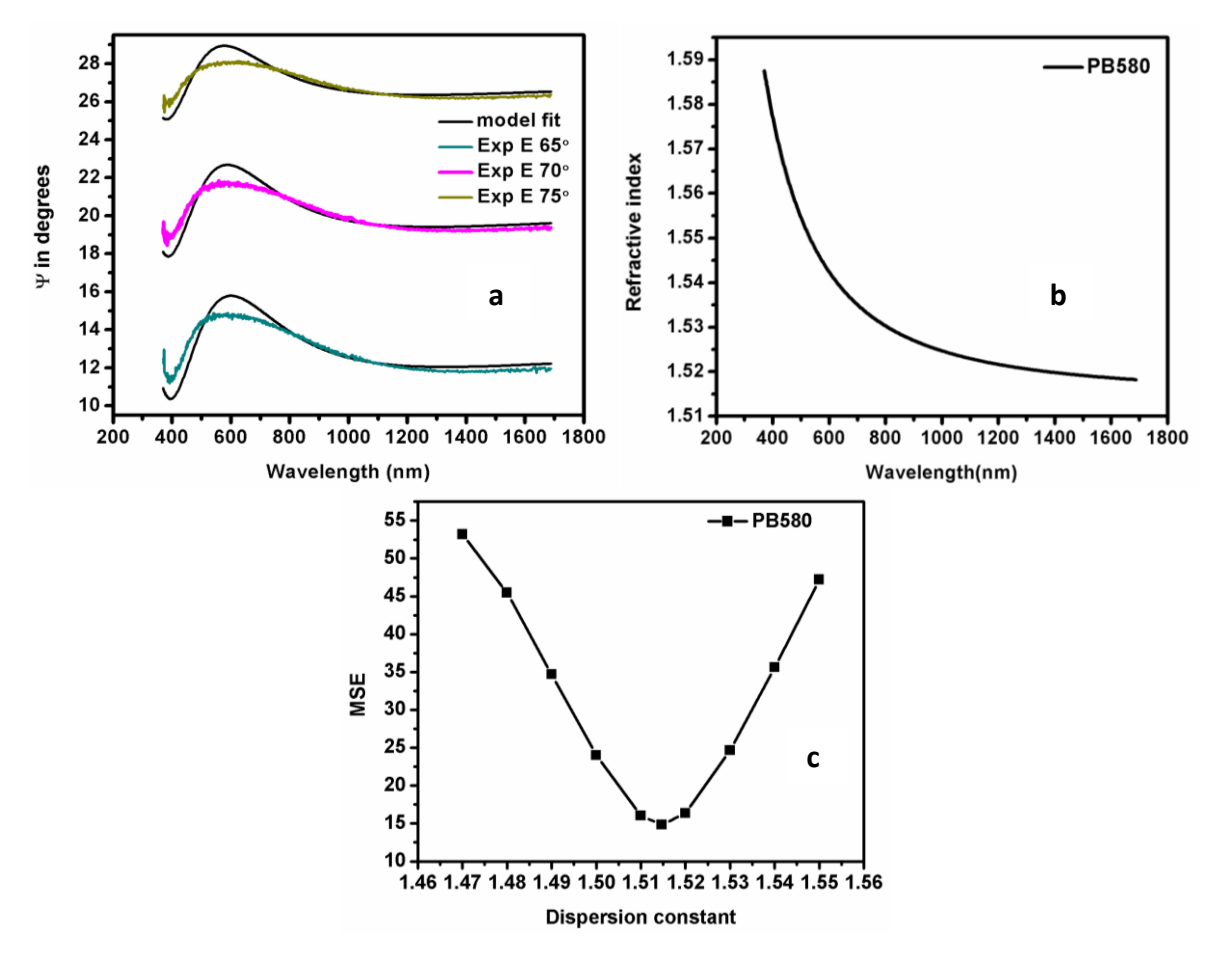


Figure 3.9: (a) Ellipsometric spectra of a sample (PB580) spin-coated on a glass substrate (experimental data and model fit are shown) (b) variation of refractive index with wavelength and (c) uniqueness fit for the sample PB580.

For a better understanding of the trend in change of RI with increasing concentration of polyphosphates, the values are plotted with respect to weight percentages of P5 and P6, as shown in figure 3.10(b) and 3.11(c). Refractive indices at three different wave lengths and the maximum value of RI for a particular sample are tabulated (Table 3.3).

In PB5 series, the general observation is that the addition of P5 into the PMMA system increases the RI of PMMA. Some of the compositions, specifically the ones with higher concentration of P5 (PB550, PB560 and PB580) showed higher RI than both the parent polymers, PMMA and P5. Also, the general trend of decrease in RI with increase in wavelength is followed intact in the PB5 series. But, the most important inference is that a refractive index tunability of 0.05 was achieved with the help of introduction of P5 into PMMA. This is quite

significant a number since a change in refractive index of about even 0.01 could bring about a change of 3.30 D actual change in its power in a perfect lens system.³⁹

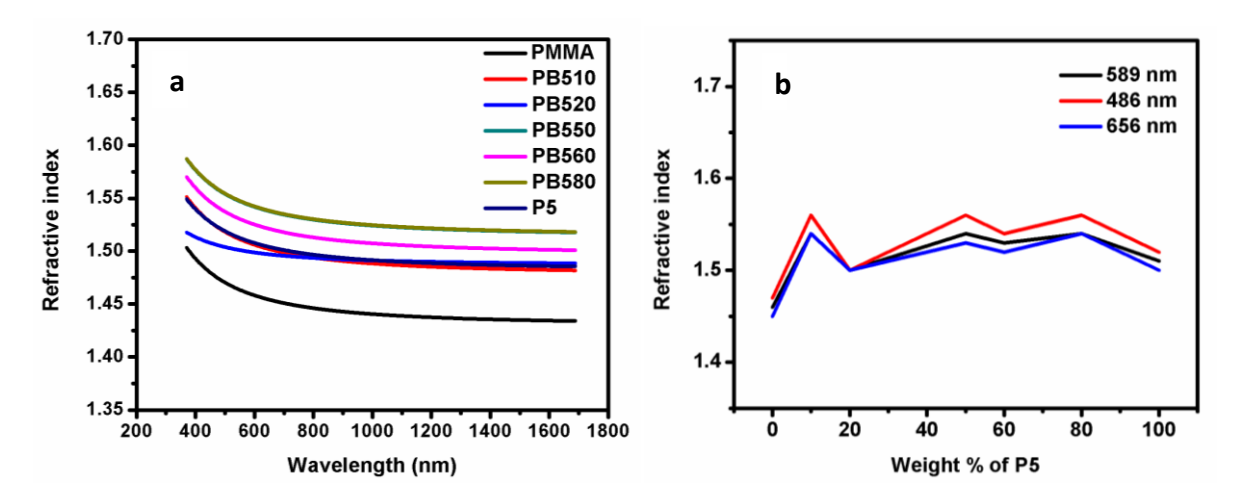


Figure 3.10: (a) Variation of refractive indices with wavelengths for PB5 series (b) Variation of refractive indices with different weight percentages for PB5 series.

3.2.5.2. PB6 series:

In contrast to the PB5 series, the PB6 series showed RI in between PMMA and P6.Most of the samples except PB660, have RI falling above PMMA but below P6. A tunability of about 0.1 in RI was observed with variation in concentration of P6. All these are valuable insights when it comes to the application point of view. The PB660 blend is showing comparatively lower RI than others in the series. As the optical properties of thin films depend on several factors like structure, thickness, homogeneity, materials used and the preparation conditions, it is difficult to estimate exactly the reason for this anomaly. However, since we have followed the same protocol for all the samples, the reason could probably be some irregularity which occurred during sample preparation.

On the other hand, the samples with higher weight percentages of P6 in the PB6 series showed increase in RI beyond a particular wavelength. This is particularly useful in designing optical filters where absorption beyond the visible range is advantageous. The reason for such a behavior can be directly correlated with the extinction coefficient graph of these blends because the imaginary part of complex refractive index is nothing but the extinction coefficient.

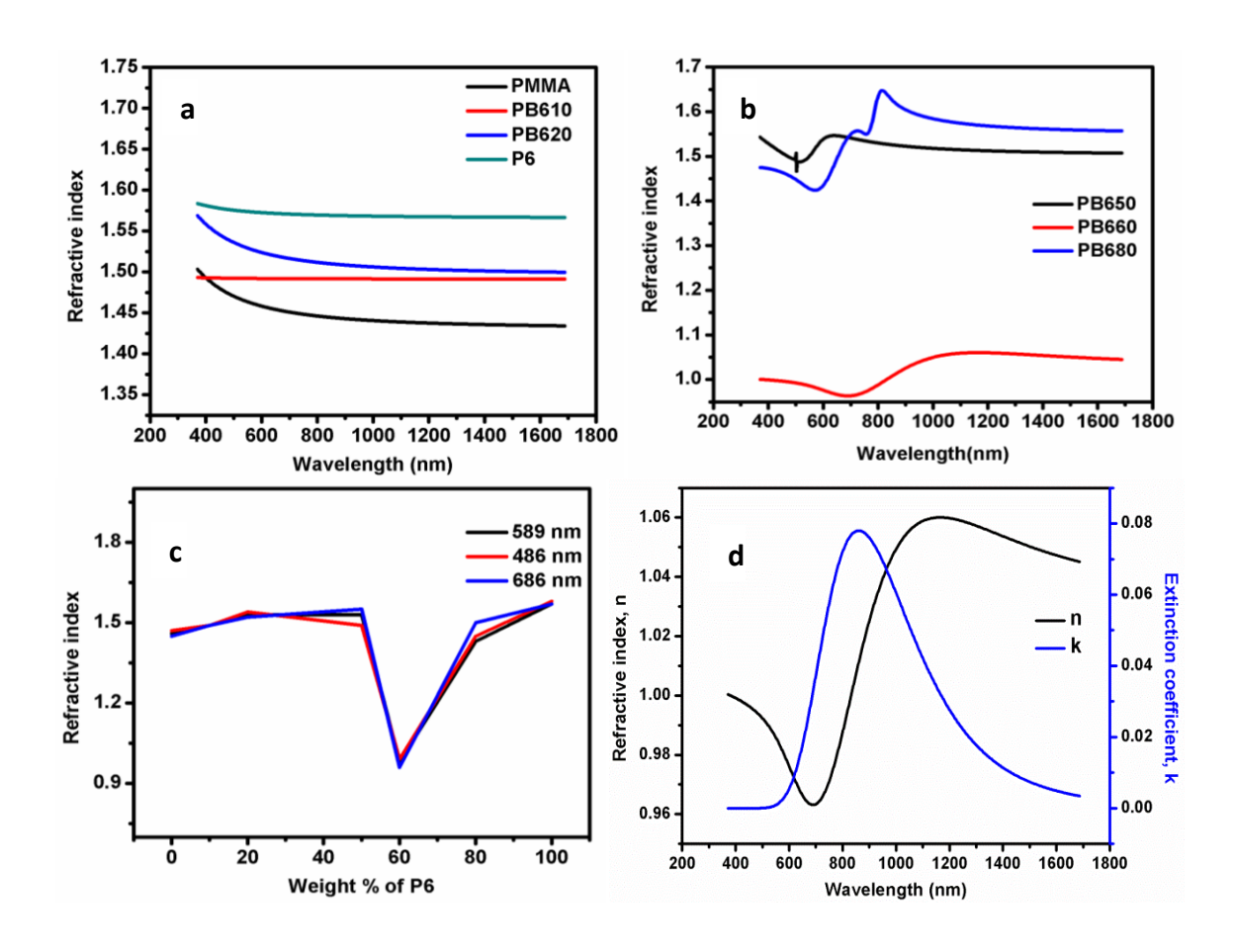


Figure 3.11: (a) Variation of refractive indices with wavelengths for PMMA, PB610, PB620 and P6 (b) Variation of refractive indices with wavelengths for PB650, PB660 and PB680 (c) Variation of refractive indices with different weight percentages for PB6 series (d) a representative plot (PB660) of variation in n and k with wavelength.

Table 3.3. Refractive indices of polyphosphate blends with PMMA

Name of the blends	Weight % of P5	n ₄₈₆	n ₅₈₉	n ₆₅₆	n _{max}
PMMA	0	1.47	1.46	1.45	1.50 (370nm)
PB510	10	1.56	1.54	1.54	1.55 (370nm)
PB520	20	1.50	1.50	1.50	1.52 (370nm)
PB550	50	1.56	1.54	1.54	1.58 (370nm)
PB560	60	1.54	1.53	1.52	1.57 (370nm)
PB580	80	1.56	1.54	1.54	1.58 (370nm)
P5	100	1.52	1.51	1.50	1.55 (370nm)
	Weight % of P6	n ₄₈₆	n ₅₈₉	n ₆₅₆	n _{max}

PMMA	0	1.47	1.46	1.45	1.50 (370nm)
PB610	10	1.49	1.49	1.49	1.49(constant)
PB620	20	1.54	1.53	1.52	1.57(370nm)
PB650	50	1.50	1.53	1.55	1.55(645nm)
PB660	60	0.99	0.98	0.97	1.06(1164nm)
PB680	80	1.45	1.43	1.50	1.65 (815nm)
P6	100	1.58	1.57	1.57	1.58(370nm)

3.2.6. Tunability in optical properties of PB5 and PB6 blends

Abbe's number (V_D) is an essential parameter of optical materials indicating its optical dispersion and is given by the equation:

$$V_D = \frac{n_{D-1}}{n_F - n_C}$$

In this equation, n_D , n_F , and n_C are the refractive indices of material at the wavelengths of the sodium D (589.3 nm), hydrogen F (486.1 nm), and hydrogen C (656.3 nm) lines, respectively. Therefore, the abbe's numbers of PB5 series were calculated (Table 3.4.). The Abbe values are generally denoted only for transparent glass like materials to account for its optical dispersion and hence could not be calculated for PB6 series. Interestingly, all PB5 blends showed values within the acceptable range of abbe values of optical lens materials with a maximum of 56 for PB520 (figure 3.12).

In short, PMMA which has a refractive index of about 1.48 upon blending with these polyphosphates, showed tunability of RI from 0.97- 1.55 at 589nm. Also as discussed in section 3.2.5.2., the blends in PB6 series with higher concentrations of P6 (PB650, PB660 and PB680) reflects a similar trend in refractive index as the extinction coefficients of these samples. Hence these may not be suitable candidates for lens kind of applications, but they may be suitable for optical filter kind of applications where absorption over a certain wavelength range is highly preferred. While all the blends in PB5 series and the first two blends of PB6 series, fall under the same category showing a regular trend of decreasing RI with increasing wavelength and these are potential candidates for lens kind of applications.

Table 3.4. Abbe values of PB5 blends

Weight %	Abbe no
of P5	
0	25
10	29
20	56
50	29
60	29
80	30
100	29

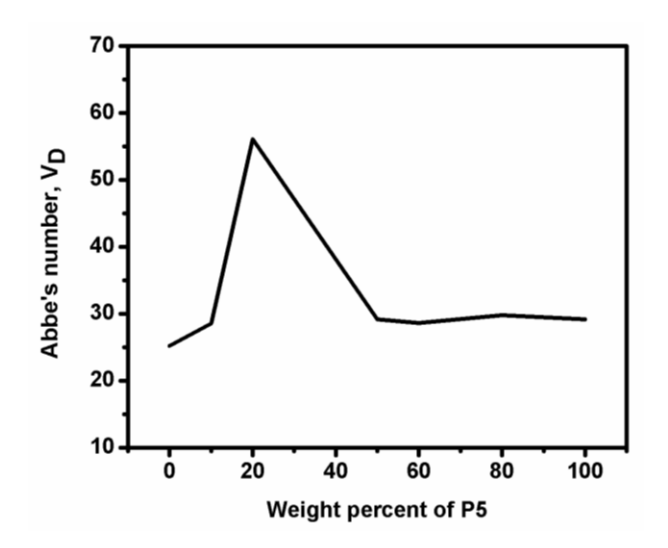


Figure 3.12: Abbe values of blends of PB5 series plotted at increasing weight percentages of P5.

3.3. Conclusions

The synthesized polymers P5 and P6 were well characterized by NMR, IR and GPC and further used for blending. We have employed a relatively simple and efficient method of solution blending and spin coating to synthesize uniform and transparent films for optical applications. The ellipsometric measurements show that the PB5 and PB6series showed a tunability in RI of about 0.05 and 0.1 respectively. Also, abbe values of PMMA blends with P5 showed an acceptable abbe value range of optical lens materials, with a maximum of 56 for PB520 blend. Blends with higher weight percentages of P6 on the other hand could be promising for optical

filters. Preliminary investigation is quite promising in a way, as of how we can engineer the desired refractive index and abbe number by incorporating the polyphosphates into PMMA. Also, PMMA is well known for its compatibility with human tissue and hence could be ideal for rigid intraocular lenses with the desired refractive index tailored by the incorporation of these polyphosphates.

3.4. Experimental section

3.4.1. Materials and instrumentation

Materials: Phenyl dichlorophosphate, Poly(methyl methacrylate) (average molecular weight 1,20,000 Da) and 1,3-dioxolane were purchased from Sigma Aldrich, 1-methyl imidazole from Merck, bisphenol A from SRL, and 4,4'-biphenol from TCI respectively.

All the NMR spectra were recorded on a Bruker Avance 500 MHz FT NMR spectrometer at R.T. Chemical shifts were reported in parts per million (δ) relative to tetramethylsilane as reference for proton and 85% H₃PO₄ for phosphorus (162 MHz). Molecular weights of the polymers were determined by Gel Permeation Chromatography (GPC) of Shimadzu 10AVP model. The separation was achieved using Phenogel mixed bed column (300 × 7.80 mm) operated at 30°C with a flow rate of 0.5 mL/min using tetrahydrofuran (THF) as the eluent and polystyrene as the standard. Absorption studies were done on a JASCO V-770 model spectrophotometer and spin coating was done with a Milman SPN4000S model spin coater. AFM was recorded in tapping mode using Oxford instruments Asylum ResearchInc. version 13.

Refractive index and associated optical parameters were obtained using a J.A. Woollam Company VASEW ellipsometer. Optical modeling and data analysis were done using the Woollam Company WVASE32 software package.

3.4.2. General synthetic procedure for the polymers P5 and P6:

A solution of phenyl dichlorophosphate (1 mmol) in 1,3-dioxolane (5mL) was added dropwise over 1 h to a stirring mixture of diol (1 mmol), 1-methylimidazole (2 mmol) and 1,3-dioxolane (5 mL) at R.T. The reaction mixture was stirred for 3h at R.T. and then the mixture was heated at 75°C. After the reaction was completed, two clear liquid phases occurred that can be easily

separated.^{26,40} The upper phase was the polymer solution and the lower phase was the pure ionic liquid. The 1,3-dioxolane solution was removed by vacuum evaporation on a rotary evaporator.

3.4.3. Sample preparation for ellipsometry and data analysis

The samples for ellipsometric measurements were prepared by spin-coating. Initially PMMA was stirred in 3mL of chloroform until the solution was homogeneous and then the as synthesized polymer P1 or P2 at definite weight ratio was added and stirred for 12 hrs to make the blend homogeneous and spin-coated on a glass substrate. The solution mixing and spin-coating ensures uniform mixing as well as uniform thickness of the film on a clean soda lime glass (SLG). The prepared sample on SLG was carefully abraded on other side in order to avoid the back reflection during ellipsometry data collection. A typical sample spin coated on a glass substrate is shown in Figure 3.2.

Refractive index and associated optical parameters were obtained using ellipsometric data analysis. Ellipsometric data (Δ and ψ) was acquired by variable angle spectroscopic ellipsometry (VASE) in a range of 400 – 1700 nm with a J.A. Woollam Co., Inc. WVASE32 spectroscopic ellipsometer, at the angle of incidence from 65° to 75°. For the PB5 series, simple two layer model with Cauchy top layer and SLG (substrate) as the bottom layer was used to generate the data. In the case of PB6 series, Cauchy dispersion model was used in the longer wave length to estimate the coating thickness, and further the model was extended to oscillator models in order to understand absorption properties. The data fitting is performed using the iterative Marquardt-Levenberg fitting algorithm. The individuality of the regression analysis has been confirmed by repeating the analysis and data collection on several locations and uniqueness fit. All the data analysis and validation processing was done using the Woollam Company WVASE32 software package.

Supporting information: ^IH NMR and ³¹P NMR of the polymers P5 and P6 are provided at the end of the chapter.

3.5. References

[1] M. Yoshida, P.N. Prasad, *Chem. Mater.*, 1996, **8**, 235–241.

- [2] P. Müller, B. Braune, C. Becker, H. Krug, H. Schmidt, *Proc. SPIE-Int. Soc. Opt. Eng.*, 1997, **3136**, 462.
- [3] C.J. Yang, S.A. Jenekhe, *Chem. Mater.*, 1994, **6**, 196–203.
- [4] T. Sugiyama, T. Wada, H. Sasabe, Synth. Met., 1989, 28, 323–328.
- [5] C.J. Yang, S.A. Jenekhe, *Chem. Mater.*, 1995, **7**, 1276–1285.
- [6] M. Liras, M. Barawi, V.A. de la Pe~na O'Shea, Chem. Soc. Rev., 2019, 48, 5454–5487.
- [7] M. Jose, M. Sakthivel, *Mater. Lett.*, 2014, **117**, 78–81.
- [8] M.R. Noor El-Din, I.M. El-Gamal, S.H. El-Hamouly, H.M. Mohamed, M.R. Mishrif, A.M. Ragab, *Colloid. Surface. Physicochem. Eng. Aspect.*, 2013, **436**, 318–324.
- [9] T.E. Kodger, J. Sprakel, Adv. Funct. Mater., 2013, 23, 475–482.
- [10] D.W. VanKrevelen, Properties of Polymers, third ed., Elsevier, Amsterdam, 1990.
- [11] Z. Fan, M.K. Serrano, A. Schaper, S. Agarwal, A. Greiner, *Adv. Mater.*, 2015, **27**(26), 3888–3893.
- [12] L.L. Beecroft, C.K. Ober, *Chem. Mater.*, 1997, **9**(6), 1302–1317.
- [13] C. Janáky, K. Rajeshwar, *Prog. Polym. Sci.*, 2015, **43**, 96–135.
- [14] R. Barbey, L. Lavanant, D. Paripovic, N. Schüwer, C. Sugnaux, S. Tugulu, H.A. Klok, *Chem. Rev.*, 2009, **109** (11), 5437–5527.
- [15] R. Okutsu, Y. Suzuki, S. Ando, M. Ueda, *Macromolecules*, 2008, 41, 6165–6168.
- [16] T. Higashihara, M. Ueda, *Macromolecules*, 2015, **48**, 1915–1929.
- [17] R.F. Hudson, Structure and Mechanism in Organo-Phosphorus Chemistry, Academic Press, London, 1965.
- [18] H.V. Babu, K. Muralidharan, *Polymer*, 2014, **55**, 83–94.
- [19] H.V. Babu, B. Srinivas, K.P.K. Naik, K. Muralidharan, *J. Chem. Sci.*, 2015, **127**, 635–641.
- [20] H.V. Babu, B. Srinivas, K. Muralidharan, *Polymer*, 2015, **75**, 10–16.
- [21] M.A. Olshavsky, H.R. Allcock, *Macromolecules*, 1997, **30**, 4179–4183.

- [22] M.A. Olshavsky, H.R. Allcock, *Macromolecules*, 1995, **28**, 6188–6197.
- [23] V. Sekharipuram, H. K. Shobha, J. E. McGrath, A. Bhatnagar, U.S. Patent, 6, 288, 210 B1, September 11, 2001.
- [24] H.K. Shobha, H. Johnson, M. Sankarapandian, Y.S. Kim, P. Rangarajan, A.D. Baird, J.E. McGrath, *J. Polym. Sci.: Polym. Chem.*, 2001, **39**, 2904–2910.
- [25] E.K. Macdonald, J.C. Lacey, I. Ogura, M.P. Shavera, Eur. Polym. J., 2017, 87, 14–23.
- [26] S. Iliescu, L. Zubizarreta, N. Plesu, L. Macarie, A. Popa, G. Ilia, *Chem. Cent. J.*, 2012, **6**, 132–145.
- [27] J.R. Van Wazer, in: F. Grayson, M. Griffin (Eds.), Topics in Phosphorus Chemistry, fifth ed., John Wiley, London, 1967.
- [28] J.R. Van Wazer, C.F. Callins, J.N. Shoolery, R.C. Jones, *J. Am. Chem. Soc.*, 1956, **78**, 5715–5726.
- [29] Y. Morisaki, Y. Ouchi, K. Tsurui, Y. Chujo, J. Polym. Sci. Polym. Chem., 2007, 45, 866–872.
- [30] H. Cavaye, F. Clegg, P.J. Gould, M.K. Ladyman, T. Temple, E. Dossi, *Macromolecules*, 2017, **50**, 9239–9248.
- [31] G. Duan, C. Zhang, A. Li, X. Yang, L. Lu, X. Wang, *Nanoscale Res. Lett.*, 2008, **3**, 118–122.
- [32] K. Gipson, K. Stevens, P. Brown, J. Ballato, J. Spectrosc., 2014, 2015, 1–9.
- [33] H. M. Alhusaiki-Alghamdi, J. Mod. Phys., 2019, **10**, 487–499.
- [34] H. M. Zidan, M. Abu-Elnader, *Physica B*, 2005, **355**, 308–317.
- [35] W.H. Hong, J. Woo, H.W. Choi, Y.S. Kim, G.D. Kim, *Appl. Surf. Sci.*, 2011, **169–170**, 428–432.
- [36] K. Murugan, J. Joardar, A.S. Gandhi, B.S. Murty, P.H. Borse, *RSC Adv.*, 2016, **6**, 43563–43573.
- [37] Y. Ouchi, Y. Morisaki, Y. Chujo, *Polym. Bull.*, 2007, **59**, 339–350.
- [38] L. D. Freedman, J. Am. Chem. Soc., 1955, 77, 6623–6624.
- [39] CRSToday, Laser-Induced refractive index change [online] Available at: https://cr stoday.com/articles/2019-apr/laser-induced-refractive-index-change/, 2019. (Accessed 16 December 2019).

[40] S. Iliescu, G. Ilia, A. Pascariu, A. Popa, N. Plesu, *Pure Appl. Chem.*, 2007, **79** (11), 1879–1884.

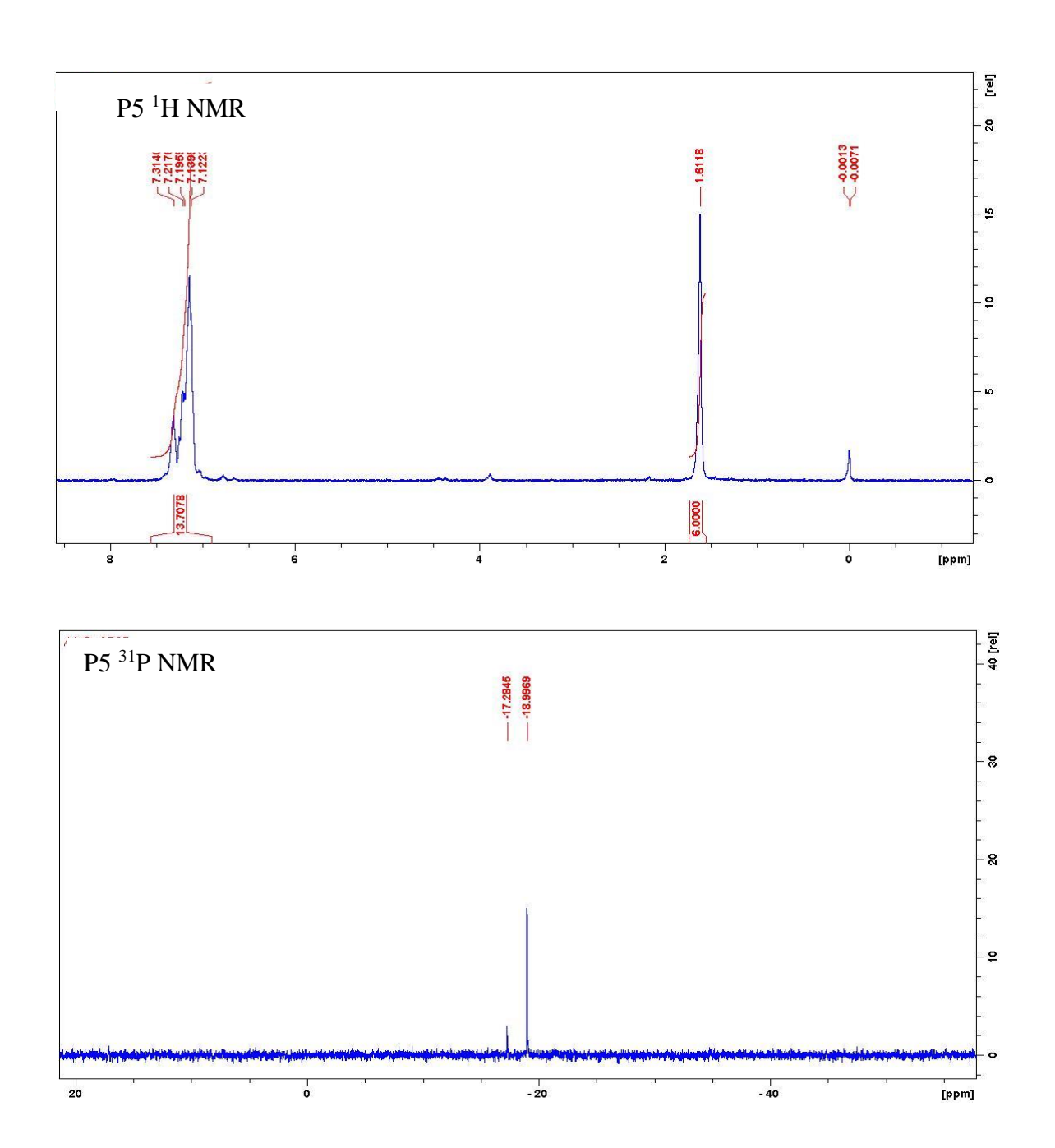
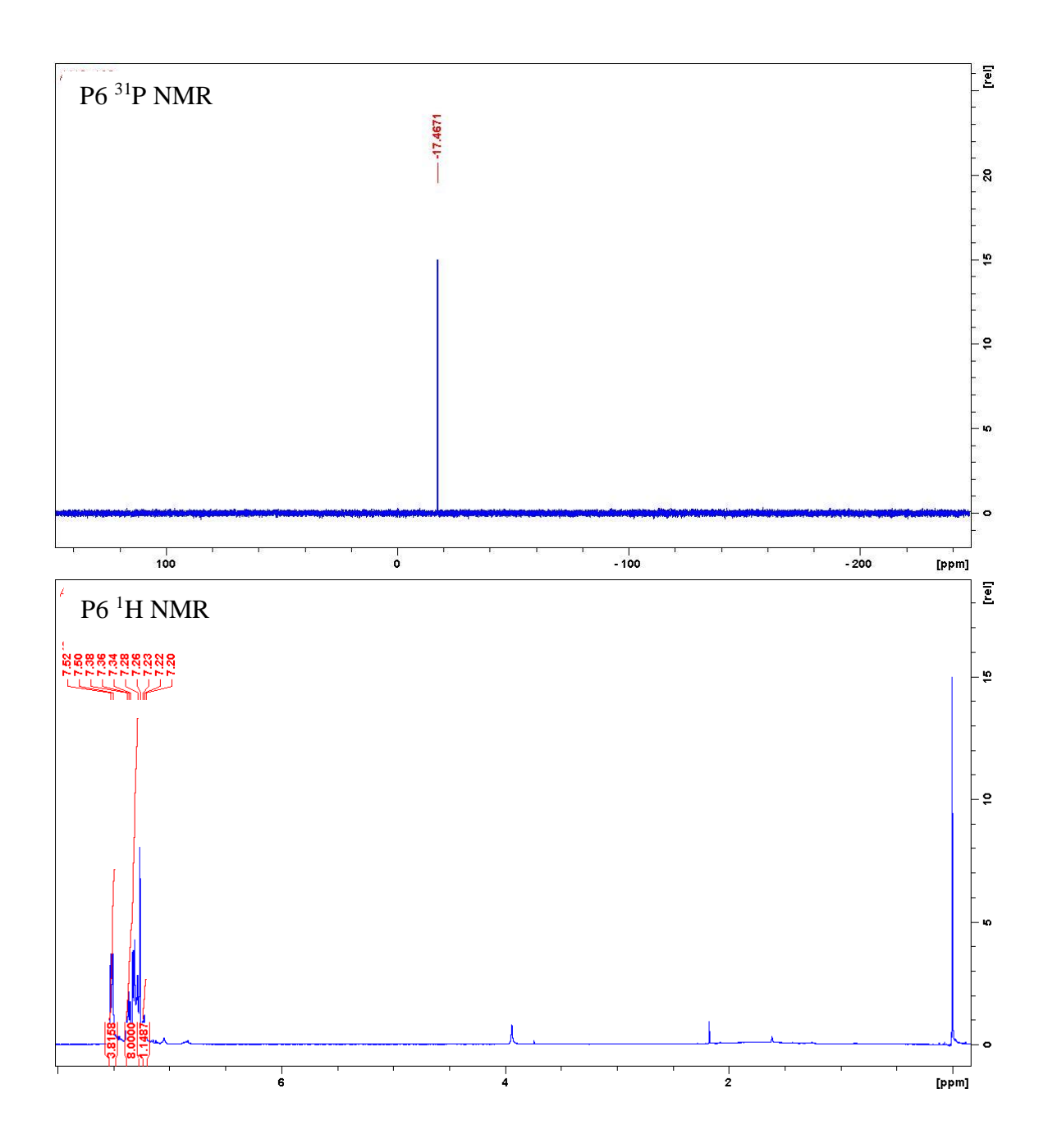


Figure 3.S1: NMR spectra of polymer P5; ³¹P NMR (top), ¹ H NMR(bottom).



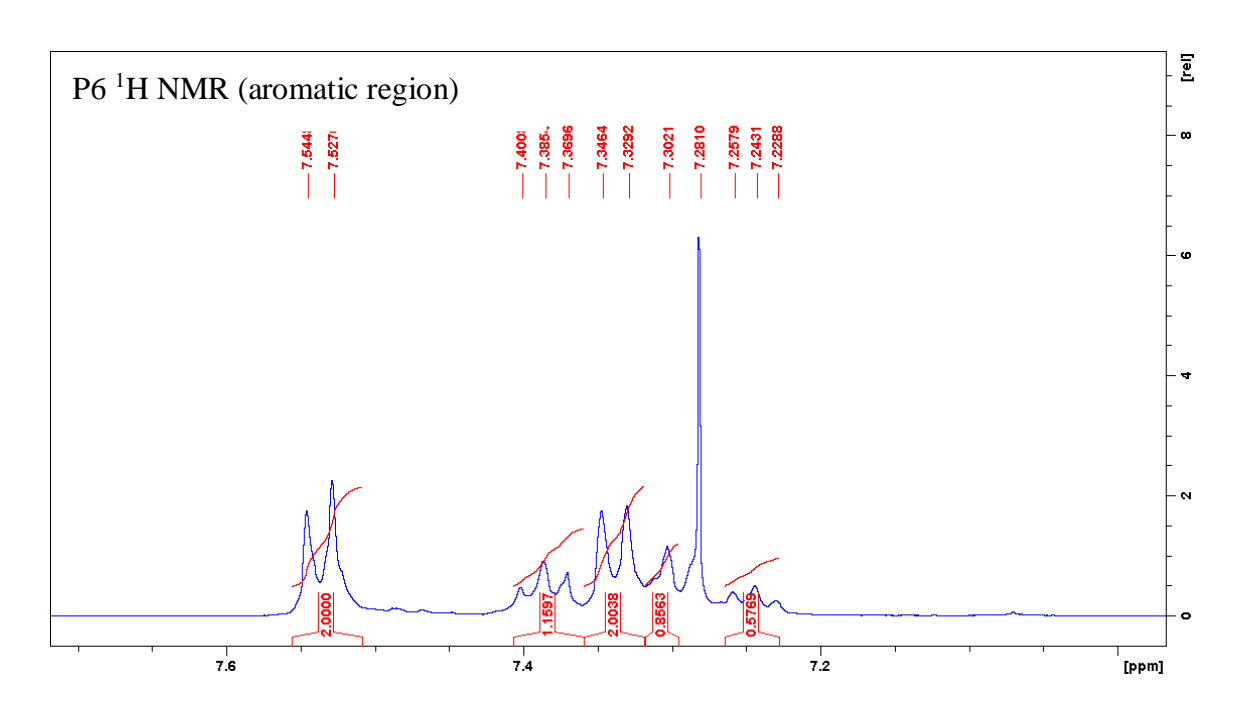


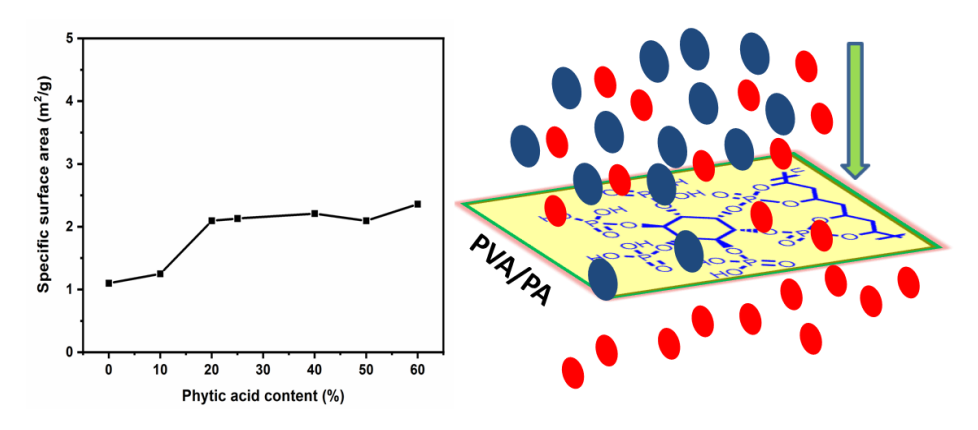
Figure 3.S2: NMR spectra of polymer P6; ³¹P NMR (top), ¹ H NMR(bottom)

Chapter 4

Polyvinyl Alcohol-Phytic Acid Polymer Films as Promising Gas/Vapor Sorption Materials

Abstract

In this chapter, we present the studies on gas/vapor sorption properties of polyvinyl alcohol/phytic acid (PVA/PA) composite polymeric films. To understand the gas sorption properties, we have performed the Brunauer–Emmet–Teller (BET) analysis of various PVA/PA polymeric films with varying weight percentages of PVA and PA. The films were mesoporous, while their specific surface area and average pore size were increasing with the gradual increase in PA compared to that of pure PVA. Observation in field emission - scanning electron microscope (FESEM) showed layered and porous morphologies of the PVA/PA polymer films, and hence they could trap gas molecules, aiding in efficient gas sorption. The tensile strength of the polymeric films decreased with the increase in quantity of PA, while the elongation at break increased with the increase in quantity PA content. Besides, vapor sorption studies provided evidence that the PVA/PA polymer films absorb water-vapor. The study showed a general trend of increasing vapor sorption with the increase in weight percent of PA. In particular, 2:3 PVA/PA polymer film showed the highest vapor sorption of 0.15 g moisture content per gram of the sample. Overall, our study reveals the potential use of PVA/PA composite polymeric films as gas/vapor sorption materials.



4.1. Introduction

Polymer membranes are used commercially as efficient gas sorption materials. They can be used to separate carbon dioxide from natural gas, oxygen, and nitrogen for oxygen enrichment and inert gas generation, water from hydrocarbons for natural gas dehydration, and hydrocarbons from the air for pollution control. In general, the separation of mixtures by adsorption is of great importance for various aspects like environmental protection and efficient use of energy. The commonly used polymer membranes for gas sorption applications include polysulfone, silicone rubber, polycarbonate, and polyimide. The efficiency of these membranes for the gas separation and storage applications is determined mainly by porosity apart from other physical properties like selectivity and permeability. Therefore, it has been a continued interest to develop polymer films that exhibit the required porosity for a given application.

Many microporous (pore size: 0.5 - 2 nm) and mesoporous (pore size: 2 - 50 nm) materials are explored as adsorbents in gas sorption applications because of their enhanced Van der Waals interaction inside the confined pores. On the other hand, macroporous (pore size: > 50 nm) materials with good porosity and interconnectivity find applications as catalysts, tissue engineering scaffolds, electrode materials, and water purifier.⁴ Microporous materials have higher selectivity and thermal stability. In comparison, macroporous materials have easy accessibility to internal pores but less selectivity compared to micropores. These drawbacks resulted in the production of mesoporous materials that maintain a balance between micro and macroporous materials. In this work, we studied the sorption properties of mesoporous polymer films designed by cross-linking polyvinyl alcohol (PVA) and phytic acid (PA) in varying weight ratios.

Phytic acid (PA) is a non-toxic substance formed during the ripening of seeds. It is the main reserve of phosphorus and energy in plants. It contains six phosphonic groups and is also called myoinositol hexaphosphoric acid.⁵⁻⁷ PA finds a variety of applications as proton conductive filler,⁸ complexing reagent,^{9,10} cross-linking reagent,¹¹ flame retardant additive,¹² anticorrosion, and coating.¹³ It is also used commercially as a preservative due to its antioxidant properties. Recently, Li et al.⁵¹ used phytic acid (PA) for cross-linking with PVA and studied mechanical and thermal properties of PVA/PA composite films. Another study explored PA as a cross-linking reagent involving the synthesis of polyaniline/PA conduction composite⁵² and

polyaniline-deposited paper composite.⁵³A cellulose-based proton-conducting membrane was prepared by Jiang et al. through doping PA into the matrix of cellulose.⁵⁴When used as a cross-linking reagent, PA improves the mechanical and electrical functioning of the material and enhances the thermal stability.

Similarly, the useful properties of PVA include easy processibility, film-forming property, high hydrophilicity, grease resistance, low toxicity, andbiocompatibility. 14-28 Therefore, PVA sponge has been utilized as absorption materials, 29, 30 in bioengineering 31 and so on. 32-34 An interesting aspect of PVA is its flexibility to be cross-linked with several cross-linking reagents, 35-50 which improves thermal stability and conductivity of PVA. The porous structure of PVA has been explored well in bioengineered tissue scaffolds. On the other hand, PA being a bulky molecule will create extra free volume for gas adsorption due to its inefficient packing in the solid-state. In this work, we show that this fact can be exploited for the preparation of PVA/PA films with improved porosity and to study their gas/vapor sorption properties. To the best of our knowledge, this aspect of PVA/PA is unexplored so far. We have synthesized and characterized PVA/PA polymer films to investigate their gas/vapor sorption properties. All the prepared PVA/PA polymer films show mesoporosity. The PVA/PA polymer films, with advantages of PVA and PA individually, are promising materials for gas/vapor sorption.

4.2. Results and discussion

4.2.1. Production of PVA/PA films and their characterization

Phytic acid (PA) is being a bulky molecule expected to interfere packing of chains of PVA. The possibility of extensive hydrogen bonding between PVA and PA molecules would create 3-D networks with pores at various places of the composite matrix. These pores are necessary for gas adsorption-desorption applications. Intending to make materials for gas sorption applications, we have produced PVA/PA composites films. The films of polyvinyl alcohol (PVA) and phytic acid (PA) were prepared easily by mixing them in the solution phase (scheme 4.1). The ratio of PVA to PA was varied (table 4.1) to produce different polymeric films. Details of weight ratios (in %) of PVA and PA in each film are given in Table 4.1. As the PA content increased gradually, the film's strength decreased, making them less elastic and more brittle. The thickness of the films produced was in the range of 0.2 - 0.5 mm. The images of the polymer films are shown in figure

4.1. The transparency and film-forming nature of these composites are evident from these images.

Scheme 4.1: Synthesis of PVA/PA polymeric films

Table 4.1. Various polymer composites synthesized and the distribution of PVA and PA in them

Composite	PVA (%)	PA (%)
PVA	100	0
9:1 PVA/PA	90	10
4:1 PVA/PA	80	20
3:1 PVA/PA	75	25
3:2 PVA/PA	60	40
1:1 PVA/PA	50	50
2:3 PVA/PA	40	60

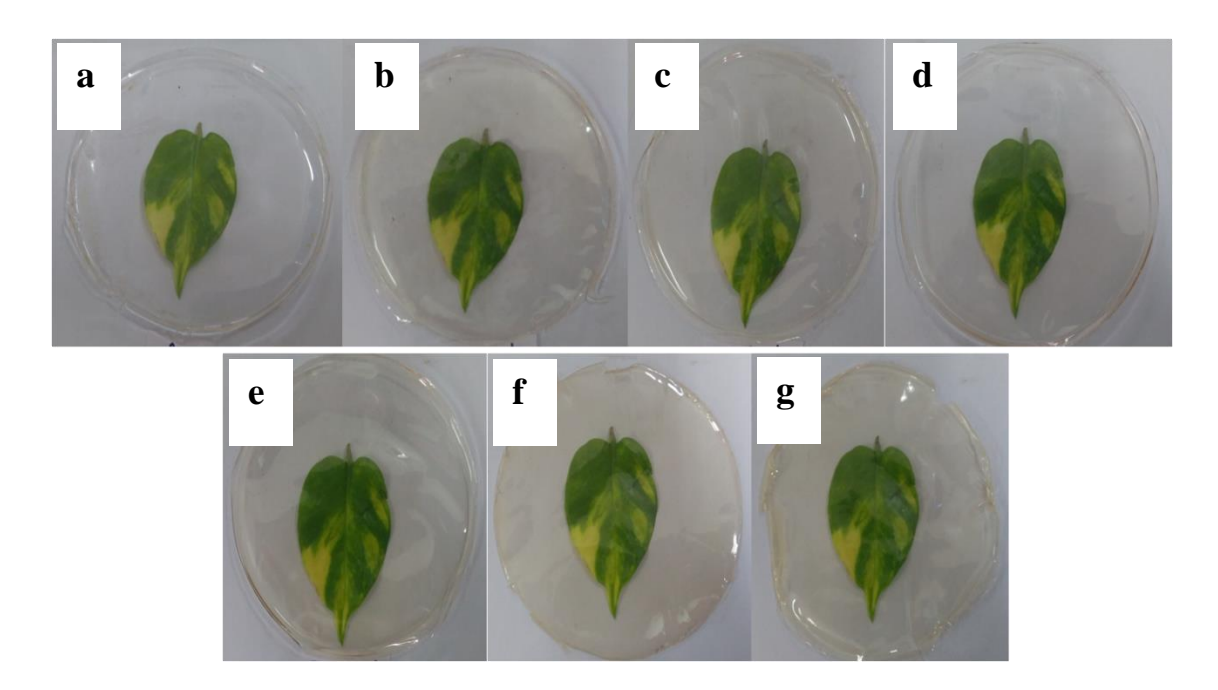


Figure 4.1: Images of various polymeric films showing its transparency and film forming nature (a) PVA (b) 9:1 PVA/PA (c) 4:1 PVA/PA (d) 3:1 PVA/PA (e) 3:2 PVA/PA (f) 1:1 PVA/PA (g) 2:3 PVA/PA.

The formation of composites was confirmed primarily by Fourier-transform infrared (FTIR) spectra (figure 4.2). The intense and broad absorption band near 3296 cm⁻¹ was assigned to the stretching vibration of OH groups (H-bonded) of PVA.^{55, 56} The peak at 2926 cm⁻¹ of IR spectra correspond to the symmetric stretching vibrations of –CH₂– moiety. CO stretching was observed at 1425 cm⁻¹, and CH bending and CH₂ twisting were observed at 995 cm⁻¹ and 1249 cm⁻¹, respectively. The band at 1720 cm⁻¹ was attributed to C=C stretching vibrations formed by intramolecular dehydration of PVA. The PA signature was found at 1080 cm⁻¹ in the spectra as a result of the P-O-C stretching vibration. The band became increasingly prominent as the PA content increased in the composite. The P-O-H stretching vibration was observed at 840 cm⁻¹.

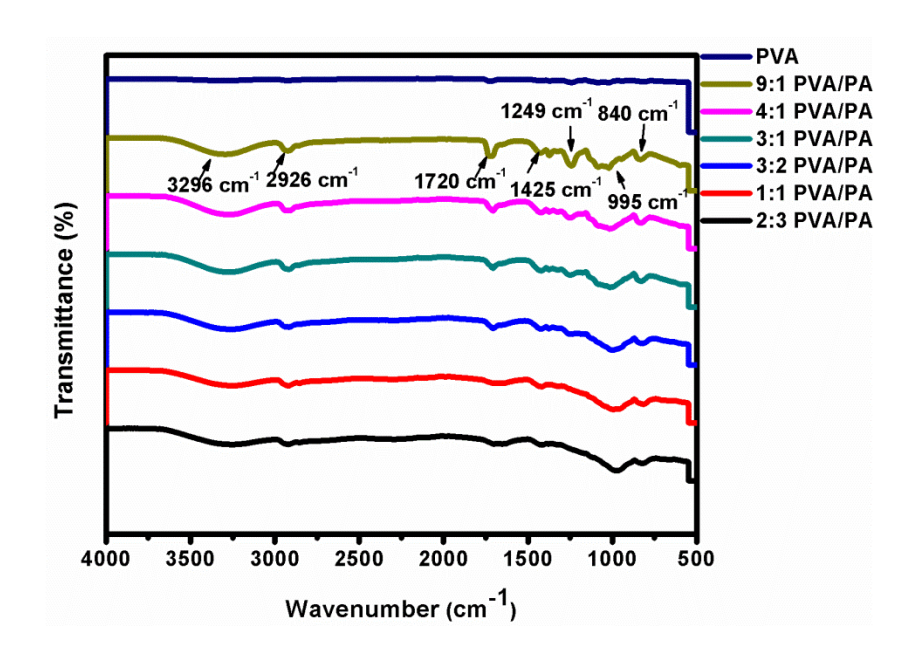


Figure 4.2: FT-IR spectra of the polymeric films.

4.2.2. Morphology of PVA/PA films

The FESEM images of the pure PVA and various films of the PVA/PA composites are shown in figure 4.3. The images (figures 4.3b - g) indicate that the polymer films produced were quite porous with layered morphology, while that of the pure polymer PVA (figure 4.3a) shows no such layered structures. Also, the multiple layers present in the cross-section morphology of the composites overlap with each other. This observation gives us preliminary evidence that the polymeric films can be useful candidates as membranes for gas/vapor sorption studies.

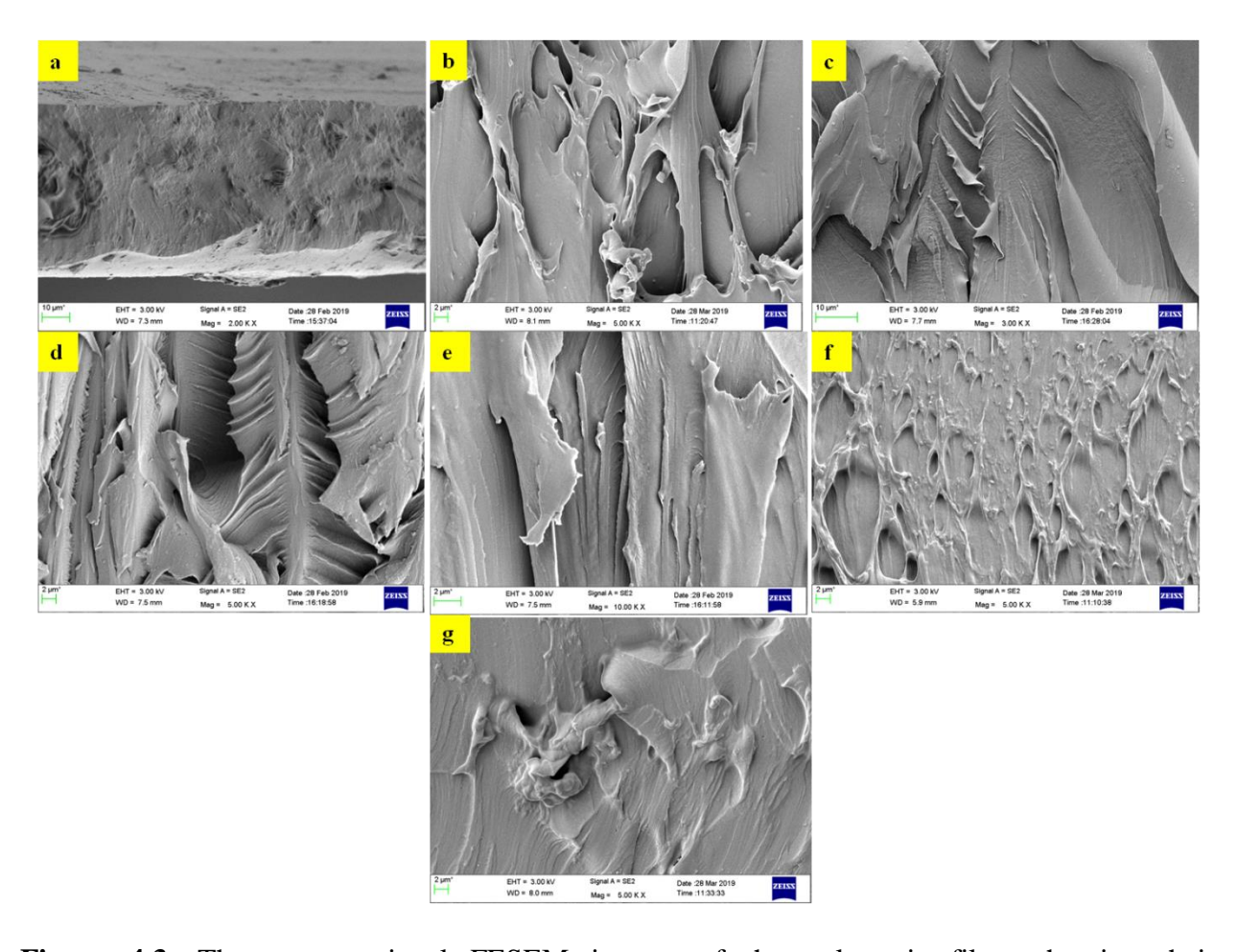


Figure 4.3: The cross-sectional FESEM images of the polymeric films showing their morphology(a) PVA (b) 9:1PVA/PA (c) 4:1 PVA/PA (d) 3:1 PVA/PA (e) 3:2 PVA/PA (f) 1:1 PVA/PA (g) 2:3 PVA/PA.

Analysis of changes happening in the cross-sectional morphology of the composite polymer films with an increase in PA loading showed that the films gradually become more porous and drift to a feather-like morphology that reaches saturation in 3:1 PVA/PA (figure 4.3d). Further, the morphology was distorted to an irregular layered morphology in 3:2 PVA/PA (figure 4.3e) and then to a highly branched root-like morphology in 1:1 PVA/PA (figure 4.3f). The sample with the highest PA content i.e., 2:3 PVA/PA, shows an irregular morphology but has considerable porosity, specific surface area, and gas/vapor sorption capabilities (section 4.2.4). A closer analysis of the cross-sectional morphology of these films illustrates that there are macropores present in polymer films. However, macroporous nature cannot be identified on the surface. Hence, there is a discrepancy in the porosity of the film on the surface and bulk. This observation will be further described in detail in section 4.2.4.

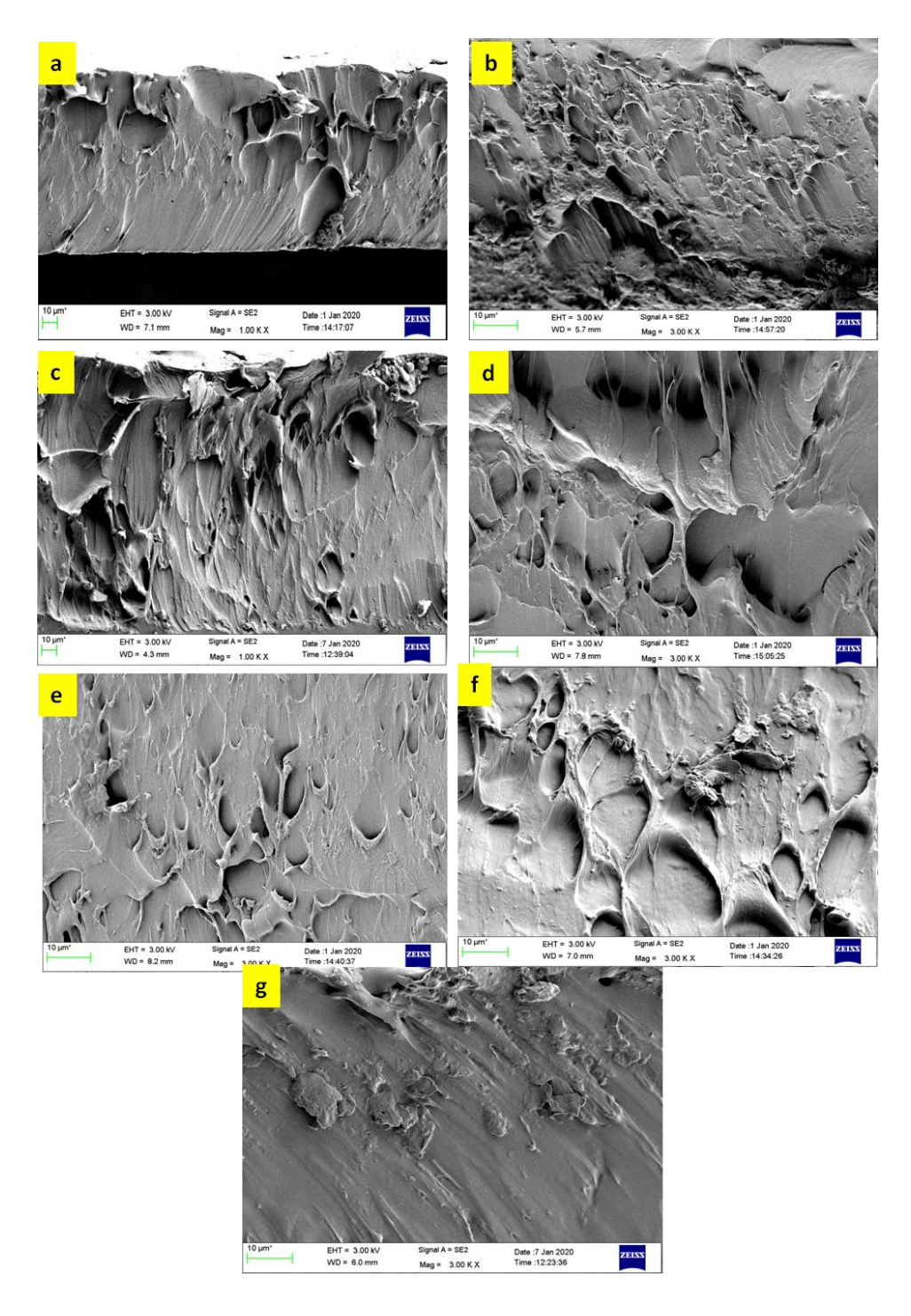


Figure 4.4: The cross-sectional FESEM images of the polymeric films showing their porosity(a) PVA (b) 9:1 PVA/PA (c) 4:1 PVA/PA (d) 3:1 PVA/PA(e) 3:2 PVA/PA (f) 1:1 PVA/PA (g) 2:3 PVA/PA

4.2.3. Thermal and mechanical properties of composite PVA/PA films

Thermogravimetric analyses PVA/PA composite film showed the losses of adsorbed water between 75 °C and 175 °C, similar to those reported by Ma et. al. ⁵⁶The condensation reaction of phosphonic groups in PA triggered further weight loss at temperature between 226 °C to 306 °C yielding pyrophosphoric acid. ⁵⁷Dehydration of the hydroxyl groups present in the chains of PVA occurred at temperature between 306 °C to 416 °C leading the formation of polyethylene kind of structures. ⁵⁸Above 426 °C, PA and PVA decomposed through breakage of phosphonate and ether bonds.

An apparent decrease in the thermal stability of PVA/PA composites was observed with an increase in PA content (figure 4.5). While PVA was stable up to 260 °C, the rest of the composites degrade, starting from 40-60 °C. Hence, these films have a limitation when it is considered for high-temperature applications. However, since the gas separation processes mostly involve physisorption, which happens at room temperature or lower temperatures, this factor should not be a real challenge, except for temperature swing adsorption techniques.

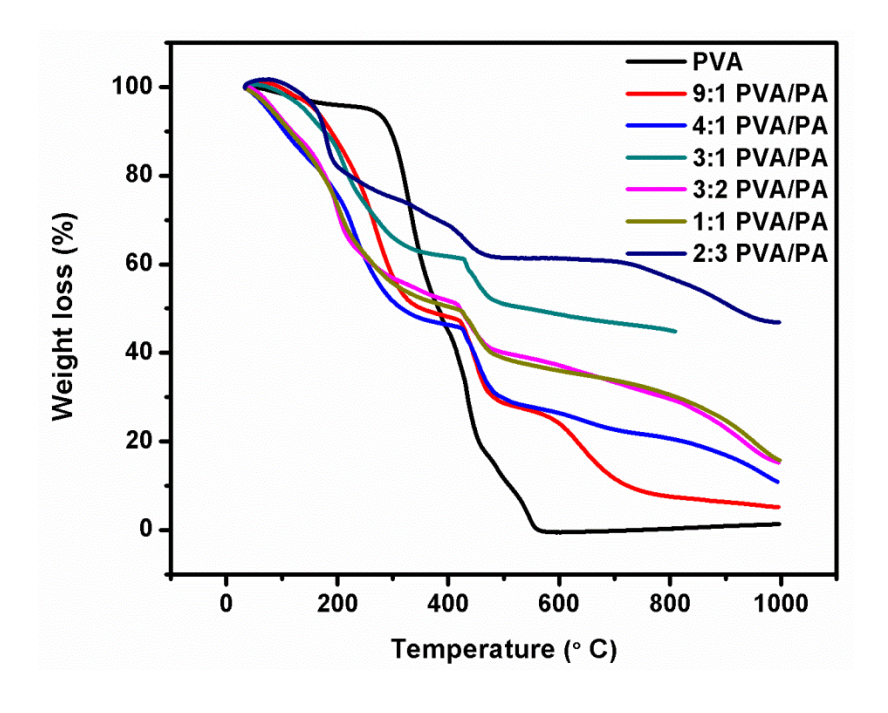


Figure 4.5: TGA spectra of the polymeric films.

The mechanical properties of a commercial adsorbent material are critical for several reasons. The material should be able to withstand both the structural and conformal deformations caused in the pore shape due to the adsorption process, and the macroscopic deformation affecting the adsorbent volume. ⁵⁹Thevalues of tensile strength and elongation at break of each of these polymeric films are tabulated (table 4.2). The stress-strain plot (figure 4.6) indicates that the tensile strength of the polymeric films gradually decreased with an increase in PA loading while the elongation at break increased with an increase in PA loading. The composite 2:3 PVA/PA showed the highest elongation at break of 372%. This value is indirectly a measure of the ductility of the material.

Table 4.2. Mechanical properties of the samples

Sample	Tensile strength (MPa)	Elongation at break (%)
PVA	30	5
9:1 PVA/PA	25	132
4:1 PVA/PA	8	182
3:1 PVA/PA	17	123
3:2 PVA/PA	11	259
1:1 PVA/PA	9	346
2:3 PVA/PA	10	372

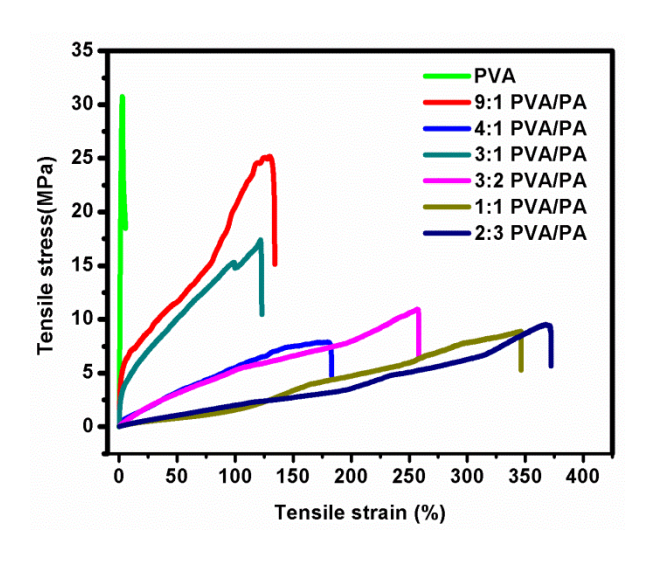


Figure 4.6: Stress-strain graph of the polymeric films.

4.2.4. Gas sorption properties of PVA/PA films

4.2.4.1. Dynamic Vapor Sorption Analysis (DVS)

Vapor sorption technique is a gravimetric analysis that measures the quantity of a solvent absorbed by a sample and time required to adsorb a particular quantity. For example, how a dry powder absorbs water. The process of sorption takes into accounts both adsorption and absorption. Although the options to use a variety of organic solvents are available, water vapor is often used. Equilibrium vapor sorption isotherms and vapor sorption kinetic experiments yield valuable data about substances that find applications in pharmaceuticals, fuel cells, and many more. Thus, the vapor sorption technique is used in various industrial processes. In this study, water vapor was used as the solvent.

Table 4.3. Vapor sorption properties of the samples

Sample	Weight (%)
PVA	106.7
9:1 PVA/PA	108.1
4:1 PVA/PA	114
3:1 PVA/PA	113.4
3: 2 PVA/PA	112.6

1:1 PVA/PA	112.5
2:3 PVA/PA	114.3

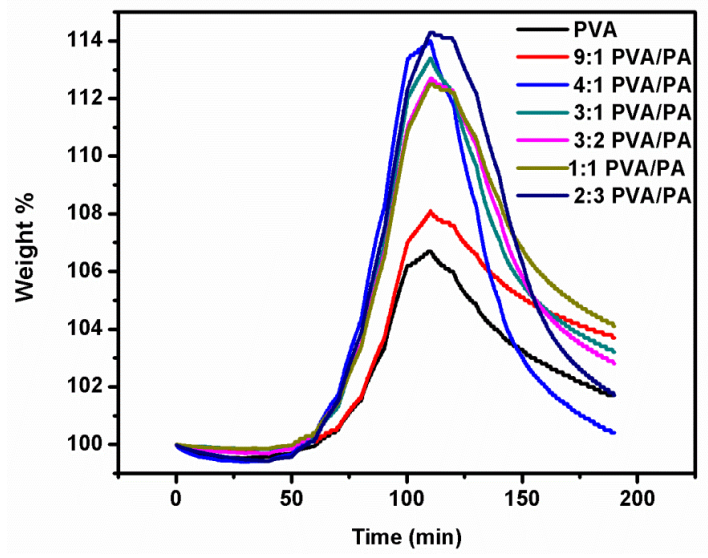


Figure 4.7: Gravimetric vapor sorption spectra of the polymeric films.

Both gravimetric vapor sorption spectra (figure 4.7) and the vapor sorption isotherms (figure 4.S1) show a general trend of increasing vapor sorption with an increase in weight percent of PA. However, the trend was not a linear and steady increase. We found that from the experiment on PVA to 4:1 PVA/PA, there was a steady increase and beyond which the sorption stays almost a constant with 2:3 PVA/PA showing maximum vapor sorption of 0.15 g moisture content per gram of sample. This study confirms the sorption properties of PVA/PA polymer membranes.

4.2.4.2. Brunauer-Emmet-Teller (BET) studies

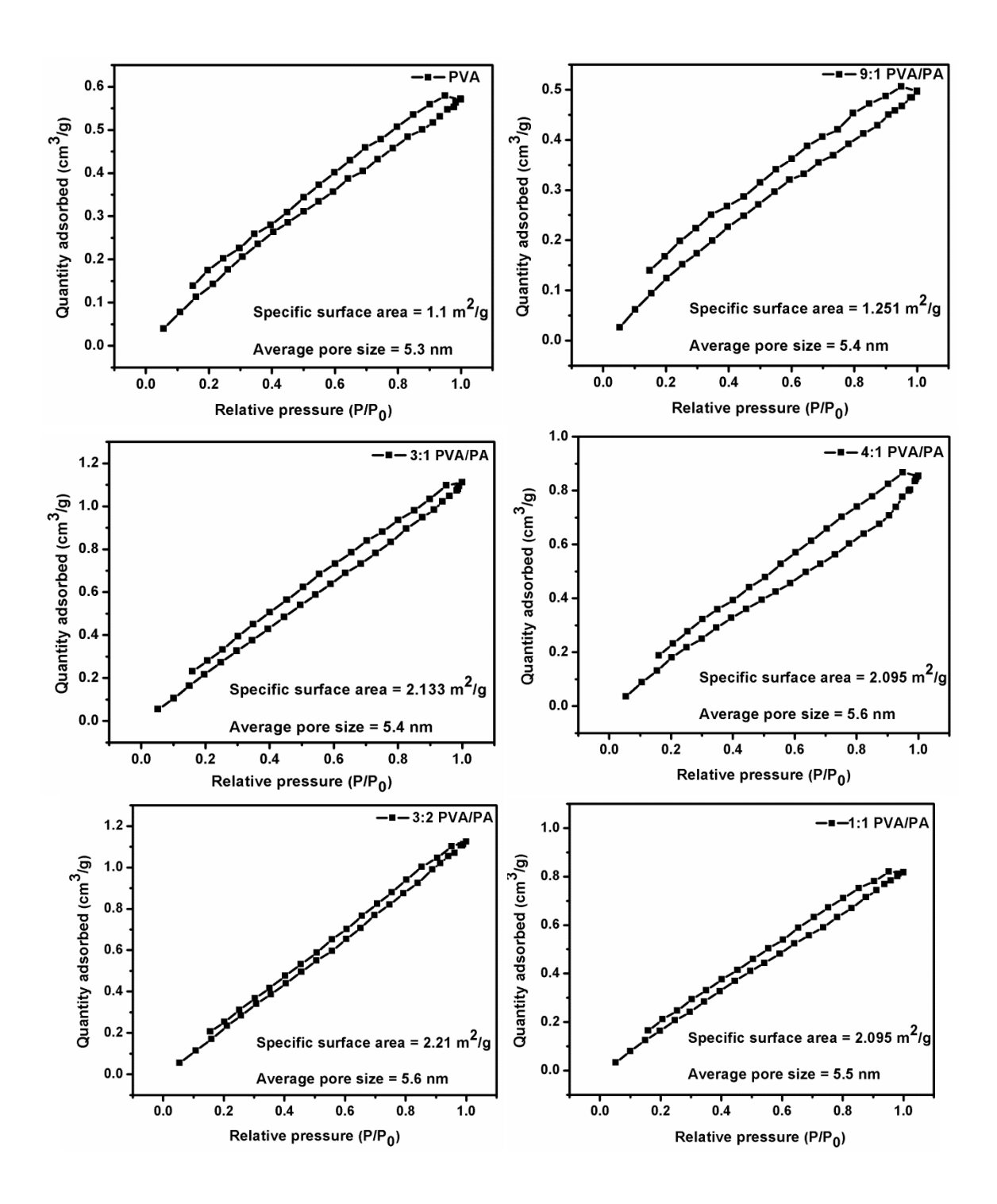
All PVA/PA composites materials prepared were subjected to the BET analysis using nitrogen gas. The BET isotherms are plotted with the quantity of adsorbate against the relative pressure of the gas. The hysteresis in the BET isotherm arises because adsorption happens by capillary condensation of nitrogen from the walls towards the core of the pores, while desorption happens because of evaporation starting from the liquid surface having different curvature. The steady rise of adsorption isotherms reveals the multilayer adsorption typical of non-uniform pore geometry. As can be seen from figure 4.8, the hysteresis loop does not close when the adsorbed gases are not desorbed completely. This trend was observed in all our samples even after

degassing for three hours before the measurement. This observation indicated that the nitrogen gas was getting trapped in some pores and found it difficult to desorb entirely at the same applied temperature and pressure.

BET analysis of the polymer films (figure 4.8) showed that all of them follow multilayer adsorption with the average pore size of 5.5 nm and specific surface area of 1-2 m²/g. Hence all the samples are mesoporous and compared to pure PVA. The PA doped samples showed the higher surface area and average pore size, indicating that the addition of PA indeed increased the adsorption capability of the membranes (figure 4.9a and b), though not drastically. 2:3 PVA/PA, which has the highest PA content, showed the highest surface area, which was 2.36 m²/g and 3:2 PVA/PA, and 3:1 PVA/PA showed the maximum average pore size which is 5.6 nm.

Table 4.4. Specific surface area and average size pores

Sample	Specific surface area (m²/g)	Average pore size (nm)
PVA	1.1	5.3
9:1 PVA/PA	1.251	5.4
4:1 PVA/PA	2.133	5.4
3:1 PVA/PA	2.095	5.6
3: 2 PVA/PA	2.21	5.6
1:1 PVA/PA	2.095	5.5
2:3 PVA/PA	2.36	5.5



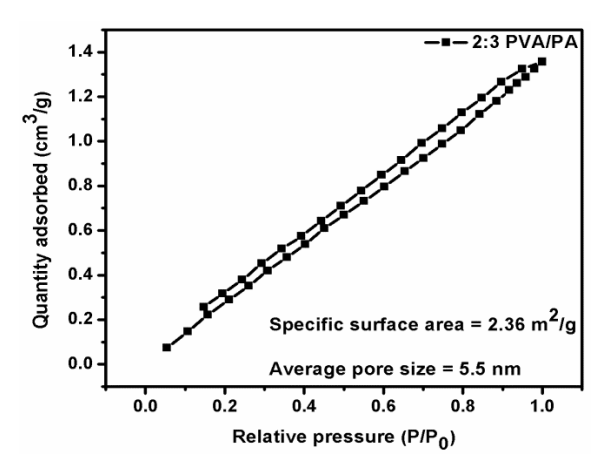


Figure 4.8: BET adsorption desorption isotherms of the polymeric films. Specific surface areas and average pore sizes of each of the samples are also shown in figure.

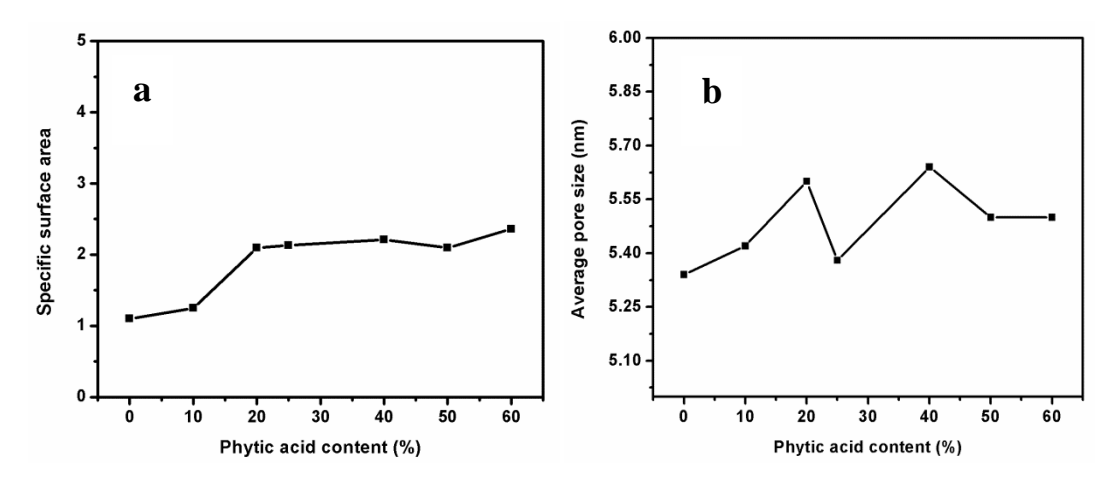


Figure 4.9: Graphs showing variation in specific surface area (a) and average pore size (b) with increasing PA content.

The BET measurement has its limitations that all the pores may not be accessible within the timescale of the measurement. Such pores are considered as closed pores. Those pores which are accessible within the timescale of measurement are called open pores. These open pores could be either the ones on the surface or those connected by channels to the pores on the surface so that the gas can slowly diffuse and reach those inner pores. Hence the macropores, what we observed in FESEM cross-sectional morphology, could be the inaccessible closed pores, and hence BET cannot estimate them adequately. Also, the BET study analyses the bulk sample, whereas FESEM is more localized in nature as compared to it. Hence, within the BET realm and taking into account the accessibility of the pores, these materials could be considered mesoporous.

Most of the non-polar gases commonly used for gas separation applications like nitrogen, methane, and carbondioxide, all have diameters well below the average pore sizes of the polymeric films described in this study ($CH_4 = 0.38$ nm, $N_2 = 0.36$ nm, $CO_2 = 0.33$ nm, see table 4.4 for average pore sizes of polymeric films). ⁶⁰Hence these gases can easily fit these pore sizes and prove to be potential adsorbates, provided the other parameters for adsorption like selectivity, and interaction energy is appropriate. These properties are yet to be explored to determine the applicability of these polymeric membranes for practical purposes.

4.3. Conclusions

PVA/PA polymeric films of different ratios were synthesized and characterized successfully. The BET analyses of the samples indicated that the introduction of PA into PVA has increased both the surface area and pore size of PVA. While 2:3 PVA/PA showed the maximum surface area of 2.36 m²/g, the 3:2 PVA/PA showed the maximum average pore size of 5.64 nm. From FESEM analysis, the morphology of these films was found to be layered and porous, which helped in trapping gas molecules aiding gas adsorption-desorption. The mechanical properties of these films are also quite impressive with 2:3 PVA/PA film showing the highest elongation at break of 372%. Vapor sorption analysis shows clearly that these films can absorb vapors of water and show a general trend of increasing vapor sorption with an increase in the weight percentage of PA. In particular, 2:3 PVA/PA polymer film showed the highest vapor sorption with 0.15 g moisture content per gram of the sample.

4.4. Experimental section

4.4.1. Materials and instrumentation

Materials: Polyvinyl alcohol (average molecular weight 88,000 Da) and phytic acid were purchased from TCI Chemicals and Sigma Aldrich respectively.

Instruments: The Thermo Scientific Nicolet iS5 spectrometer was used to record FTIR-spectra of the composite films. To study thermal stability of polymeric films, we have used the Perkin Elmer (Pyris STA 6000 model) thermogravimetric analyzer. The decomposition behavior of polymers was studied from 50 °C to 995 °C under the nitrogen flow with a heating rate of 20 °C/min. Ultra 55 Carl Zeiss instrument was used to obtain the FESEM images. The tensile strength (stress-strain relationship) of the polymer membranes was measured on a universal

testing machine (INSTRON 5965) using 5 (KN) load cell. Citizon digital ultrasonic cleaner was used for sonication.

4.4.2. General Synthetic Protocol

PVA/PA polymer composites were produced as follows. Firstly, phytic acid was added into the beaker having 10 mL of distilled water and irradiated with ultrasound. After 1 min, phytic acid solution changes from neutral to acidic due to the dissolution of protons of phosphonic groups in phytic acid. Afterward, PVA dissolved in 15 mL of distilled water was added to this beaker at around 100 °C and sonicated. The esterification reaction of PVA and PA was completed upon irradiation for 2 h. Then, the solution was allowed to stand for at least three hours for the foam to settle and to avoid bubbles. Further, the solution of composite was poured into a Petri dish and dried at room temperature.

4.4.3. Testing of mechanical strength

A Universal Testing Machine (UTM) was used to determine the tensile and compressive strengths of the composite materials. Dumbbell shaped specimens (Type IV specimen) were prepared from membranes according to the ASTM standard D638. Tensile properties of all the samples were measured at room temperature with a crosshead speed of 10 mm/min. Three readings were taken for each sample to check the reproducibility.

4.4.4. Gas sorption experiments

All gas sorption experiments were performed using the PVA/PA composite films cut in the form of tiny pieces. For DVS studies, water vapor was used as the solvent, and the experiment was performed by means of measuring the change in mass when the vapor concentration surrounding the sample varies. In the case of BET, nitrogen gas was used to study the adsorption-desorption, and the samples were degassed 3 h prior to the experiment.

Supporting information: Vapor sorption isotherms of the various polymer membranes are provided at the end of the chapter in figure 4.S1.

4.5. References

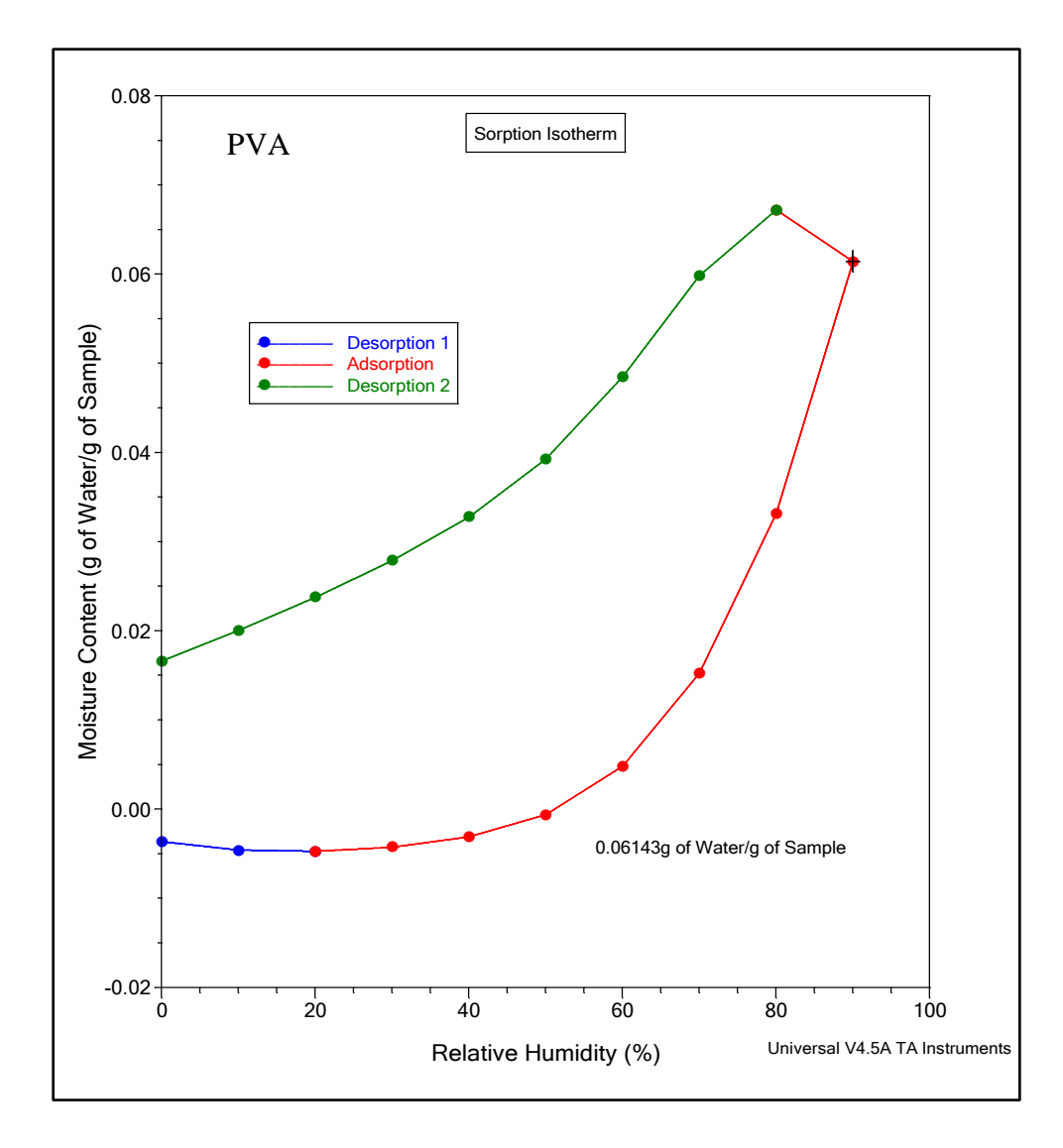
[1] J. A. Nollet, J. Membr. Sci., 1995, 100, 1.

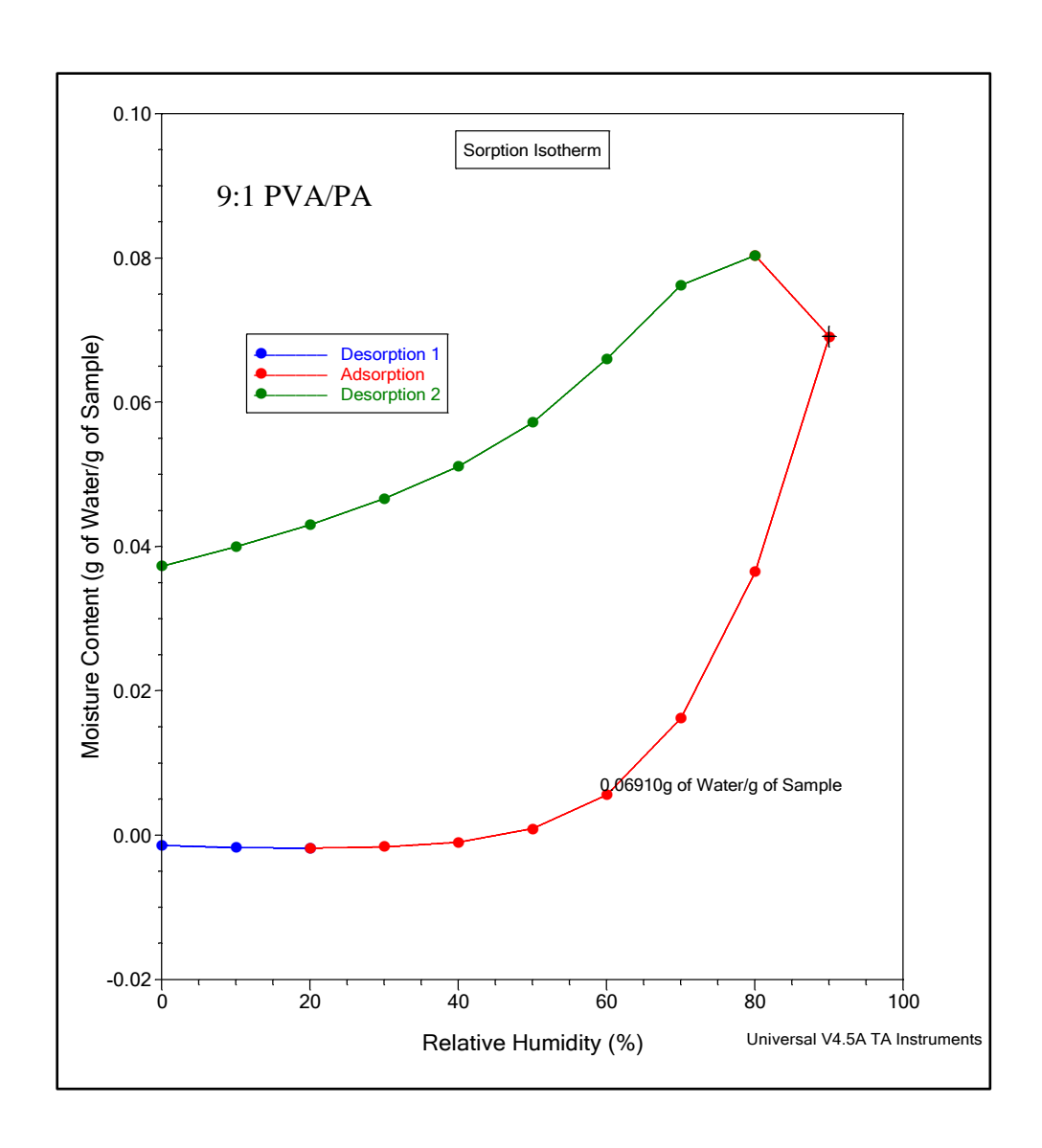
- [2] R. Abedini, A. Nezhadmoghadam, *Petroleum & Coal*, 2010, **52**(2), 69-80.
- [3] L. M. Robeson, Current Opinion in Solid State and Materials Science, 1999, 4, 549–552.
- [4] F. Wang, Y. Zhu, H. Xu and A. Wang, Front. Chem., 2019,7, 603.
- [5] B. Samotus, S. Schwimmer, *Nature*, 1962, **194**, 578–579.
- [6] A. J. Hatch, J. D. York, Cell, 2010, 143, 1030.
- [7] L. Pan, G. Yu, D. Zhai, H. R. Lee, W. Zhao, N. Liu, H. Wang, B. C. Tee, Y. Shi, Y. Cui, *Proc. Natl. Acad. Sci.USA*, 2012, **109**, 9287–9292.
- [8] G. Jiang, J. Qiao, F. Hong, *Int. J. Hydrogen Energy*, 2012, **37**, 9182–9192.
- [9] A. W. Xu, Q. Yu, W. F. Dong, M. Antonietti, H. Cölfen, Adv. Mater., 2005, 17, 2217–2221.
- [10] G. Zhang, G. Wang, Y. Liu, H. Liu, J. Qu, J. Li, J. Am. Chem. Soc., 2016, 138, 14686– 14693.
- [11] H. Wu, G. Yu, L. Pan, N. Liu, M. T. McDowell, Z. Bao, Y. Cui, Nat. Commun., 2013, 4.
- [12] Y. Zhou, C. Ding, X. Qian, X. An, *Carbohyd.Polym.*, 2015, **115**, 670–676.
- [13] X. Gao, K. Lu, L. Xu, H. Xu, H. Lu, F. Gao, S. Hou, H. Ma, *Nanoscale*, 2016, **8**, 1555–1564.
- [14] C. C. DeMerlis, D. R. Schoneker, Food Chem. Toxicol., 2003, 41, 319–326.
- [15] H. Yu, Z. Z. Chong, S. B. Tor, E. Liu, N. H. Loh, RSC Adv., 2015, 16, 8377–8388.
- [16] F. Y. Li, H. S. Xia, J. Appl. Polym. Sci., 2017, 134.
- [17] F. Hadi, F. Mohammad, H. Mahdi, N. Nooshin, *Carbohyd. Polym.*, 2017, **167**, 79–89.
- [18] T. Schuman, M. Wikstrom, M. Rigdahl, Surf. Coaf. Tech., 2004, 183, 96–105.
- [19] X. D. Zhai, J. Y. Shi, X. B. Zou, S. Wang, C. Jiang, J. Zhang, X. Huang, W. Zhang, M. Holmes, *Food Hydrocolloid.*, 2017, **69**, 308–317.
- [20] Q. Yu, A. Xie, F. Huang, S. Li, Y. Xiao, Y. Shen, *Mater. Sci. Eng. C- Mater.*, 2017, **76**, 918–924.

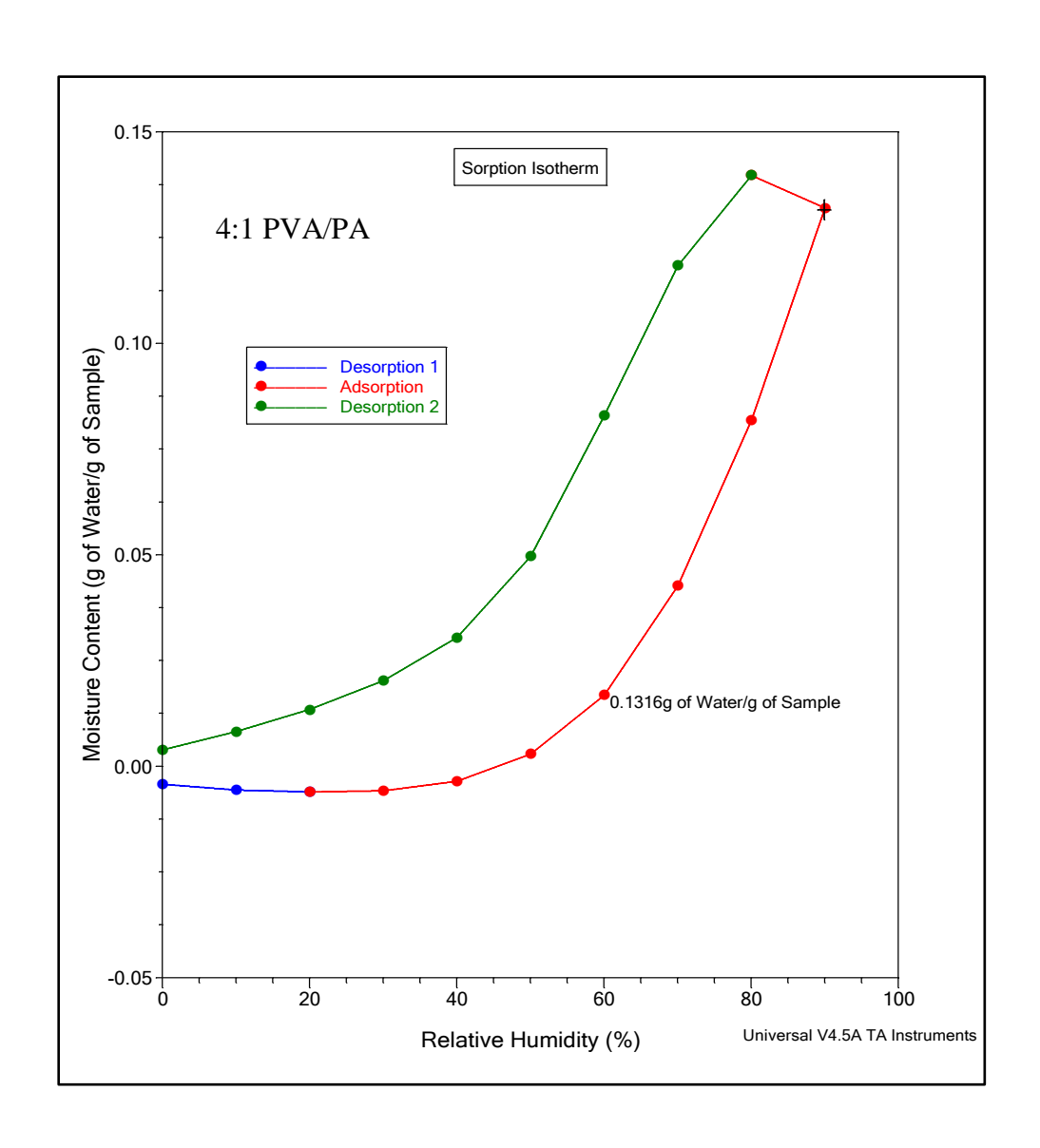
- [21] S. Mallakpour, F. Motirasoul, *Ultrason.Sonochem.*, 2017, **37**, 623–633.
- [22] F. Ni, G. C. Wang, H. B. Zhao, J. Appl. Polym. Sci., 2017, 134.
- [23] H. Anwar, M. Ahmad, M. U. Minhas, S. Rehmani, Carbohyd. Polym., 2017, 166, 183-194.
- [24] Y. X. Wang, C. Y. Chang, L. N. Zhang, *Macromol. Mater. Eng.*, 2010, **295**, 137–145.
- [25] J. S. Gonzalez, A. S. Maiolo, C. E. Hoppe, V. A. Alvarez, *Proc. Mater. Sci.*, 2012, **1**, 483–490.
- [26] A. P. N. Mário, V. R. Hélder, C. B. F. Pedro, M. H. L. Ribeiro, *Appl. Biochem. Biotechnol.*, 2010, **160**, 2129–2147.
- [27] A. Karimi, M. Navidbakhsh, A. M. Haghi, Adv. Polym. Tech., 2014, 33.
- [28] A. Karimi, M. Navidbakhsh, M. Alizadeh, R. Razaghi, *Biomed. Tech.*, 2014, **59**, 439–446.
- [29] C. Cheng, J. Wang, X. Yang, A. Li, C. Philippe, J. Hazard. Mater., 2014, 264, 332–341.
- [30] Y. Pan, Z. Liu, W. Wang, C. Peng, K. Shi and X. Ji, J. Mater. Chem. A, 2016, 4, 2537–2549.
- [31] S. Barachini, S. Danti, S. Pacini, D. D'Alessandro, V. Carnicelli, L. Trombi, S. Moscato, C. Mannari, S. Cei, M. Petrini, *Micron*, 2014, **67**, 155–168.
- [32] Z. Cheng, J. Liao, B. He, F. Zhang, F. Zhang, X. Huang, L. Zhou, *ACS Sustain. Chem. Eng.*, 2015, **3**, 1677–1685.
- [33] P. Hyojin, K. Dukjoon, J. Biomed. Mater. Res. A., 2006, **78**, 662–667.
- [34] C. Sharmila, R. Vinuppriya, C. Selvi, C. Jincy, B. Chandarshekar, *J. Appl. Res. Technol.*, 2016, **14**, 319–324.
- [35] L. Yao, T. W. Haas, A. Guiseppi-Elie, G. L. Bowlin, D. G. Simpson, and G. E. Wnek, *Chem. Mat.*, 2003, **15**, 1860–1864.
- [36] Y. B. Li, S. Yao, *Polym. Degrad. Stabil.*, 2017, **137**, 229–237.
- [37] S. Mallakpour, and A. N. Ezhieh, *Carbohyd. Polym.*, 2017, **166**, 377–386.
- [38] K. Ashwini, K. Awanish, *Mater. Sci. Eng.* C, 2017, **73**, 333–339.

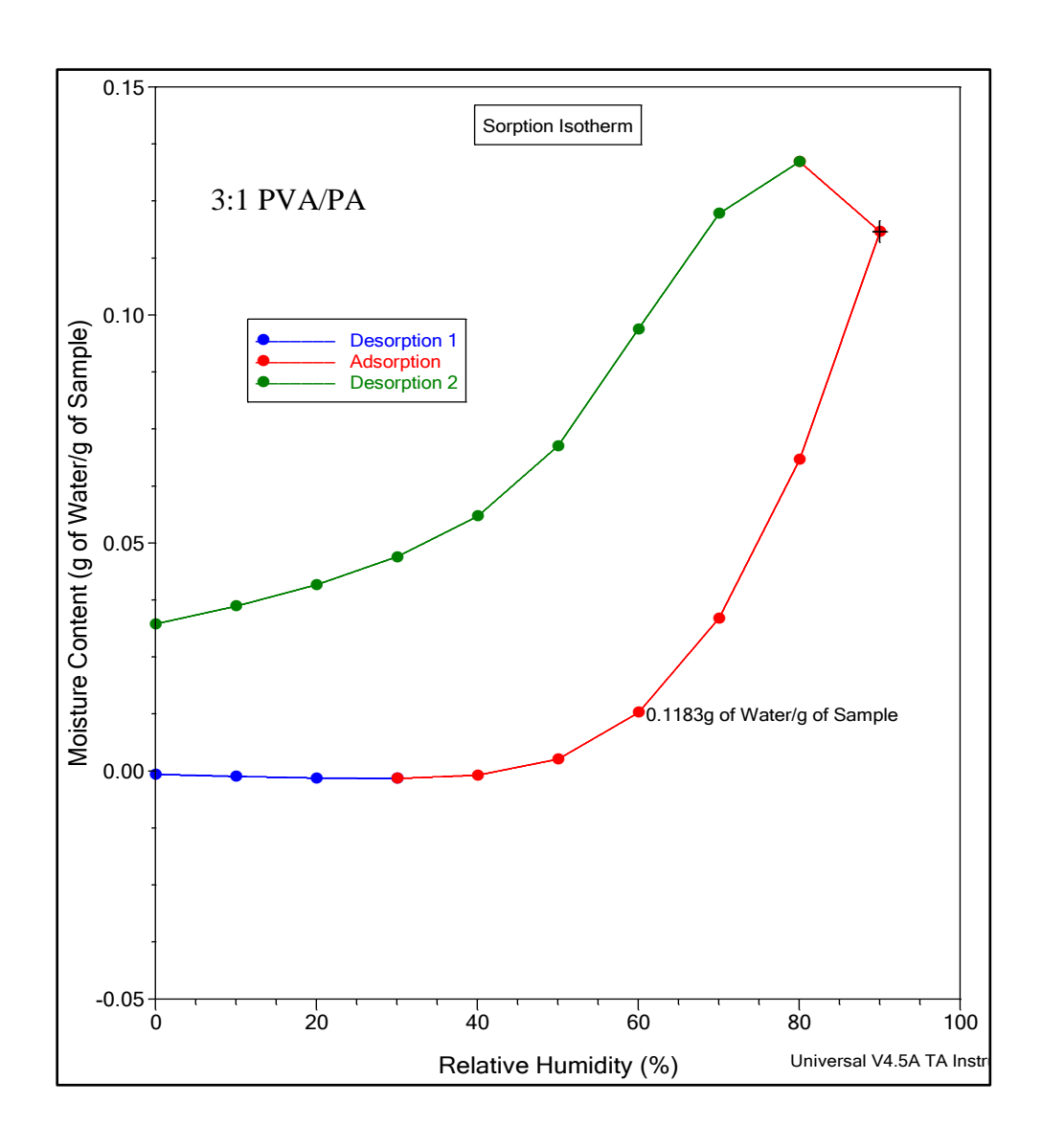
- [39] A. G. Destaye, C. K. Lin, C. K. Lee, ACS Appl. Mater. Interfaces, 2013, 5, 4745–4752.
- [40] A. K. Sonker, H. D. Wagner, R. Bajpai, R. Tenne, X. M. Sui, Compos. Sci. Technol., 2016, 127, 47–53.
- [41] A. K. Sonker, N. Tiwari, R. K. Nagarale, V. Verma, J. Polym. Sci. Pol. Chem., 2016, 54, 2515–2525.
- [42] J. Li, Y. Li, S. Niu, J. Liu, L. Wang, J. Porous Mater., 2007, 1–10.
- [43] Y. Chen, X. Cao, P. R. Chang, M. A. Huneault, *Carbohyd. Polym.*, 2008, **73**, 8–17.
- [44] C. H. Zhang, F. L. Yang, W. J. Wang, B. Chen, Sep. Purif. Technol., 2008, 61, 276–286.
- [45] R. H. M. Marcilli, M. G. de Oliveira, *Colloid. Surf. B*, 2014, **116**, 643–651.
- [46] Q. Tang, K. Huang, G. Q. Qian, B. C. Benicewicz, J. Power Sources, 2013, 229, 36–41.
- [47] M. E. Gouda, S. K. Badr, M. A. Hassan, E. Sheha, *Ionics*, 2011, 17, 255–261.
- [48] D. S. Kim, H. B. Park, J. W. Rhim, Y. M. Lee, J. Membrane Sci., 2004, 240, 37–48.
- [49] J. W. Rhim, H. B. Park, C. S. Lee, J. H. Jun, D. S. Kim, Y. M. Lee, *J. Membrane Sci.*, 2004, **238**, 143–151.
- [50] L. Q. Liu, A. H. Barber, S. Nuriel, H. D. Wagner, Adv. Funct. Mater., 2005, 15, 975–980.
- [51] J. Li, Y. Li, Y. Song, S. Niu, N. Li, *Ultrason. Sonochem.*, 2017, **39**, 853-862.
- [52] H. Wu, G. Yu, L. Pan, N. Liu, M.T. McDowell, Z. Bao, Y. Cui, Nat. Commun., 2013, 4.
- [53] Y. Zhou, C. Ding, X. Qian, X. An, Carbohyd. Polym., 2015, 115, 670–676.
- [54] G. Jiang, J. Qiao, F. Hong, Int. J. Hydrogen Energy, 2012, 37, 9182–9192.
- [55] L Carol, M Jord, R Catal R. Gavara, P. H. Muňoz, J. Agric. Food Chem., 2011, 59, 11026–11033.
- [56] C. B. Ma, B. J. Du, E. K. Wang, *Adv. Funct. Mater.*, 2017, **27**, 1–8.
- [57] C. B. Ma, B. J. Du, E. K. Wang, Adv. Funct. Mater., 27 (2017) 1–8.
- [58] Y. Li, Y. Song, J. Li, Y. Li, N. Li, S. Niu, *Ultrason. Sonochem.*, 2018, 42, 18–25.

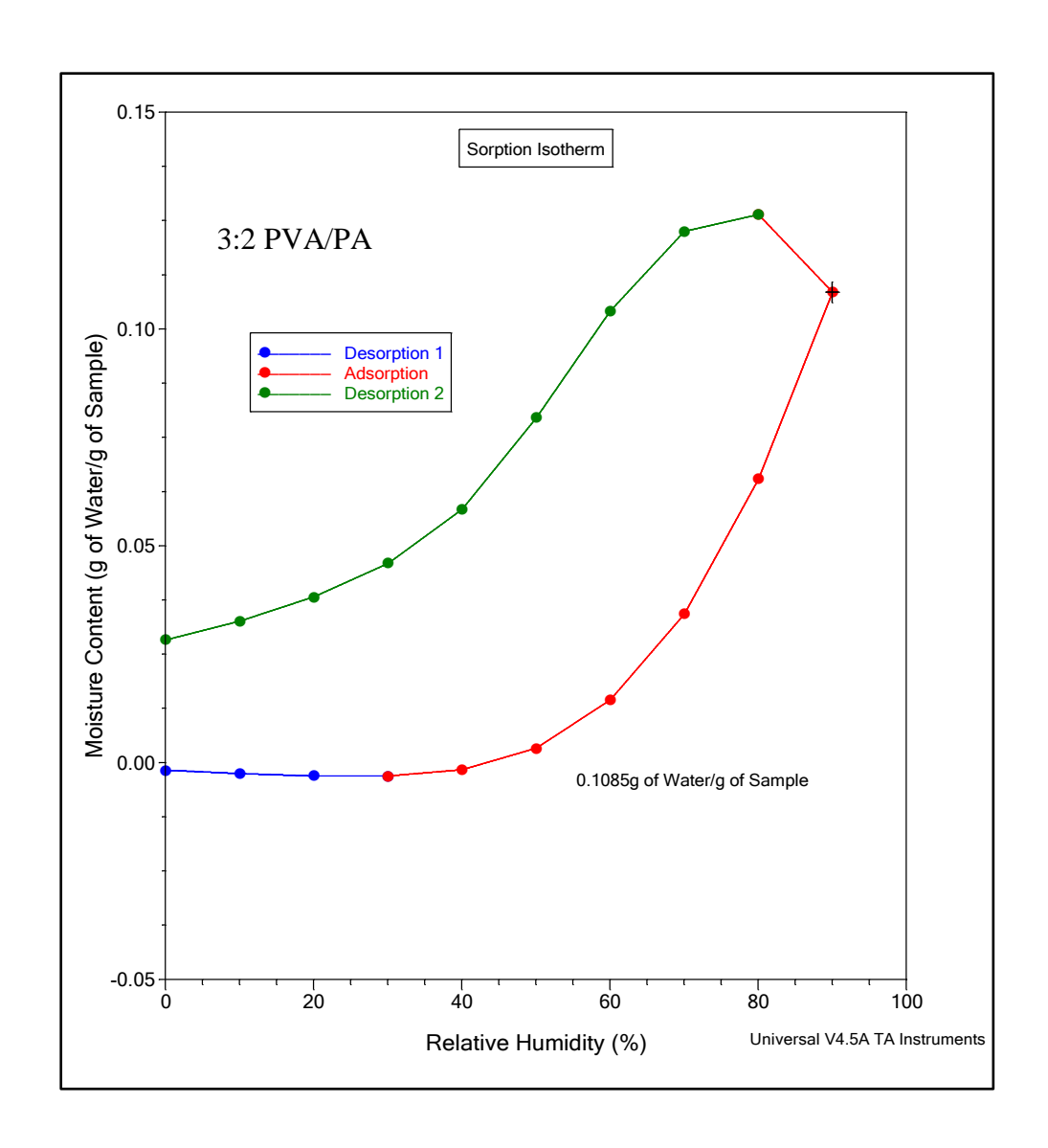
- [59] Daniel W. Siderius, Nathan A. Mahynski, and Vincent K. Shen, Adsorption, 2017, 593-602.
- [60] R. T. Yang, Adsorbents: Fundamentals and Applications, Wiley Interscience, New York, 2003.
- [61] R. Zaleski, W. Stefaniak, M. Maciejewska, J. Goworek, J. Porous Mater., 2009, 16, 691–698.

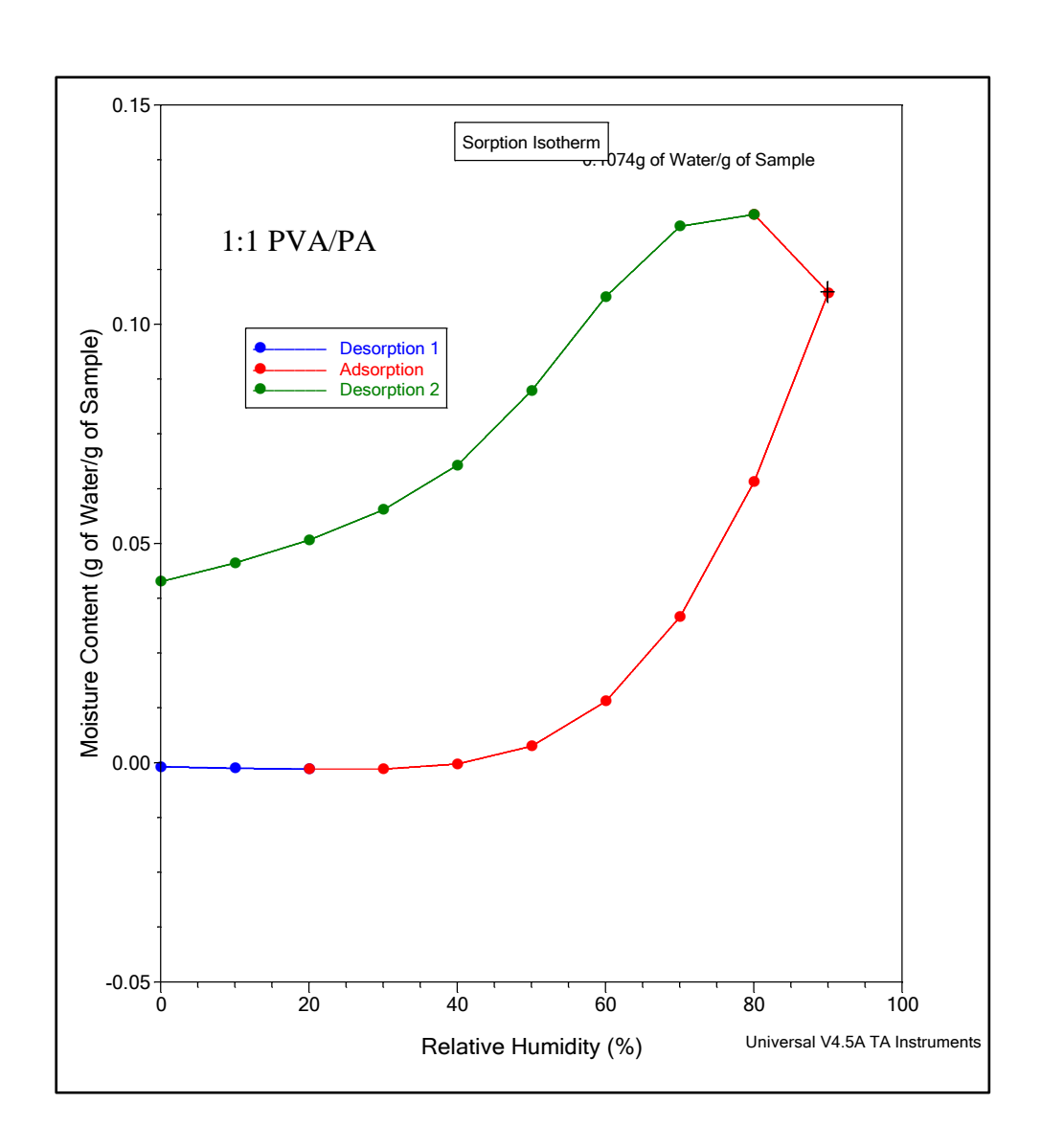












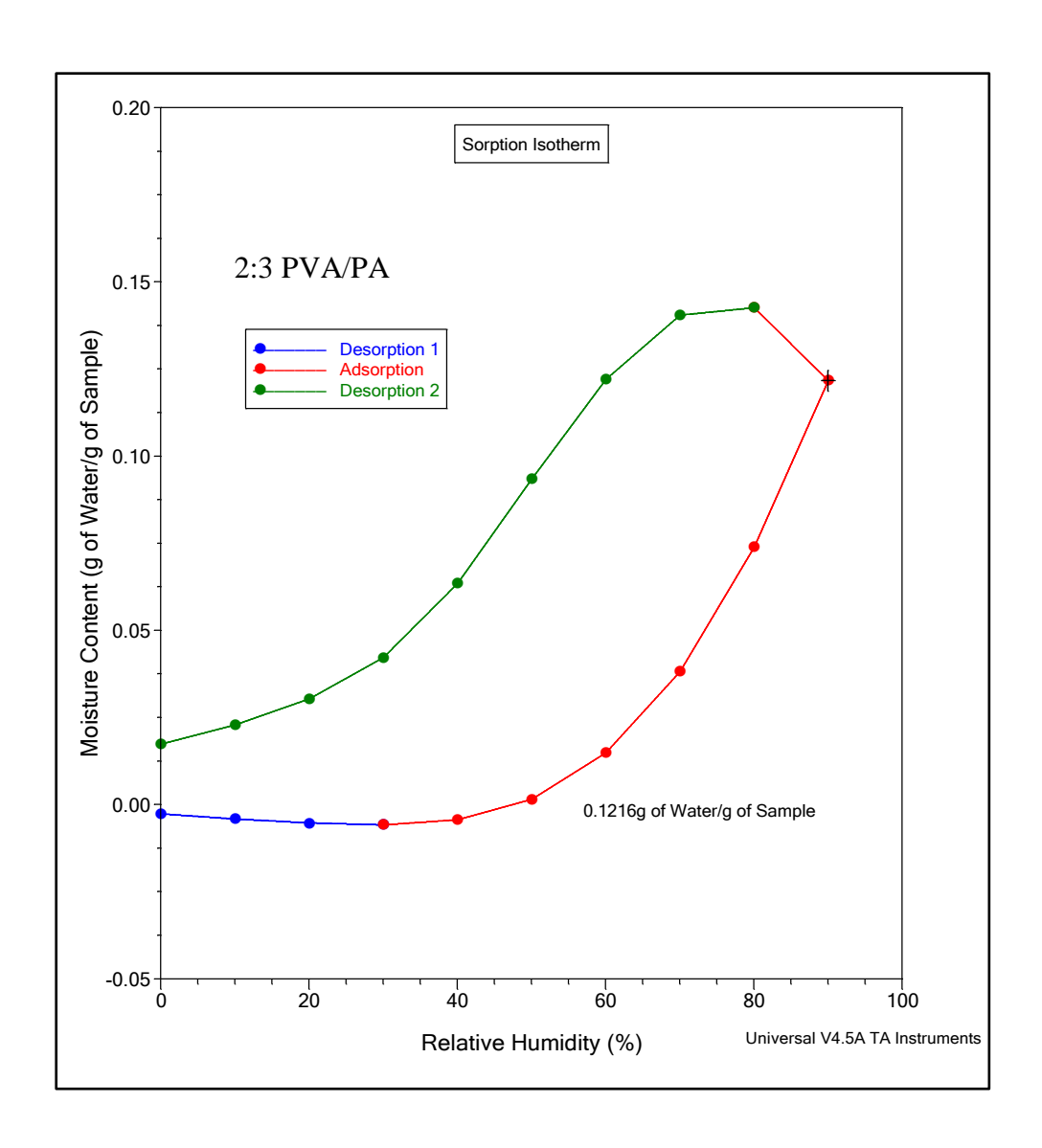


Figure 4.S1: Vapor sorption isotherms of the polymeric films.

Chapter 5

Summary and Future perspective

Polymers and small molecules of phosphorus find diverse applications and still more left unexplored. The applications that have been studied in this thesis are quite distinct. Furthermore, the requirements for each of those applications vary drastically.

In chapter 2, four different polyphosphates were synthesized, and their possible applicability in Li-ion batteries is studied. The synthesized polymers were highly stable solids at room temperature and porous, as seen from FESEM. P1-P4 showed thermal stability above 200° C, which is very important for practical applications. Due to continuous usage, the Li-ion battery may get heated up, and the electrolyte inside has to withstand these temperatures to avoid thermal runaway. The Li-ion conductivity values obtained were also quite impressive. SPE3 (20%) was found to have a Li-ion conductivity of 1.4×10^{-3} Scm⁻¹, SPE3 (40%) 1.0×10^{-3} Scm⁻¹ and SPE1 (40%) 1.2×10^{-3} Scm⁻¹ at 80 °C. The higher conductivities obtained for these polymers is explained by the microstructure of polymer molecules dictated by the bulky and rigid groups.

The Li-Li symmetric cell fabrication was done with polymer P1 as a coating on lithium foil, and their charge-discharge cycles were studied at a current density of 20 mA.cm⁻² and a cycling capacity of 10 mAh.cm⁻². A constant variation of overpotential was observed, which indicated controlled dendrite growth in P1 and showed a stable cycling behavior for about 2000 cycles. Lithiophilic sites of polyphosphate polymer are responsible for controlled Li electrodeposition during electrochemical cycling. The presence of phosphorus is expected to impart flame-retardant property to the SPEs. These polymers being stable solids and showing good conductivity are quite promising for solid-state Li-ion batteries.

Polymer electrolytes have no internal shortage, no leakage of electrolytes, and no non-combustible reaction products at the electrode surface. Nevertheless, the major challenge still is their low ionic conductivity at ambient temperature and low Li transference number. To achieve such SPEs is still a challenge. Hence intense research has to be done in this direction to overcome these problems.

In chapter 3, two phosphate polymers P5 and P6 were synthesized and blended with different ratios of PMMA, and their applicability in optics is studied. These polymers were well characterized by NMR, IR, and GPC and further used for blending. A relatively simple and efficient solution blending and the spin coating methods were employed to produce uniform and transparent films. Ellipsometric studies showed that PB5 and PB6 series of blends showed tunability in RI of about 0.05 and 0.1, respectively. The significance of these values stems from the fact that a change in RI of about 0.01 could bring about a 3.3 D change in the perfect lens system. Also, abbe values of PB5 blends showed an acceptable abbe value range of optical lens materials, with a maximum of 56 for PB520 blend.

On the other hand, blends with higher weight percentages of P6 could be promising for optical filters. This investigation is quite promising in a way, as of how we can engineer the desired RI and abbe number by incorporating the polyphosphates into PMMA. PMMA, well known for its compatibility with human tissue, could be ideal for rigid intraocular lenses with the desired RI tailored by the incorporation of polyphosphates.

It is essential to tune the RI of a material for specific applications, especially when graded-index is important. At the molecular level, RI is tuned by incorporating elements like sulfur, halogen, and phosphorus, while at the bulk level by adding inorganic fillers or blending. Blending organophosphorus polymers is quite promising, as we have seen from our study. This method is quite an easy method of RI tunability if we understand the variation in trend by studying the change in optical properties systematically in each variant.

Chapter 4 described the production of PVA/PA polymeric films of different ratios and the study of their sorption properties. The gas sorption properties of PVA/PA films have not been explored so far. Observation in FESEM revealed layered leaf-like morphology of films that could help in trapping gas molecules and help in gas adsorption-desorption. These films' mechanical properties were also impressive with 2:3 PVA/PA film showing the highest elongation at break value as 372%.

Vapor sorption analysis of the polymeric films provided the first substantial evidence that these films can adsorb and desorb gaseous molecules. The general trend of increasing vapor sorption with an increase in weight percent of phytic acid was observed. In particular, 2:3 PVA/PA polymer film showed the highest vapor sorption with 0.15g moisture content per gram

of the sample. BET analysis showed that the introduction of PA into PVA had increased both the surface area and pore size of PVA with 2:3 PVA/PA showing the maximum surface area of 2.36 m²/g and 3:2 PVA/PA showing the maximum pore size of 5.6 nm. All the films produced were mesoporous. Further, the selectivity and permeability to various gases have to be studied systematically to determine the actual applicability of these polymer films for gas separation kind of applications. Also, PVA/PA sponges could be interesting for studying their sorption properties.

Publications from thesis

- [1] **A. K. Othayoth**, B. Srinivas, K. Murugan and K. Muralidharan, Poly (methylmethacrylate)/polyphosphate blends with tunable refractive indices for optical applications, *Opt. Mat.*, 2020, **104**, 109841-109851.
- [2] **A. K. Othayoth**, B. Srinivas, H. V. Babu and K. Muralidharan, Tunable microstructure-assisted Li-ion conductivity in catechol based polyphosphates for solid electrolytes in Li-ion battery (Manuscript submitted, under revision).
- [3] **A. K. Othayoth**, and K. Muralidharan, Polyvinyl Alcohol-Phytic acid polymer films as promising gas/vapor sorption materials (Manuscript to be communicated).

Other publications

[1] B. Vijayakumar, **K. O. Anjana** and G. Ranga Rao, Polyaniline/clay Nanocomposites: Preparation, Characterization and Electrochemical Properties, IOP Conf. Ser. Mat. Sci. Eng.2015, **73**, 012112.

Poster and oral presentations:

- [1] Anjana K.O. presented a poster in **Chem-Fest**, **2017**, held at University of Hyderabad, India. Poster title: Synthesis and characterization of phosphorus containing polymers for Li-ion batteries.
- [2] Anjana K.O. attended International Collaborative & Cooperative Chemistry Symposium (ICCCS-8), 2017, held at University of Hyderabad, India.
- [3] Anjana K.O. participated in the "Workshop on Development of Binders and Plasticizers for Energetic Applications", held at Advanced Centre of Research in High Energy Materials, University of Hyderabad, India on 15th December 2017.
- [4] Anjana K.O. and K. Muralidharan presented a poster in **Chem-Fest**, **2018**. held at University of Hyderabad, India from 9-10 March, 2018.

Poster title: Phosphorus containing polymers and their nanocomposites for high refractive index. [5] Anjana K.O., B. Srinivas and K. Muralidharan presented a poster at **SPSI** - **Macro 2018**, **15**th **International Conference on Polymer Science and Technology,** held at IISER Pune, India from 19-22 December, 2018.

Poster title: Phosphorus containing polymers: Synthesis and Applications.

[6] Anjana K.O. delivered an oral presentation on "Phosphorus containing polymers: Synthesis, characterization and their lithium ion conductivities" at **International Conference on Materials Science and Technology (ICMST)**, **2019**, held at VSSC Trivandrum from 10-13th October, 2018.

[7] Anjana K.O. delivered an oral presentation on "Phosphorus containing polymers: Synthesis and Applications" in **Chem-Fest**, **2019**, held at University of Hyderabad, India.

ELSEVIER

Contents lists available at ScienceDirect

Optical Materials

journal homepage: http://www.elsevier.com/locate/optmat





Poly(methyl methacrylate)/polyphosphate blends with tunable refractive indices for optical applications

Anjana K. Othayoth^a, Billakanti Srinivas^a, Karuppiah Murugan^{b,**}, Krishnamurthi Muralidharan^{a,*}

- a School of Chemistry, University of Hyderabad, Hyderabad, 500 046, India
- b International Advanced Research Centre for Powder Metallurgy & New Materials (ARCI), Balapur, Hyderabad, 500 005, India

ARTICLE INFO

Keywords: Refractive index Transparency Phosphate PMMA Ellipsometry Tunability

ABSTRACT

Tuning the refractive index of the transparent materials is essential for optical applications. Herein, we report novel materials with a tunable refractive index that are prepared by blending poly(methyl methacrylate) (PMMA) with different concentrations of two polyphosphate hybrid polymers (P1 and P2), having phosphorus in the main chain. The refractive indices and associated optical parameters of these polymers and hybrid materials (PB1 and PB2 series) are investigated using ellipsometry and optical modelling method to find their applicability in optics. Refractive indices of these materials are fine-tuned by altering the ratio of PMMA to P1 or P2. This approach is simple and ideal for obtaining homogeneous blends. Refractive index tunability of 0.05 and 0.1 are achieved for PB1 and PB2 series, respectively, by this approach. Abbe numbers of these blends are reasonable for PB1 series compared to the conventional lens materials, with a maximum value of 56 achieved in the case of PB120 blend. In addition, the trend in variation of extinction coefficient with wavelength for blends PB250, PB260 and PB280 seem promising for optical filter kind of applications. These results show that the synthesized polymer blends are promising as optical materials with refractive index tunability.

1. Introduction

Functional materials with excellent optical properties such as high refractive index (RI) and good transparency are useful for a variety of applications, including anti-reflection coatings, optical waveguides [1], ophthalmic lens [2], and adhesives for optical components. A few polymers such as aromatic heterocyclic polymers [3], polythiophene [4], and conjugated polymers [5], were reported to show the RI value higher than 1.7, so far. If the RI value of the polymer is high, the thickness of the materials required for lens manufacture is less. Further, solubility, optical dispersion, and optical transmittance in the visible region are properties that decide the practical use of a polymer. Thus, the development of high-refractive-index polymers (HRIP) with worthy optical properties is still a hot topic.

Much-dedicated efforts are on to produce polymer-inorganic hybrid materials [6], because they have enhanced thermal, mechanical, magnetic, optical, electronic, and optoelectronic properties compared with their corresponding individual polymer or inorganic component.

Nanoparticles can considerably increase the RI but may affect the transparency of the material due to agglomeration [7]. Further, these particles tend to agglomerate during dispersion in a solvent or a polymer matrix, which ultimately hinders the application. Therefore, obtaining hybrid materials with useful RI value overcoming all issues is a challenge.

RI of a material is related to molar volume and mean polarizability by the Lorentz - Lorenz equation [3,8–10]. The equation gives an estimation of the refractive index of the material from the individual molar refractions of functional groups and the repeating units.

$$\frac{n^2-1}{n^2+1} \! = \! \frac{4\pi}{3} N\alpha = \sum_{i} (R_{LL})_{i}$$

where N is the number of molecules per unit volume, α is the mean polarizability and R_{LL} is the individual molar refraction values. Therefore, as per the equation, the introduction of phosphorus, sulphur, and halogen with high molar refraction values will increase the RI of the material [11–16]. Phosphorus has higher polarizability due to its

E-mail addresses: kmsc@uohyd.ernet.in, murali@uohyd.ac.in (K. Muralidharan).

 $^{^{\}ast}$ Corresponding author.

^{**} Corresponding author.

electronic structure. Unlike nitrogen, which has a 3s-3d energy gap of 23 eV, phosphorus has an energy gap of 17 eV and is, therefore, more polarisable [17].

Organic-inorganic hybrid polymers with phosphorus as one of the atoms in the main-chains have exceptional advantages owing to their conformational flexibility introduced by the size and the fifth valence of phosphorus atoms. These properties of the phosphorus-containing polymers help in designing polymers for various applications [18–20] with tunable properties. Considering these advantages, Olshavsky and Allcock prepared a series of polyphosphazenes with high RIs and optically transparent in the visible region [21,22]. These polymers possessed moderate to high Abbe numbers and RI as high as 1.75. McGrath and co-workers synthesized aromatic polyphosphonates and studied for their use as HRIPs [23,24]. In 2001, H. K. Shobha et al. have synthesized a variant of polyphosphonates starting from phenyl phosphonic dichloride and the diol using triethyl amine as the base and phenol as an end capper [24]. Recently in 2017, Macdonald et al. have synthesized a series of similar high refractive index polymers starting from phenyl and methyl phosphonic dichloride using triethyl amine and n-methyl imidazole as bases and end capped the polymers with various endcappers [25]. The highest reported RI for a polyphosphonate is 1.64.

Mostly polyphosphonates have been explored as high refractive materials, whereas polyphosphates are less explored in this regard. Polyphosphates are similar to the polycarbonates (PC) by the structure, and they are the materials of commercial importance because of their excellent flame-retarding characteristics. Polycarbonates are wellstudied materials for optical applications. For example, in 2019, Nahida and Marwa have studied the optical constants of PC blended with PMMA, a well-known polymer for optical applications, at different concentrations and proved that a 50% blend ratio showed the best results [26]. However, PC involves high processing temperatures and is quite expensive to manufacture. On the other hand, polyphosphates are cheap and can be degradable biomaterials. Bis-phenol A-bis(diphenyl phosphate) commercially known as Fyrolflex BDP is a well-known fire retardant. In this paper, we have explored the refractive index tunability of PMMA using two polyphosphate polymers, one of which is a polymer of bisphenol A diphenyl phosphate, and the other is a biphenyl variant of the same.

One of the intriguing strategies of increasing the RI of a polymer is making hybrid materials [27,28] by combining a typical organic polymer with the hybrid polymer having phosphorus atoms. Therefore, we have synthesized two polyphosphates, and the present work describes a novel approach of tailoring the refractive index of PMMA by mixing with varied weight ratios of synthesized polyphosphates. PMMA is a ubiquitous amorphous polymer in various optical components. Further, PMMA finds a wide variety of applications because of its several desirable qualities, including toughness, durability, transparency, biocompatibility and refractive index tunability [29]. The flexibility of tuning the optical properties is crucial for the practical use of material. Consequently, polyphosphates described here are blended with PMMA by simple solution mixing to ensure homogeneous mixing of composition. The RI values and Abbe's number (ν D) of these blends were tunable compared to that of individual polymers showing the advantages of the present study described here.

2. Experimental section

2.1. Materials and instrumentation

Materials: Phenyl dichlorophosphate, poly(methyl methacrylate) (average molecular weight 1,20,000 Da) and 1,3-dioxolane were purchased from Sigma Aldrich, 1-methyl imidazole from Merck, bisphenol A from SRL, and 4,4'-biphenol from TCI respectively.

Instruments: A Bruker Avance 500 MHz, FT NMR spectrometer was used to record all NMR spectra at room temperature. Chemical shifts in the spectra were determined in parts per million (δ) with reference to

tetramethylsilane for 1H spectra and 85% $\rm H_3PO_4$ for $^{31}P\{^1H\}$ spectra. Shimadzu 10AVP model Gel Permeation Chromatography (GPC) instrument was used to determine the molecular weights of polymers. Separation of polymer molecules in this GPC instrument was achieved using Phenogel mixed bed column (300 \times 7.80 mm) operated at 30 $^{\circ}C$ with a flow rate of 0.5 mL/min using tetrahydrofuran (THF) as the eluent and polystyrene as the standard. JASCO V-770 model spectrophotometer was used for absorption studies, while Milman SPN4000S model spin coater was used for coating the samples. Oxford Instruments Asylum Research Inc. version 13 was utilized to record AFM in tapping mode. Refractive index and associated optical parameters were obtained using a J. A. Woollam Company VASEW ellipsometer, and the optical modelling and data analysis were performed using WVASE32 software package.

2.2. General synthetic procedure for the polymers P1 and P2

A solution of phenyl dichlorophosphate (1 mmol) in 1, 3-dioxolane (5 mL) was added dropwise over 1 h to a stirring mixture of aromatic diol (1 mmol) (structure of aromatic diols are shown in Scheme 1), 1-methylimidazole (2 mmol) and 1, 3-dioxolane (5 mL) at room temperature. The reaction mixture was stirred for 3 h, and then the mixture was heated at 75 °C. After the reaction was completed, two clear liquid phases occurred, which was separated easily [30,31]. The upper phase was the polymer solution, and the lower phase was the pure ionic liquid. The 1, 3-dioxolane solution was removed by vacuum evaporation using a rotary evaporator. The characterization data of the polymers are displayed in Table 1.

2.3. Sample preparation for ellipsometry

Refractive index and associated optical parameters were obtained using ellipsometric data analysis. The samples for ellipsometric measurements were prepared by spin-coating. Initially, PMMA was stirred in 3 mL of chloroform until the solution was homogeneous, and then the polymer P1 or P2 at a defined weight ratio was added. It was stirred for 12 h to obtain a solution of a homogeneous blend. This solution was spin-coated on a glass substrate, i.e., soda-lime glass (SLG) by solvent casting. The solution mixing and spin-coating ensured a uniform mixing as well as the uniform thickness of the film on SLG. The prepared sample on SLG was abraded carefully on the other side in order to avoid the back reflection during ellipsometry data collection. A typical sample spin-coated on a glass substrate is shown in Fig. 2(b).

2.4. Analysis of ellipsometry data

Ellipsometric data (Δ and ψ) was acquired by variable angle spectroscopic ellipsometry (VASE) in the range of 400-1700 nm with a J. A. Woollam Co., Inc. WVASE32 spectroscopic ellipsometer, at the angle of incidence from 65° to 75°. For the PB1 series, simple or graded Cauchy dispersion model, considering SLG (substrate) as the bottom layer was used to generate the data. In the case of PB2 series, Cauchy dispersion model was used in the longer wave length to estimate the coating thickness, and further the model was extended to oscillator models in order to understand absorption properties. The models facilitate to estimate the coating thickness as well as RI separately [32-34]. The data fitting is performed using the iterative Marquardt - Levenberg fitting algorithm. The individuality of the regression analysis has been confirmed by repeating the analysis and data collection on several locations and uniqueness fit. All the data analysis and validation processing was done using the Woollam Company WVASE32 software package.

A.K. Othayoth et al. Optical Materials 104 (2020) 109841

$$CI = P - CI$$

$$OH = P - CI$$

Scheme 1. Schematic representation for the syntheses of polymers P1 and P2.

Table 1 Characterization data of polyphosphates, P1 and P2.

Polymer	31 P NMR in CDCl $_3$ δ (ppm)	1 H NMR in CDCl $_{3}$ δ (ppm)	Mn (Da)	Mw (Da)	PDI	DP
P1	-17.2 (s) and -18.9 (s)	7.2–7.4 (m, 13H), 1.6 (s, 6H)	32372	64331	1.98	88
P2	-17.46 (s)	7.2–7.5 (m, 13H)	6639	10983	1.65	20

3. Results and discussion

3.1. Preparation of polyphosphates and their blends with PMMA

Typical condensation polymerization (Scheme 1) involving the formation of P-O bonds yielded polyphosphates, P1 and P2, and released HCl as a side product. M. Gao and Y. Sun reported [35] the oligomer of the polyphosphate, P1 in 2013. They have synthesized Epoxy Resins containing bisphenol A bis (diphenyl phosphate) oligomer starting from POCl₃ and bisphenol using AlCl₃ as the catalyst, by a two-step synthesis and end-capping with phenol. Herein, we have produced polyphosphates in a single step synthesis [31], starting from phenyl dichloro phosphate and the corresponding diols. These reactions yielded polymers of sufficiently large average molecular weights with reasonable Polydispersity Index (PDI) for practical applications. GPC analyses provided their molecular weight distribution (Table 1). P1 showed a higher average molecular weight than P2, both in terms of Mn and Mw. The degree of polymerization (DP) was calculated from the number average molecular weight and repeat unit molecular weight (Table 1). As expected, P1 has a higher DP than P2 owing to its higher average molecular weight.

The NMR spectral data confirmed the structure of repeating units in the polymers. The two signals in the ^{31}P NMR spectrum of the polymer P1 are assigned to the phosphorus in the repeat unit and the phosphorus at the end chain. The polymers P1 and P2 were purified by repeated precipitation from chloroform into hexane, and therefore there is no possibility of any unreacted phosphorous source used in the reaction. Usually, if chain length is small, it is expected to show two distinguishable peaks in the ^{31}P NMR spectrum. Similar observations of two phosphorus peaks in ^{31}P NMR have been reported by many researchers [18,31,36–39]. However, in our case, the higher molecular weight polymer P1 showed two ^{31}P signals. The reason for this observation is

explained, presumably based on the high polydispersity index (PDI). In general, higher PDI value reflects the heterogeneity in chain length, *i.e.*, the presence of more random arrangement. As PDI is more for P1, there should be a considerable variation in molecular weights of each chain of the polymer whose average is given as 32,372 Da (Mn). So the presence of smaller chains where the two phosphorus environments are distinguishable may be resulting in two ³¹P NMR peaks in P1. The chain length of P2 could be longer than these smaller chains in P1 and hence cannot differentiate the two phosphorus environments.

Many phosphorus-containing polymers are known in the literature, and these phosphorus-containing polymers can be categorised as polymers with phosphorus atoms in the main chain or an organic pendant group containing phosphorus. The polymers with P-N, P-C, P-O, and P-B bonds in the main chain constitute the first category of polymers while the second group comprises mostly phosphonates or phosphinates attached to typical carbon polymers. In this study, we have synthesized polymers with P-O bonds wherein phosphates form a part of the repeating units. In P1 and P2, the phosphate part provide thermal stability (Tg value) [40], whereas the aromatic organic groups provide the opportunity for tuning the property and film-forming nature. Ab initio calculation using contemporary density functional theory (DFT) procedures predicted the substantial charge separation in case of the P-C and P-O bond suggesting an increase in bond dissociation energies dissociations of P-C and P-O bonds. Many experimental results have verified the thermal stability of phosphorus-containing polymers [41].

The polymers P1 and P2 possessed unusual film-forming nature, as depicted in Fig. 1. These films were formed by simple solvent casting from chloroform solution and drying at room temperature. However, the films of P1 and P2 were brittle and non-transparent; therefore, they were blended with PMMA since it is known to form a transparent film. The blends were prepared in chloroform by mixing P1 and P2 separately with PMMA in varying weight ratios (Fig. 2 and Fig. S6). First, phosphates were mixed with PMMA in such a way to contribute 10% of the weight of the blend. Then, the weight contribution of the phosphates was increased while decreasing the amount of PMMA. These blends were coated directly on the soda-lime glass. The name of the blends and their respective weight ratios are displayed in Table 2. The detailed analysis of RI of polymer blends is done by the ellipsometric method (Section 3.5).

3.2. Absorption behaviour of polyphosphates

The absorption behaviour of PMMA was studied well and reported

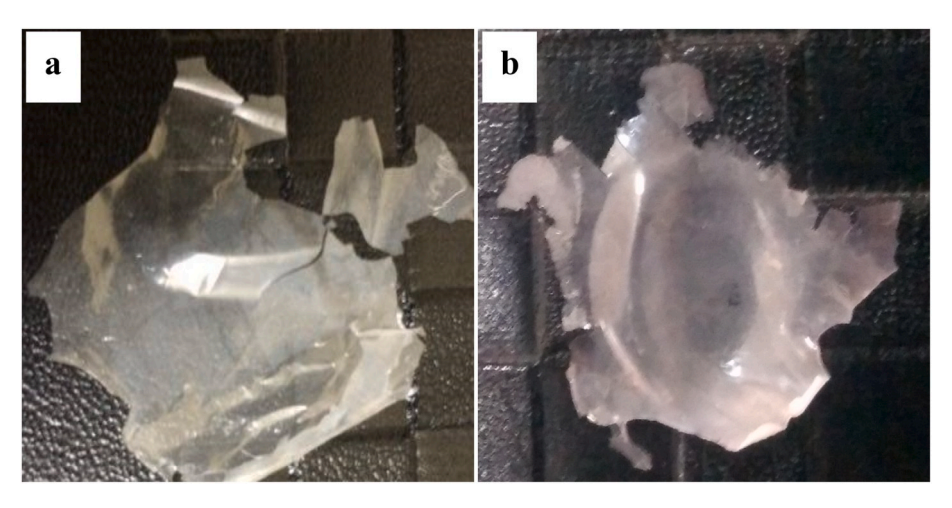


Fig. 1. Polymers P1 (a) and P2 (b) casted into films by solvent casting. The images illustrate the film forming tendency of the polymers.

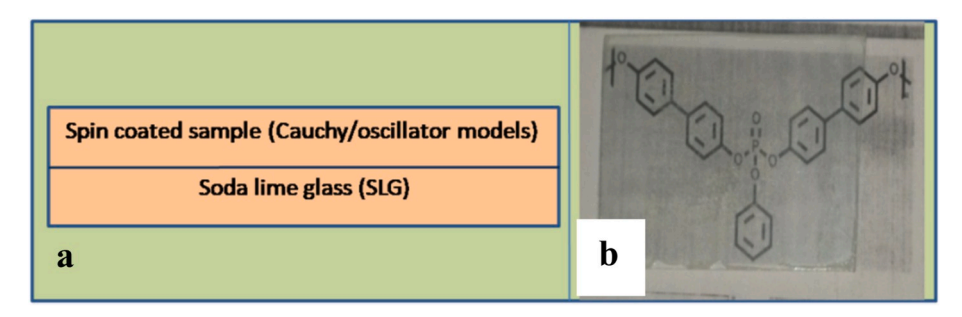


Fig. 2. (a) A schematic representation of the sample coated on SLG as considered for optical modelling (b) A typical sample spin-coated on a glass slide illustrated for its transparency (See Fig. S6 for the images of rest of the samples).

Table 2 Phosphates (P1 or P2) and PMMA blends and their weight ratio.^a

Name of the polymer blend	Polyphosphate (P1 or P2)	Percentage of P1 or P2 in the blend	Weight ratio PMMA: P1 or P2
PB110	P1	10	4:1
PB120	P1	20	3:2
PB150	P1	50	1:1
PB160	P1	60	2:3
PB180	P1	80	1:4
PB210	P2	10	4:1
PB220	P2	20	3:2
PB250	P2	50	1:1
PB260	P2	60	2:3
PB280	P2	80	1:4

^a The nomenclature of polymer blends based on weight percentage of PMMA and polyphosphate (P1 or P2) and their weight ratios are given.

elsewhere [42,43]. The absorption of polyphosphates and their blends with PMMA at the UV–Vis–NIR region were recorded to understand their optical behaviour. Fig. 3 depicts the absorption spectra of P1 and P2 in the region of 1400–200 nm. The absorption of P1 in visible and NIR region is almost zero from 1400 nm to 370 nm compared to the baseline. In the case of P2, in the visible region, an additional absorption peak shows broadband centered at 480 nm with an onset absorption of 520 nm (see inset of Fig. 3(a)). It has been reported that the visible light absorbance has several contributions, such as intrinsic absorbance (actual absorbance due to electronic excitation), scattering (apparent absorption due to scattering with respect to particle or grain size), and the dopant effect [44]. In this case, the additional absorption in P2 at λ max around 480 nm is probably due to inter band transition. On the other hand, in the UV region (300 -200 nm, inset), multiple oscillations were observed in the sample P1 (λ max 240, 260, 270, and 285 nm),

whereas **P2** shows only a single oscillation having λ max 250 nm. These peaks are mainly due to π - π^* band of the benzene ring [45]. All the above peaks in the UV region are characteristic absorption of biphenyl derivatives with phosphorus in the main chain as reported by Freedman [46].

Fig. 3(b) shows the extinction co-efficient of the **P2** blended samples. The PB1 polymer blends, on the other hand, showed negligible or zero extinction coefficients and hence not explicitly plotted. The samples PB210 and PB220 are not showing any additional characteristic absorption in the range 1400 to 370 nm, similar to P2. Upon increasing the P2 weight percentage further, the sample PB250 shows the characteristic absorption around 590 nm. Similarly, a further increase in the P2 concentration shifts the absorption peak to the lower energy side. The heavily doped sample PB280 shows multiple oscillations in the range of 400-1000 nm. From this observation, it is clear that the processing conditions and the addition of polyphosphates into PMMA change the optical properties by entering into the basic network of the PMMA. Doping affects the overall film absorption and the band gap of the film depending upon the concentration [44]. Such controllable absorption behaviour depending upon the weight percentage of polyphosphates are highly recommended for tuning the optical properties depending upon the applications.

3.3. FT-IR spectra and interaction between polymers in blend

The characteristic FT-IR bands of PMMA are observed at 1386 cm $^{-1}$ and 750 cm $^{-1}$ corresponding to vibrations of the α -methyl group while the 1141 cm $^{-1}$ and 1188 cm $^{-1}$ bands correspond to the C-O-C stretching (Fig. 4(a) and (b)). C-H bending is observed at 1434 cm $^{-1}$, and the carbonyl stretching band is observed at 1721 cm $^{-1}$. At 2949 cm $^{-1}$ and 2992 cm $^{-1}$, the C-H stretching of CH $_2$ and CH $_3$ are observed respectively

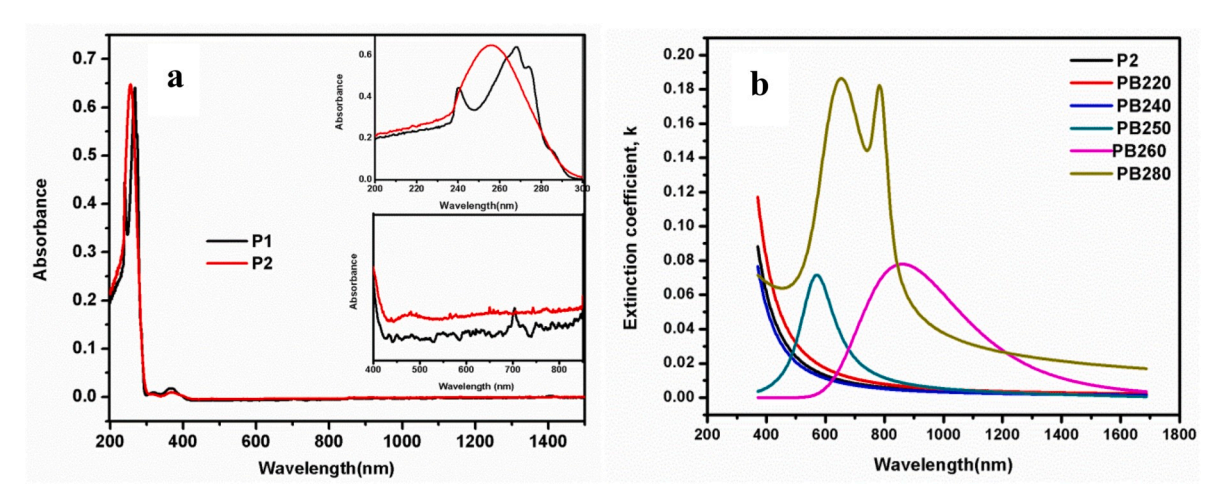


Fig. 3. (a) Absorption spectra of P1 and P2 from 200 to 1500 nm (The inset shows the range 200–300 nm as well as 400–850 nm for close observation and identification of peaks) (b) Variation in extinction coefficients with wavelength for P2 and the blends of P2.

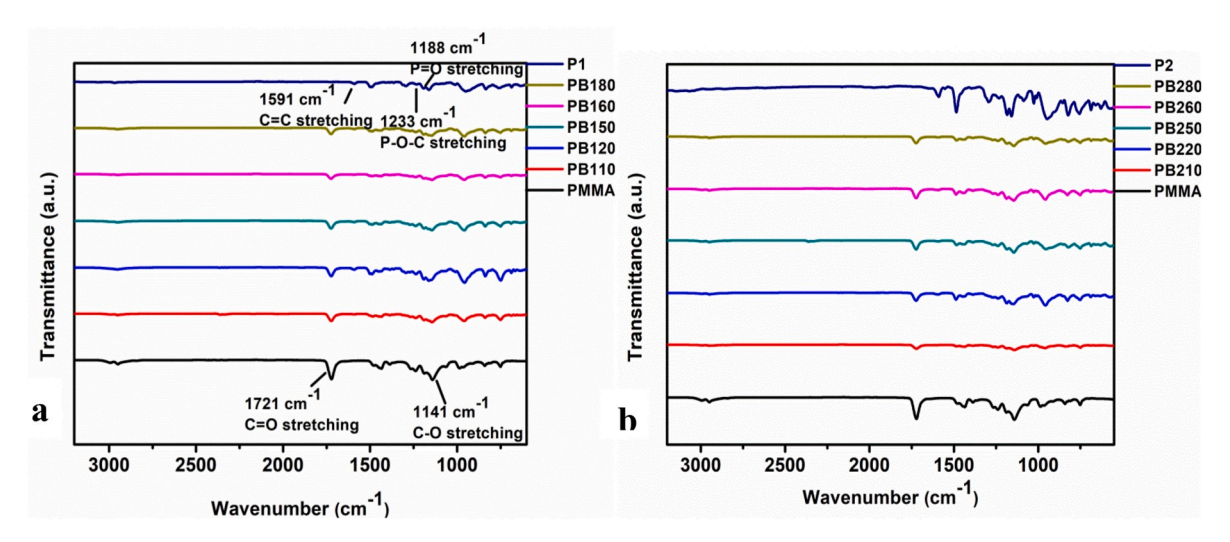


Fig. 4. (a) FT-IR spectra of P1, PMMA and their blends for comparison (b) FT-IR spectra of P2, PMMA and their blends for comparison.

[47,48]. After blending with the polyphosphates, the characteristic phosphate bands at 1233 cm-1 and 1191 cm $^{-1}$ corresponding to P-O-C and P=O stretching are observed in the blended samples along with the C=C stretching at 1591 cm $^{-1}$. This observation confirms the formation of the blend.

The nature of interactions between the polyphosphates and PMMA is explained from the evidence of hydrogen bonding in blends. The presence of broad peaks in the region $3200\text{-}3500~\text{cm}^{-1}$ is indicative of the intermolecular hydrogen bonding between polyphosphates and PMMA (Fig. S3(b)). Hydrogen bonding could take place between the carbonyl oxygen of PMMA and methyl groups of P1 [49]. Similarly, phosphoryl oxygen of P1 and P2 can interact with methyl of PMMA. However, since the hydrogen bonding is quite weak, there is no considerable red-shift observed in the IR frequencies corresponding to those hydrogen-bonded groups.

3.4. Thermal analysis of the polyphosphates and their blends

All the blends in PB1 and PB2 series showed thermal stability of about $180\,^{\circ}\text{C}$ on an average, which is quite reasonable for a variety of optical applications (Fig. 5(a) and b). Analysis of glass transition temperatures of the blends in PB1 series indicates that they are completely miscible blends since their Tg lie in between the parent polymers, as shown in Fig. 5 (c). In the case of PB2 series also, the Tg of the blends lie

almost in the same range (50–55 $^{\circ}$ C) as the blends of PB1 series and are all below that of parent polymer PMMA (105 $^{\circ}$ C) (Fig. 5(d)). However, since the polymer **P2** shows a gradual weight loss starting from around 45 $^{\circ}$ C itself, the DSC analysis of the polymer could not be performed.

3.5. Study of refractive indices of polymer blends

3.5.1. PB1 series

The refractive indices of the polymer blends listed in Table 2 were determined using ellipsometer, and the values were deduced from theoretical model fitting. The data was measured at three different wavelengths (486, 589, and 656 nm). A representative sequence of graphs one of the blends (PB180) showing the whole process of data collection is presented in Fig. 6. As can be seen from Fig. 6(a), the theoretical model is found to be in close agreement with the experimental data. The RI data is then derived from this fitting shown (Fig. 6(b)). The uniqueness of the fit was analysed to check the reliability of the data obtained as is represented in Fig. 6(c). The fit was obtained employing minimum MSE and Kramers-Kronig consistency.

Refractive indices at three different wavelengths and the maximum value of RI for a particular sample is shown in Table 3. The general trend of decrease in RI with an increase in wavelength is followed intact in the PB1 series (Fig. 7(a)). In Fig. 7(b), the RI values of blends are plotted with respect to weight percentages of P1 and P2. This helps to

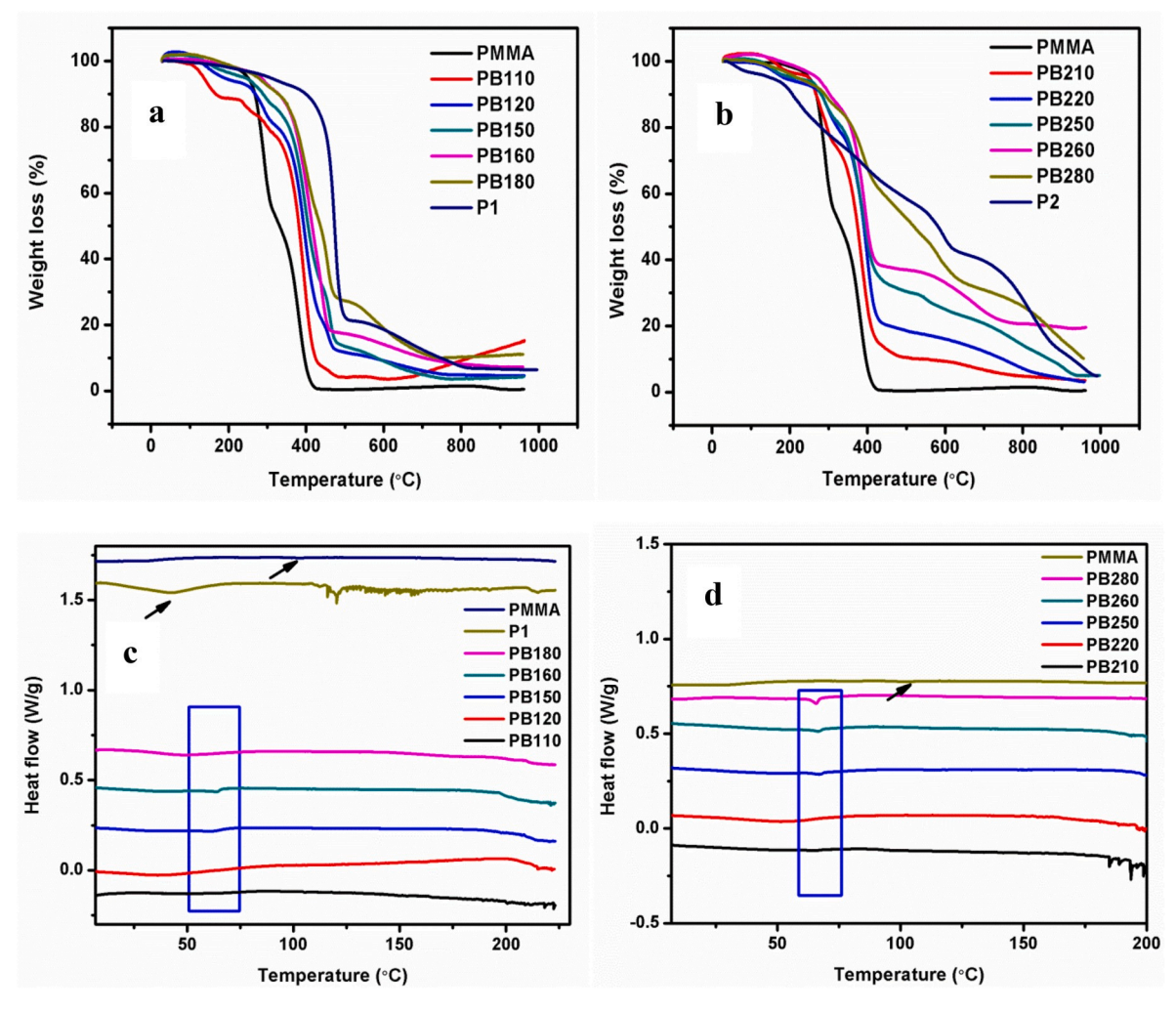


Fig. 5. The thermogravimetric analyses of all the samples in PB1 and PB2 series are shown in Figs (a and b), respectively and their corresponding glass transition temperatures, measured by DSC, are illustrated in figure c and d respectively.

understand the variation of RI with respect to concentration of polyphosphates P1 and P2. In the PB1 series, the overall observation is that the addition of P1 into the PMMA system increases the RI of PMMA (Fig. 7(b)). Some of the compositions, specifically the ones with a higher concentration of P1 (PB150, PB160, and PB180), showed higher RI than both the parent polymers, PMMA, and P1. Nevertheless, the most important inference is that a refractive index tunability of 0.05 was achieved with the help of the introduction of P1 into PMMA. This number is quite significant since a change in the RI of about even 0.01 could bring about a change of 3.30 D actual change in its power in a perfect lens system [50].

3.5.2. PB2 series

In contrast to the PB1 series, the PB2 series showed RI in between PMMA and P2 (Table 3). Most of the samples except PB260, have RI falling above PMMA but below P2. A tunability of about 0.1 in RI was observed with variation in concentration of P2. All these are valuable insights when it comes to the application point of view. The PB260 blend is showing comparatively lower RI than others in the series. As the optical properties of thin films depend on several factors like structure, thickness, homogeneity, materials used, and the preparation conditions, it is not very easy to estimate precisely the reason for this anomaly. However, since we have followed the same protocol for all the samples, the reason could probably be some irregularity that occurred during sample preparation.

The trend in RI for the blends in PB2 series can be categorised into

two parts. The blends with lower percentage of P2 (PB210 and PB220) behave almost like the PB1 series. They have no significant absorption losses and hence follow the general trend of decreasing RI with increasing wavelengths (Fig. 8(a)). On the other hand, the blends with higher weight percentages of P2 showed an increase in RI beyond a particular wavelength (Fig. 8(b)). The reason for such a behaviour can be directly correlated with the extinction coefficient graph (Fig. 3(b)) of these blends because the imaginary part of the complex refractive index is nothing but the extinction coefficient from the equation,

$$\tilde{\mathbf{n}} = n + i\mathbf{k}$$

here \tilde{n} is the complex refractive index, n is real part of refractive index and k is the extinction coefficient. This fact is further illustrated by Fig. 8 (d) where n and k compensate each other. And interestingly, this property of absorption beyond the visible range makes these blends useful in designing optical filters.

3.6. Tunability in optical properties of PB1 and PB2 blends

Abbe's number (V_D) is an essential parameter of optical materials indicating its optical dispersion and is given by the equation:

$$V_D = \frac{n_{D-1}}{n_E - n_C}$$

In this equation, n_D , n_F , and n_C are the refractive indices of material at the wavelengths of the sodium D (589.3 nm), hydrogen F (486.1 nm),

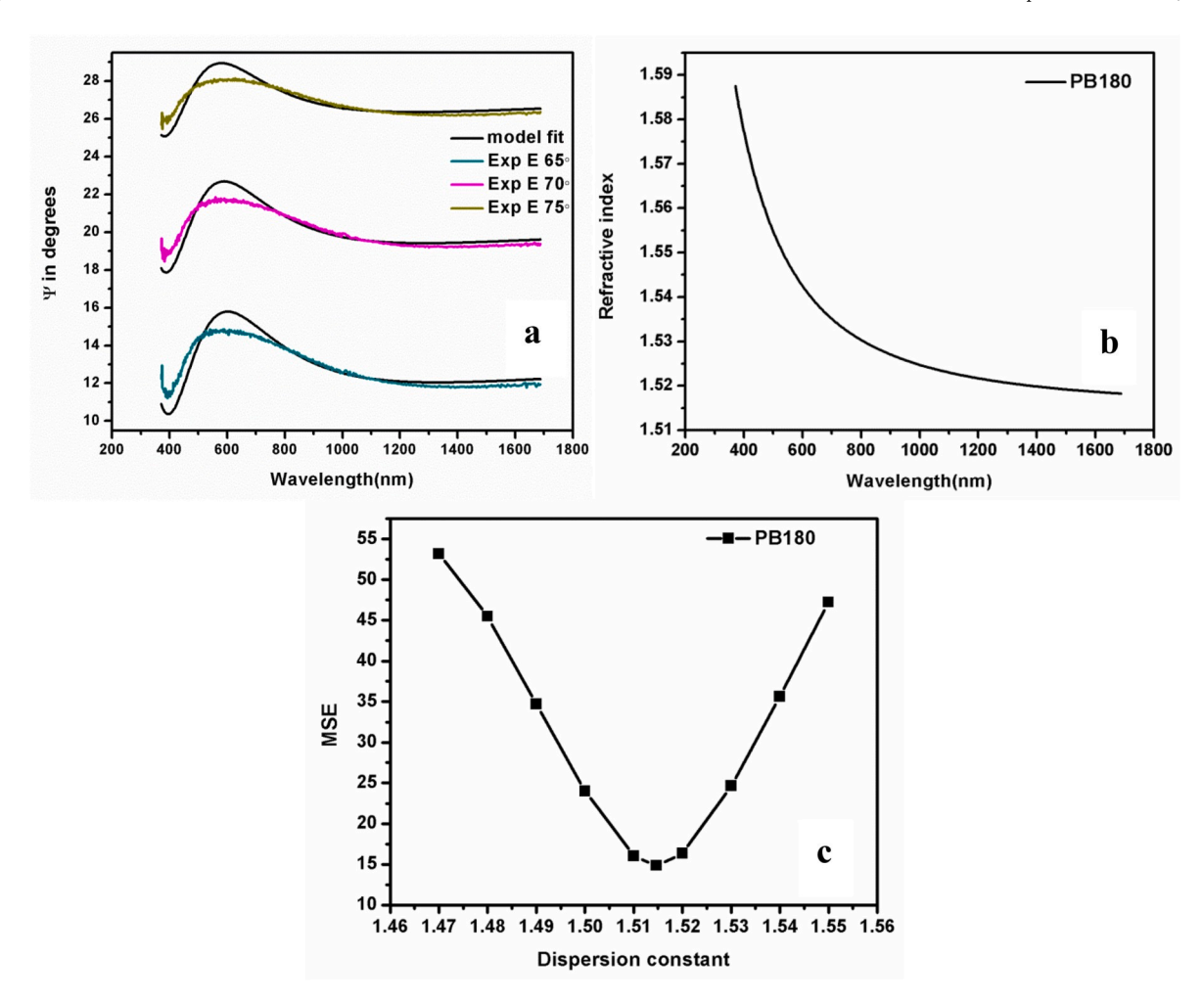


Fig. 6. (a) Ellipsometric spectra of a sample (PB180) spin-coated on a glass substrate (experimental data and model fit are shown) (b) variation of refractive index with wavelength and (c) uniqueness fit for the sample PB180.

Table 3Refractive indices of polyphosphate blends with PMMA.

Name of the blends	Weight % of P1	n ₄₈₆	n ₅₈₉	n ₆₅₆	n _{max}
PMMA	0	1.47	1.46	1.45	1.50 (370 nm)
PB110	10	1.56	1.54	1.54	1.55 (370 nm)
PB120	20	1.50	1.50	1.50	1.52 (370 nm)
PB150	50	1.56	1.54	1.54	1.58 (370 nm)
PB160	60	1.54	1.53	1.52	1.57 (370 nm)
PB180	80	1.56	1.54	1.54	1.58 (370 nm)
P1	100	1.52	1.51	1.50	1.55 (370 nm)
	Weight % of P2	n ₄₈₆	n ₅₈₉	n ₆₅₆	n _{max}
PMMA	Weight % of P2	n ₄₈₆	n ₅₈₉	n ₆₅₆	n _{max} 1.50 (370 nm)
PMMA PB210	•				
	0	1.47	1.46	1.45	1.50 (370 nm)
PB210	0 10	1.47 1.49	1.46 1.49	1.45 1.49	1.50 (370 nm) 1.49 (constant)
PB210 PB220	0 10 20	1.47 1.49 1.54	1.46 1.49 1.53	1.45 1.49 1.52	1.50 (370 nm) 1.49 (constant) 1.57 (370 nm)
PB210 PB220 PB250	0 10 20 50	1.47 1.49 1.54 1.50	1.46 1.49 1.53 1.53	1.45 1.49 1.52 1.55	1.50 (370 nm) 1.49 (constant) 1.57 (370 nm) 1.55 (645 nm)

and hydrogen C (656.3 nm) lines, respectively. The abbe's numbers of all the samples in PB1 series were calculated and tabulated in Table 4. The Abbe values are generally denoted only for transparent glass-like materials to account for its optical dispersion. Hence, V_D is not calculated for PB2 series (especially the blends with higher concentrations of P2) because of their significant absorption indicated by the extinction coefficient values. Interestingly, all PB1 blends showed values within the acceptable range of abbe values of optical lens materials with a

maximum of 56 for PB120 (Fig. 10).

In short, PMMA, which has a refractive index of about 1.48 upon blending with these polyphosphates, showed a tunability of RI from 0.97 to 1.55 at 589 nm. Since polyphosphates have a similar structure to polycarbonates (PC), the RIs of the P1/P2 blended with PMMA with that of PC-PMMA blends reported in literature are compared [26]. A plot of RI at 486 nm as a function of weight percent of the blends of P1, P2 and PC is shown in Fig. 9. It is clear from the plot that, as the concentration is varied RI of PB1 and PB2 series varies gradually whereas a large change in RI value was observed for PC blends. The advantage of polymers used here is they can be blended with PMMA in a simple process and expected to provide thermal and mechanical stability.

Also, as discussed in Section 3.5.2., the blends in PB2 series with higher concentrations of P2 (i.e. PB250, PB260, and PB280) reflect a similar trend in the RI as the extinction coefficients of these samples. Hence these may not be suitable candidates for lens kind of applications, but they may be suitable for optical filter kinds of applications where absorption over a specific wavelength range is highly preferred. On the other hand, all the blends in PB1 series and the first two blends of PB2 series, fall under the same category, showing a regular trend of decreasing RI with increasing wavelength. Therefore, these are potential candidates for use as lens because of their transparency, RI tunability and high abbe number.

4. Conclusions

We have synthesized two polyphosphate polymers (P1 and P2) and

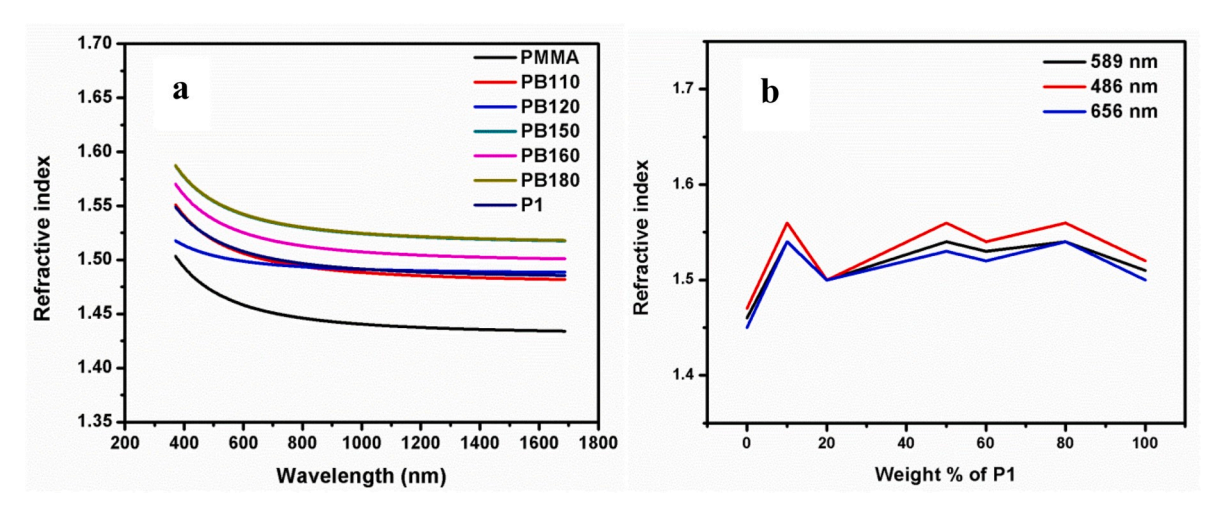


Fig. 7. (a) Variation of refractive indices with wavelengths for PB1 series (b) Variation of refractive indices with different weight percentages for PB1 series.

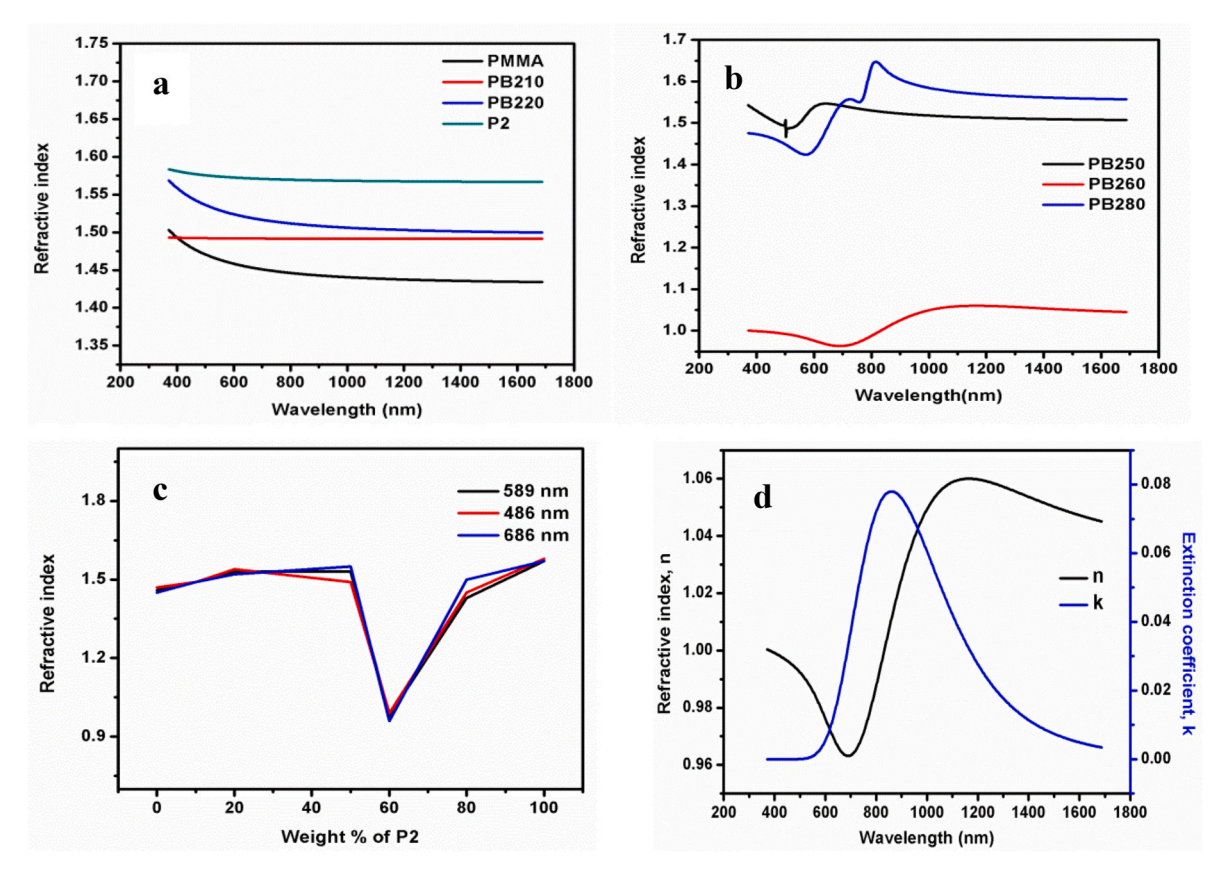


Fig. 8. (a) Variation of refractive indices with wavelengths for PMMA, PB210, PB220 and P2 (b) Variation of refractive indices with wavelengths for PB250, PB260 and PB280 (c) Variation of refractive indices with different weight percentages for PB2 series (d) a representative plot (PB260) of variation in n and k with wavelength.

characterized them thoroughly. These polymers are blended with PMMA to produce uniform and transparent polymer films (PB1 and PB2 series) by simple spin-coating from solution for optical applications. The hydrogen-bonding interactions between PMMA and the polyphosphates, as evidenced by IR spectra, ensures the homogeneity of the blend. Thermal analysis of PB1 series indicates these blends to be completely miscible.

The incorporation of polyphosphates has resulted in the tunability of RI of PMMA. The ellipsometric measurements of prepared blends (PB1 and PB2 series) showed a tunability in RI of about 0.05 and 0.1,

respectively. Also, blends of PB1 series showed an acceptable Abbe value in the range of optical lenses with a maximum of 56 achieved for PB120 blend. On the other hand, blends with higher weight percentages of P2 in PB2 series could be promising for optical filters owing to its ability to filter some wavelengths as seen from their extinction coefficients.

The preliminary investigation on blends of P1 and P2 with PMMA is quite promising in the way of engineering the desired refractive index and Abbe number by altering the polyphosphates content. Also, PMMA, which is well known for its compatibility with human tissue, could be ideal for rigid intraocular lenses with the desired refractive index

Table 4 Abbe values of P1 and their blends^a.

Weight % of P1	Abbe no
0	25
10	29
20	56
50	29
60	29
80	30
100	29

^a 0 wt % of P1 indicate that it is pure PMMA and 100 wt % of P1 indicate that it is P1 polymer.

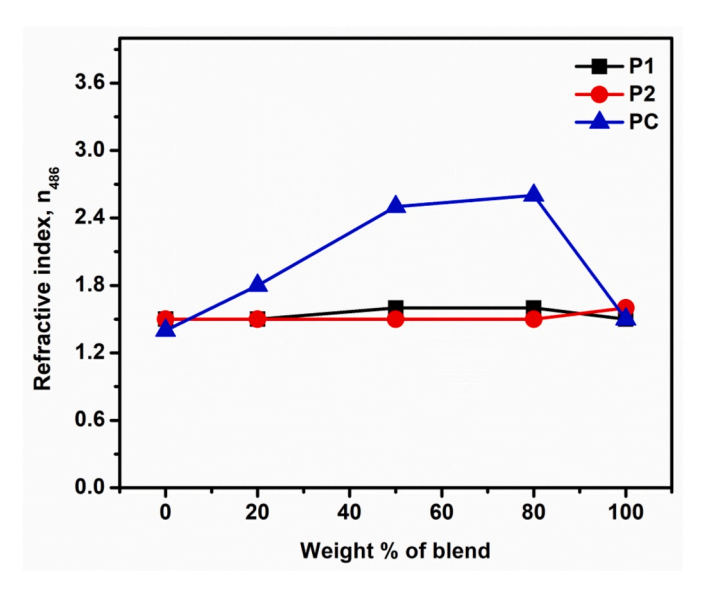


Fig. 9. Variation of RI with different weight % of P1, P2 and PC blended with PMMA.

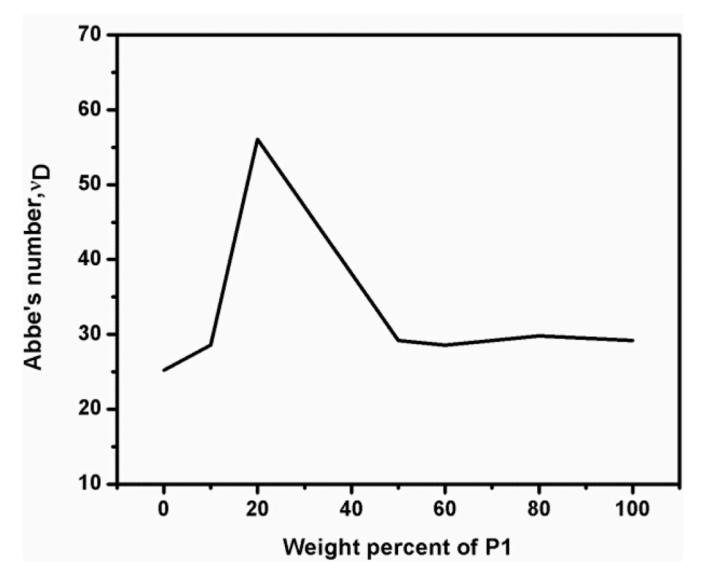


Fig. 10. Abbe values of blends of PMMA with P1 plotted with increasing weight percentages of P1.

tailored by the incorporation of these polyphosphates.

Declaration of competing interest

The authors declare that they have no known competing financial interests or personal relationships that could have appeared to influence the work reported in this paper.

CRediT authorship contribution statement

Anjana K. Othayoth: Conceptualization, Investigation, Formal analysis, Writing - original draft. Billakanti Srinivas: Conceptualization. Karuppiah Murugan: Investigation, Formal analysis, Writing - review & editing. Krishnamurthi Muralidharan: Supervision, Writing - review & editing.

Acknowledgment

A.K.O. acknowledges UGC-BSR for fellowship. Financial and infrastructure support from the University Grants Commission, New Delhi, India (through the UPE and CAS programs) and the Department of Science and Technology, New Delhi, India (through the PURSE and FIST programs) are gratefully acknowledged. We also thank ARCI, Hyderabad, India for ellipsometric measurements.

Appendix A. Supplementary data

Supplementary data to this article can be found online at https://doi.org/10.1016/j.optmat.2020.109841.

Abbreviations

PMMA	Poly (methyl methacrylate)
RI	refractive index
NMR	Nuclear magnetic resonance
IR	infrared
UV	ultraviolet
PB	polymer blend
SLG	soda lime glass
PDI	polydispersity index
GPC	gel permeation chromatography
TGA	thermogravimetric analysis
DSC	dynamic scanning analysis

References

- M. Yoshida, P.N. Prasad, Sol-Gel-Processed SiO₂/TiO₂/poly(vinylpyrrolidone) composite materials for optical waveguides, Chem. Mater. 8 (1996) 235–241.
- [2] P. Müller, B. Braune, C. Becker, H. Krug, H. Schmidt, Proc. SPIE-Int. Soc. Opt. Eng. 3136 (1997) 462.
- [3] C.J. Yang, S.A. Jenekhe, Effects of structure on refractive index of conjugated polyimines, Chem. Mater. 6 (1994) 196–203.
- [4] T. Sugiyama, T. Wada, H. Sasabe, Optical nonlinearity of conjugated polymers, Synth. Met. 28 (1989) 323–328.
- [5] C.J. Yang, S.A. Jenekhe, Group contribution to molar refraction and refractive index of conjugated polymers, Chem. Mater. 7 (1995) 1276–1285.
- [6] M. Liras, M. Barawi, V.A. de la Peña O'Shea, Hybrid materials based on conjugated polymers and inorganic semiconductors as photocatalysts: from environmental to energy applications, Chem. Soc. Rev. 48 (2019) 5454–5487.
- [7] M. Jose, M. Sakthivel, Synthesis and characterization of silver nanospheres in mixed surfactant solution, Mater. Lett. 117 (2014) 78–81.
- [8] M.R. Noor El-Din, I.M. El-Gamal, S.H. El-Hamouly, H.M. Mohamed, M.R. Mishrif, A.M. Ragab, Rheological behavior of water-in-diesel fuel nanoemulsions stabilized by mixed surfactants, Colloid. Surface. Physicochem. Eng. Aspect. 436 (2013) 318–324.
- [9] T.E. Kodger, J. Sprakel, Thermosensitive molecular, colloidal, and bulk interactions using a simple surfactant, Adv. Funct. Mater. 23 (2013) 475–482.
- [10] D.W. VanKrevelen, Properties of Polymers, third ed., Elsevier, Amsterdam, 1990.
- [11] Z. Fan, M.K. Serrano, A. Schaper, S. Agarwal, A. Greiner, Polymer/nanoparticle hybrid materials of precise dimensions by size-exclusive fishing of metal nanoparticles, Adv. Mater. 27 (26) (2015) 3888–3893.

- [12] L.L. Beecroft, C.K. Ober, Nanocomposite materials for optical applications, Chem. Mater. 9 (6) (1997) 1302–1317.
- [13] C. Janáky, K. Rajeshwar, The role of (photo) electrochemistry in the rational design of hybrid conducting polymer/semiconductor assemblies: from fundamental concepts to practical applications, Prog. Polym. Sci. 43 (2015) 96–135.
- [14] R. Barbey, L. Lavanant, D. Paripovic, N. Schüwer, C. Sugnaux, S. Tugulu, H.A. Klok, Polymer brushes via surface-initiated controlled radical polymerization: synthesis, characterization, properties, and applications, Chem. Rev. 109 (11) (2009) 5437–5527
- [15] R. Okutsu, Y. Suzuki, S. Ando, M. Ueda, Poly(thioether sulfone) with high refractive index and high abbe's number, Macromolecules 41 (2008) 6165–6168.
- [16] T. Higashihara, M. Ueda, Recent progress in high refractive index polymers, Macromolecules 48 (2015) 1915–1929.
- [17] R.F. Hudson, Structure and Mechanism in Organo-Phosphorus Chemistry, Academic Press, London, 1965.
- [18] H.V. Babu, K. Muralidharan, Polyethers with phosphate pendant groups by monomer activated anionic ring opening polymerization: syntheses, characterization and their lithium-ion conductivities, Polymer 55 (2014) 83–94.
- [19] H.V. Babu, B. Srinivas, K.P.K. Naik, K. Muralidharan, Polymerization behavior of butyl bis(hydroxymethyl)phosphine oxide: phosphorus containing polyethers for Li-ion conductivity, J. Chem. Sci. 127 (2015) 635–641.
- [20] H.V. Babu, B. Srinivas, K. Muralidharan, Design of polymers with an intrinsic disordered framework for Li-ion conducting solid polymer electrolytes, Polymer 75 (2015) 10–16.
- [21] M.A. Olshavsky, H.R. Allcock, Polyphosphazenes with high refractive Indices: optical dispersion and molar refractivity, Macromolecules 30 (1997) 4179–4183.
- [22] M.A. Olshavsky, H.R. Allcock, Polyphosphazenes with high refractive indices: synthesis, characterization, and optical properties, Macromolecules 28 (1995) 6188-6197
- [23] Sekharipuram, V.; Shobha, H. K.; McGrath J. E.; Bhatnagar, A. High Refractive Index Thermoplastic Polyphosphonates. U.S. Patent 6,288,210 B1, September 11, 2001.
- [24] H.K. Shobha, H. Johnson, M. Sankarapandian, Y.S. Kim, P. Rangarajan, A.D. Baird, J.E. McGrath, Synthesis of high refractive-index melt-stable Aromatic polyphosphonates, J. Polym. Sci.: Polym. Chem. 39 (2001) 2904–2910.
- [25] E.K. Macdonald, J.C. Lacey, I. Ogura, M.P. Shavera, Aromatic polyphosphonates as high refractive index polymers, Eur. Polym. J. 87 (2017) 14–23.
- [26] J.H. Nahida, R.F. Marwa, Study of the optical constants of the PMMA/PC blends, AIP Conf. Proc. 1400 (2011) 585–595.
- [27] N.M. Noriega, M. Hinojosa, V. Gonz_alez, S.E. Rodil, Polymer-based composite with outstanding mechanically tunable refractive index, Opt. Mater. 58 (2016) 18–23.
- [28] N.M. Deghiedy, S.M. El-Sayed, Evaluation of the structural and optical characters of PVA/PVP blended films, Opt. Mater. 100 (2020) 109667–109677.
- [29] A. Zhanga, W. Xub, R. Chena, Z. Wanga, Q. Yana, Y. Miao, H. Jiab, B. Xub, W. Yeung Wong, Program controlling the emission color of blend polymer phosphors containing Eu(III), Tb(III), Be(II) ions for WLEDs, Opt. Mater. 89 (2019) 250–260
- [30] S. Iliescu, G. Ilia, A. Pascariu, A. Popa, N. Plesu, Organic solvent-free synthesis of phosphorus containing polymers, Pure Appl. Chem. 79 (11) (2007) 1879–1884.
- [31] S. Iliescu, L. Zubizarreta, N. Plesu, L. Macarie, A. Popa, G. Ilia, Polymers containing phosphorus groups and polyethers: from synthesis to application, Chem. Cent. J. 6 (2012) 132–145.

- [32] K. Vedam, R. Rai, F. Lukes, R. Srinivasan, Ellipsometric method for the determination of all the optical parameters of the system of an isotropic nonabsorbing film on an isotropic absorbing substrate. Optical constants of silicon, J. Opt. Soc. Am. 58 (526) (1968) 64–71.
- [33] K. Li, S. Wang, L. Wang, H. Yu, N. Jing, R. Xue, Z. Wang, Fast and sensitive ellipsometry-based biosensing, Sensors 18 (15) (2018) 1–13.
- [34] D. Pristinski, V. Kozlovskaya, S.A. Sukhishvili, Determination of film thickness and refractive index in one measurement of phase-modulated ellipsometry, J. Opt. Soc. Am. A 23 (10) (2006) 2639–2644.
- [35] M. Gao, Y. Sun, Flame retardancy and thermal degradation behaviors of Epoxy Resins containing bisphenol A bis (diphenyl phosphate) oligomer, Polym. Eng. Sci. 53 (5) (2013) 1125–1130.
- [36] J.R. Van Wazer, in: F. Grayson, M. Griffin (Eds.), Topics in Phosphorus Chemistry, fifth ed., John Wiley, London, 1967.
- [37] J.R. Van Wazer, C.F. Callins, J.N. Shoolery, R.C. Jones, Principles of phosphorus chemistry. II. Nuclear Magnetic Resonance Measurements1, J. Am. Chem. Soc. 78 (1956) 5715–5726
- [38] Y. Morisaki, Y. Ouchi, K. Tsurui, Y. Chujo, Synthesis of optically active polymers containing chiral phosphorus atoms in the main chain, J. Polym. Sci. Polym. Chem. 45 (2007) 866–872.
- [39] H. Cavaye, F. Clegg, P.J. Gould, M.K. Ladyman, T. Temple, E. Dossi, Primary Alkylphosphine—Borane polymers: synthesis, low glass transition temperature, and a predictive capability thereof, Macromolecules 50 (2017) 9239–9248.
- [40] K. Hemelsoet, F.V. Durme, V.V. Speybroeck, M.F. Reyniers, M. Waroquier, Bond dissociation energies of organophosphorus compounds: an assessment of contemporary ab initio procedures, J. Phys. Chem. 114 (2010) 2864–2873.
- [41] R. Chen, X. Huang, R. Zheng, D. Xie, Y. Mei, R. Zou, Flame-retardancy and thermal properties of a novel phosphorus-modified PCM for thermal energy storage, Chem. Eng. J. 380 (2020) 122500–122510.
- [42] H.M. Zidan, M. Abu-Elnader, Structural and optical properties of pure PMMA and metal chloride-doped PMMA films, Physica B 355 (2005) 308–317.
- [43] W.H. Hong, J. Woo, H.W. Choi, Y.S. Kim, G.D. Kim, Optical property modification of PMMA by ion-beam implantation, Appl. Surf. Sci. 169–170 (2011) 428–432.
- [44] K. Murugan, J. Joardar, A.S. Gandhi, B.S. Murty, P.H. Borse, Photo-induced monomer/dimer kinetics in methylene blue degradation over doped and phase controlled nano-TiO₂ films, RSC Adv. 6 (2016) 43563–43573.
- [45] Y. Ouchi, Y. Morisaki, Y. Chujo, Synthesis of optically active dendrimers having chiral bisphosphine as a core, Polym. Bull. 59 (2007) 339–350.
- [46] L.D. Freedman, The ultraviolet absorption spectra of some biphenyl derivatives of phosphorus and arsenic, J. Am. Chem. Soc. 77 (1955) 6623–6624.
- [47] G. Duan, C. Zhang, A. Li, X. Yang, L. Lu, X. Wang, Preparation and characterization of mesoporous zirconia made by using a poly (methyl methacrylate) template, Nanoscale Res. Lett. 3 (2008) 118–122.
- [48] K. Gipson, K. Stevens, P. Brown, J. Ballato, Infrared spectroscopic characterization of photoluminescent polymer nanocomposites, J. Spectrosc. 2015 (2014) 1–9.
- [49] H.M. Alhusaiki-Alghamdi, Effect of silicon carbide (SiC) nanoparticles on the spectroscopic properties and performance of PMMA/PC polymer blend, J. Mod. Phys. 10 (2019) 487–499.
- [50] CRSToday, Laser-Induced refractive index change [online] Available at: https://crstoday.com/articles/2019-apr/laser-induced-refractive-index-change/, 2019. (Accessed 16 December 2019).

Organophosphorus polymers, blends and composites: Applications in Li-ion batteries, optics and gas sorption

by Anjana K O

Submission date: 24-Jul-2020 07:56PM (UTC+0530)

Submission ID: 1361601453

File name: Anjana Theis Combined for antiplagiarism.pdf (6.7M)

Word count: 18982 Character count: 99475 UNIVERSITY TRANSPORTS OF THE PARTY TO THE PA

Organophosphorus polymers, blends and composites: Applications in Li-ion batteries, optics and gas sorption

2	3%	4%	21%	4%
SIMILA	ARITY INDEX	INTERNET SOURCES	PUBLICATIONS	STUDENT PAPERS
PRIMAR	Y SOURCES		•	
1	Karuppial Muralidha methacry tunable re	Othayoth, Billal n Murugan, Krish aran. "Poly(meth late)/polyphosph efractive indices ns", Optical Mat	nnamurthi yl nate blends with for optical	K. MURALIDHARAN Professor School of Chemistry University of Hyderabad Hyderabad - 500 046.
2	Krishnam polymers	Vignesh Babu, Burthi Muralidhar with an intrinsic conducting solid 2015	an. "Design of disordered fram	ework %
3	link.spring	ger.com		<1%
4	journal.ch	nemistrycentral.c	om	<1%
5	www.hinc	lawi.com	·	%

UNITY GO JAN BOOD DAG

6	pubs.rsc.org Internet Source	<1%
7	hdl.handle.net Internet Source	<1%
8	www.examsegg.com Internet Source	<1%
9	Nagaraj Goud Ireni, Ramanuj Narayan, Pratyay Basak, K.V.S.N. Raju. "Poly(thiourethane-urethane)-urea as anticorrosion coatings with impressive optical properties", Polymer, 2016	<1%
10	Benny D. Freeman. "Basis of Permeability/Selectivity Tradeoff Relations in Polymeric Gas Separation Membranes", Macromolecules, 1999	<1%
11	Rui Zhang, Xiang Chen, Xin Shen, Xue-Qiang Zhang, Xiao-Ru Chen, Xin-Bing Cheng, Chong Yan, Chen-Zi Zhao, Qiang Zhang. "Coralloid Carbon Fiber-Based Composite Lithium Anode for Robust Lithium Metal Batteries", Joule, 2018	<1%
12	Babu, Heeralal Vignesh, Billakanti Srinivas, and Krishnamurthi Muralidharan. "Design of polymers with an intrinsic disordered framework for Li-ion conducting solid polymer electrolytes"	<1%

1. Va Julian Constitution Ones

13	Heeralal Vignesh Babu, Krishnamurthi Muralidharan. "Polyethers with phosphate pendant groups by monomer activated anionic ring opening polymerization: Syntheses, characterization and their lithium-ion conductivities", Polymer, 2014 Publication	<1%
14	bmcchem.biomedcentral.com Internet Source	<1%
15	iopscience.iop.org Internet Source	<1%
16	Submitted to University of Sydney Student Paper	<1%
17	Submitted to University of Hong Kong Student Paper	<1%
18	en.wikipedia.org Internet Source	<1%
19	Submitted to Pondicherry University Student Paper	<1%
20	Submitted to University of Sheffield Student Paper	<1%
21	Kim, Joo Gon, Byungrak Son, Santanu Mukherjee, Nicholas Schuppert, Alex Bates,	<1%

Osung Kwon, Moon Jong Choi, Hyun Yeol Chung, and Sam Park. "A review of lithium and non-lithium based solid state batteries", Journal of Power Sources, 2015.

Publication

22	Submitted to Universiti Teknologi MARA Student Paper	<1%
23	Submitted to Universiti Teknologi Petronas Student Paper	<1%
24	www.mdpi.com Internet Source	<1%
25	Submitted to Monash University Student Paper	<1%
26	Nathaniel W Alcock, Howard J Clase, David J Duncalf, Suzanne L Hart, Andrew McCamley, Peter J McCormack, Paul C Taylor. "Synthesis of racemic chiral-at-metal complexes of the Group 4 metals", Journal of Organometallic Chemistry, 2000	<1%
27	Submitted to Curtin University of Technology Student Paper	<1%
28	Mahinder Ramdin, Theo W. de Loos, Thijs J.H. Vlugt. "State-of-the-Art of CO Capture with Ionic Liquids ", Industrial & Engineering Chemistry Research, 2012	<1%

29	Submitted to Canyons School District Student Paper	<1%
30	Hong-Cang Zhou, Zhao-Ping Zhong, Bao-Sheng Jin, Rui Xiao, Ya-ji Huang. "REMOVAL OF PAHs BY SORBENT FROM FLUE GAS DURING MSW INCINERATION", Polycyclic Aromatic Compounds, 2005	<1%
31	"Transmission Electron Microscopy Characterization of Nanomaterials", Springer Science and Business Media LLC, 2014	<1%
32	Jian Wu, Zhao Jin, Qing Zhang. "Synthesis and characterization of conjugated polymer based on tetracyano-anthraquinodimethane", Polymer Bulletin, 2015	<1%
33	Nanda Gopal Sahoo, Yong Chae Jung, Jae Whan Cho. "Electroactive Shape Memory Effect of Polyurethane Composites Filled with Carbon Nanotubes and Conducting Polymer", Materials and Manufacturing Processes, 2007	<1%
34	open.library.ubc.ca Internet Source	<1%
	1 . Company	

35	Submitted to Coastal Carolina University Student Paper	<1%
36	Submitted to Institute of Graduate Studies, UiTM Student Paper	<1%
37	Submitted to University of Minnesota System Student Paper	<1%
38	Submitted to University College London Student Paper	<1%

Exclude quotes

On

Exclude bibliography

On

Exclude matches

14 words

. Wild Interest and